

University of Louisville

ThinkIR: The University of Louisville's Institutional Repository

Electronic Theses and Dissertations

5-2023

The alphaviral capsid protein inhibits IRAK1-dependent TLR signaling to promote pathogenesis.

V. "Trey" Landers
University of Louisville

Follow this and additional works at: <https://ir.library.louisville.edu/etd>



Part of the [Virology Commons](#)

Recommended Citation

Landers, V. "Trey", "The alphaviral capsid protein inhibits IRAK1-dependent TLR signaling to promote pathogenesis." (2023). *Electronic Theses and Dissertations*. Paper 4061.
<https://doi.org/10.18297/etd/4061>

This Doctoral Dissertation is brought to you for free and open access by ThinkIR: The University of Louisville's Institutional Repository. It has been accepted for inclusion in Electronic Theses and Dissertations by an authorized administrator of ThinkIR: The University of Louisville's Institutional Repository. This title appears here courtesy of the author, who has retained all other copyrights. For more information, please contact thinkir@louisville.edu.

THE ALPHAVIRAL CAPSID PROTEIN INHIBITS IRAK1-DEPENDENT TLR
SIGNALING TO PROMOTE PATHOGENESIS

By

V “Trey” Douglas Landers
B.S. Lipscomb University, 2015
M.S. Lipscomb University, 2016
M.S. University of Louisville, 2019

A Dissertation
Submitted to the Faculty of the
School of Medicine of the University of Louisville
in Partial Fulfillment of the Requirements
for the Degree of

Doctor of Philosophy in Microbiology and Immunology

Department of Microbiology and Immunology
University of Louisville
Louisville, Kentucky
May 2023

THE ALPHAVIRAL CAPSID PROTEIN INHIBITS IRAK1-DEPENDENT TLR
SIGNALING TO PROMOTE PATHOGENESIS

By

V “Trey” Douglas Landers
B.S. Lipscomb University, 2015
M.S. Lipscomb University, 2016
M.S. University of Louisville, 2019

A Dissertation Approved on

April 14th 2023

by the following Dissertation Committee:

Dr. Kevin Sokoloski

Dr. Donghoon Chung

Dr. Juhi Bagaitkar

Dr. Thomas Mitchell

Dr. Igor Lukashevich

DEDICATION

This work is dedicated to my family and friends for always supporting me and believing that I could accomplish whatever I set my mind to.

ACKNOWLEDGMENTS

First, thank you Dr. Kevin Sokoloski for letting me join your lab. My time at UofL under your mentorship has helped me develop into a better scientist. You've always been a supportive mentor and do what you can to make sure your students succeed.

I would like to thank my committee members, Drs. Chung, Lukashevich, Bagaitkar, and Mitchell for their advice and input over the years.

None of this would have been possible without my lab mates, Autumn, Claire, Milton, Cierra, and Deepa. Thank you for the support and help and for making coming into work enjoyable.

To my other friends I've made while at UofL, Drew, Sarah, and Will. You've been just as great as my lab mates, and I can't imagine my time at UofL without you.

Finally, I'd like to thank my family for always supporting me. From encouraging me to pursue a degree in biology to believing in me when I said I wanted to get a PhD.

ABSTRACT

THE ALPHAVIRAL CAPSID PROTEIN INHIBITS IRAK1-DEPENDENT TLR SIGNALING TO PROMOTE PATHOGENESIS

V Douglas “Trey” Landers

March 24th 2023

Alphaviruses are positive-sense RNA viruses spread by mosquitos. They can cause a severe multi-joint febrile arthritis or encephalitis resulting in death or life-long cognitive impairments. To date there are no approved antiviral therapeutics or vaccine strategies for the treatment of alphaviruses creating a critical need to better understand the host pathogen interactions of alphaviruses that enable pathogenesis. It is known that alphaviruses evade innate immune responses by shutting down host transcription and translation, but these methods are dependent on viral gene expression and leave a critical time frame during early infection before viral gene expression has begun that the virus can be identified and responded to by host cells. In order to identify potential viral products that could serve to mask the virus during early infection Sindbis virus, a model alphavirus, was tested for the expression of proteins that could interfere with intracellular immune defenses.

Through these efforts we discovered that the alphavirus capsid protein (CP) interacts with host Interleukin 1 Receptor Associated Kinase 1 (IRAK1) in order to block Toll-Like Receptor Signaling (TLR). IRAK1 is a key signaling kinase for several pro-inflammatory immune pathways and CP interacting with it provides a possible mechanism of inhibiting detection by host cells. Pursuing this interaction, we discovered that CP from several members of the *Alphavirus* family are capable of binding IRAK1 and inhibiting IRAK1-dependent TLR signaling. We were able to map the necessary interaction determinates on CP which, when mutated, ablated IRAK1 binding and restored IRAK1-depdent signaling. Host cells infected with this mutant virus increased their expression of IFN- β *in vitro*, relative to cells infected with wild-type Sindbis virus. The mutant virus was also impaired in an *in vivo* model of infection where it failed to cause symptoms of alphavirus infection. Collectively these data show a novel interaction between alphavirus CP and host IRAK1 that allows the virus to evade the immune detection during early infection a crucial time when the virus has yet not been able to shut down host transcription and translation. This interaction was also found to be crucial for viral pathogenesis and the absence of it leaves the virus attenuated.

The data presented in this dissertation offer insight into a newly observed method *Alphavirus* uses to evade detection by the innate immune system which could be a potential target for therapeutic intervention as well as a mutant virus that could be a candidate for a live-attenuated vaccine.

TABLE OF CONTENTS

LIST OF FIGURES	ix
CHAPTER 1	1
Alphavirus Overview.....	1
Genetic Organization.....	4
Overview of Viral Lifecycle	6
Nonstructural Proteins.....	10
Structural Proteins.....	14
Arthritic Infection Mouse Models	19
Encephalitic Infection Mouse Models	21
Evasion of Innate Immune Response.....	23
CHAPTER 2	26
Toll-Like Receptor Overview	26
TLR Structure, Trafficking, and Maturation / Activation	28
The Functional Detection of PAMPs by TLRs	30
Signaling Pathways	33
NF- κ B Signaling During TLR Signaling	36
Interferon Expression and Signaling After TLR Activation.....	37
Toll-Like Receptors in Alphavirus Infections.....	39
Rationale	42
CHAPTER 3	44
Introduction	44
Materials and Methods	47
Results	62
Discussion.....	91

Conclusions.....	101
CHAPTER 4	102
Synopsis.....	102
Introduction	103
Methods	107
Results	120
Discussion.....	149
CHAPTER 5	157
Research Summary.....	157
Mechanism of Action	160
IRAK1 Interaction Conservation	161
IRAK1 Role in IL-1 Signaling.....	165
Capsid:IRAK1 in Non-permissive Cells	166
Capsid:IRAK1 as Therapeutic Target.....	166
Capsid:IRAK1 as a Live-Attenuated Vaccine Candidate	167
RII as an Anti-inflammatory	169
Future Directions	170
REFERENCES	176
GLOSSARY.....	225
CURRICULUM VITAE	231

LIST OF FIGURES

Figure 1.1- Schematic of the Genomic Organization of Alphaviruses.....	5
Figure 1.2- The <i>Alphavirus</i> Lifecycle	7
Figure 2.1- TLR Signaling.....	34
Figure 3.1- The Identification of the Host–Pathogen Interactions of the SINV Capsid Protein	64
Figure 3.2- Ontological Analysis of the SINV CP–Protein Interactants Reveals Novel Host–Pathogen Interfaces	68
Figure 3.3- The CP–IRAK1 Interaction Is Genuine, and Widely Conserved across the Genus <i>Alphavirus</i>	73
Figure 3.4- The SINV Capsid Protein Inhibits IRAK1-Dependent Signaling in a Specific Manner.....	77
Figure 3.5- Old-World Alphavirus Capsid Proteins Inhibit IRAK1-Dependent TLR7 Signaling.....	80
Figure 3.6- The SINV Infection Inhibits IRAK1-Dependent TLR Signaling	84
Figure 3.7- The SINV Capsid Protein Delivered by Incoming Infectious and Non- Infectious Particles Is Sufficient to Inhibit IRAK1-Dependent TLR Signaling	88

Figure 3.8- A Diagram of the Roles of the Nucleocapsid Components Early during Infection	99
Figure 4.1- Functional Mapping of Capsid to IRAK1 Interaction	124
Figure 4.2- Functional Analysis of Different Capsid Fragments to Block IRAK1 Related Signaling	127
Figure 4.3 RI and Protease Domain are Incapable of Repressing TLR Activity	128
Figure 4.4 Deletion of RII Ablates the IRAK1 Interaction Without Disrupting Viral Replication.....	131
Figure 4.5 Mutation of the Leading 15 Amino Acids of RII Ablates TLR Repression	132
Figure 4.6- <i>In Vivo</i> infections of SINV.ΔRII Shows Attenuation of the Virus	135
Figure 4.7- Intracranial Infections with SINV.ΔRII Cause a Less Severe Disease Than SINV.WT	139
Figure 4.8- RNAseq of Intracranial Infected Brains 3dpi.....	141
Figure 4.9 Down Regulated Biological Processes from Intracranial Infected Mice	143
Figure 4.10- C57BL/6 Mice Derived Macrophages Showed Increased IFN-β Induction in SINV.ΔRII Infections.....	147
Figure 4.11- Proposed Model for SINV CP:IRAK1 Interaction.....	150

Figure 5.1- Conservation of RI and RII Regions Across Several Arthritogenic
Alphavirus Members.....164

CHAPTER 1

ALPHAVIRUS INTRODUCTION

Alphavirus Overview

Alphavirus is a positive-sense RNA genus of viruses in the *Togaviridae* family; they are spread through various mosquito species, including members of the *Aedes* and *Culex* genera [1]. Alphaviruses are distributed globally and were originally classified as either Old World or New World based on their geographic location. Due to climate change increasing the habitable zones of vector mosquitos and increases in global travel, more immunologically naïve populations are at an increased risk of being exposed to *Alphavirus* infections. This geographic redistribution has also resulted in the classic Old World and New World divisions falling out of favor as a naming convention, and it has largely been replaced by groupings based on the disease they cause, with alphaviruses being either the arthritic alphaviruses or encephalitic alphaviruses. For the past century, there have been large-scale outbreaks of alphaviruses every decade, with each outbreak infecting thousands of people, with each outbreak resulting in a severe burden of disease [2-4]. To date, there are no effective antiviral treatments or vaccines available, which limits therapeutic intervention causing a drastic need for a better understanding of the molecular interactions that alphaviruses use to promote pathogenesis to help identify targets for therapeutic intervention.

Arthritic alphaviruses include members such as Sindbis virus (SINV), Chikungunya virus (CHIKV), Semliki Forest virus (SFV), and Ross River virus (RRV). These alphaviruses tend to cause febrile arthritis in patients along with headaches, rash, and myalgia [5-8]. The percentage of patients who present clinical disease can vary, CHIKV has shown a range of 3.8%-27.7% asymptomatic cases, while RRV has been shown to have a rate of 50% asymptomatic cases[9, 10]. While mortality for these viruses is low, the morbidity is uncharacteristically high for an RNA virus, and up to 60% of patients experience prolonged arthritis that can range from a few months to up to 3 years after clearance of the virus [11]. This creates a large economic burden on households that are dependent on manual labor for financial support [12, 13]. CHIKV has been classified as an emerging virus and Mayaro virus infections are rising in South America, and along with seasonal outbreaks of SINV and RRV the arthritic alphaviruses are a growing threat to public health [10, 14-21].

Encephalitic alphaviruses include Venezuelan Equine Encephalitis virus (VEE), Eastern Equine Encephalitis virus (EEE), and Western Equine Encephalitis virus (WEE). Clinically these are rarer than the arthritic members with less than 5% of EEEV infections presenting in encephalitis and 0.1% WEEV of infections presenting encephalitis[22, 23]. Similar to the arthritogenic alphaviruses, the encephalitic alphaviruses can cause fever, headaches, and rashes, but the potential for the development of clinical viral encephalitis gives them a higher mortality rate with a range of 40-70% of symptomatic patients dying of infection [24-27]. Approximately 80% of patients that do survive clinical *Alphavirus* induced

encephalitis end up with lifelong cognitive impairments and require assistance in living or significant physical and mental rehabilitation during recovery [28].

As alphaviruses are transmitted through mosquito vectors, they are classified as arthropod-borne viruses (arbovirus). The transmission cycle of alphaviruses begins when a mosquito takes a blood meal from an infected vertebrate. Upon uptake into the mosquito, the virus arrives in the mosquito's midgut where it must replicate in midgut epithelia and neuroepithelia to escape out of the midgut and into the hemolymph [29, 30]. Once in the hemolymph, the virus can spread to secondary tissues throughout the body, with the most important being the salivary glands. Once infection of the salivary glands is established, the virus can be spread the next time the mosquito takes a blood meal [29]. It has been shown to take a week for virus to escape into the salivary glands and replicate to levels where it will be infectious upon the mosquito's next blood meal [31]. When an infected mosquito takes a blood meal from a vertebrate, the virus is released from the salivary glands into the site of infection. This also releases salivary proteins from the mosquito which has been shown to multiple effects to potentiate viral infection including, retaining virus in the site of infection, inhibiting the innate immune response, as well as loosening the endothelial barrier of the capillaries [32-35]. From there, local cells such as fibroblasts, dendritic cells, and keratinocytes become infected [36]. Following localized infection, the tissue-resident macrophages, such as Langerhans cells, become infected and migrate to the draining lymph nodes. This allows the virus to escape into the blood [37, 38]. Once viremic, the secondary site of infection is dependent on the type of

alphavirus, but generally arthritic members track to muscle cells and cells associated with joints, while the encephalitic members migrate to the brain through both antegrade transport of peripheral neurons and caveola-mediated transcytosis of the blood-brain barrier [39-43]. Once disseminated to secondary sites of infection the alphaviruses begin to replicate in the local cells of the target tissue and produce the pathogenesis associated with their respective diseases. While normally large vertebrates like humans have been a dead-end host for viral transmission, more recent outbreaks have shown a potential for alphaviruses to adapt to the human environment and become transmissible to uninfected mosquito vectors during a blood meal taken from an infected human [3].

Genetic Organization

Alphaviruses have a genome of ~11.5kb with a 5' cap and 3' poly A tail [44-46]. From the genomic RNA, the nonstructural proteins are translated and early during infection the polyprotein P123 and nsP4 form a complex to generate negative-sense RNA from the genomic template strand (Fig 1.1) [44]. This negative-sense strand is then used by the replication complex to generate more genomic RNA. Later during infection, the P123 polyprotein is fully cleaved into nsP1, 2, and 3 which along with nsP4 form a replication complex responsible for the production of genomic and sub-genomic RNA from the negative-stranded RNA synthesized earlier. The sub-genomic RNA is responsible for encoding the structural proteins.

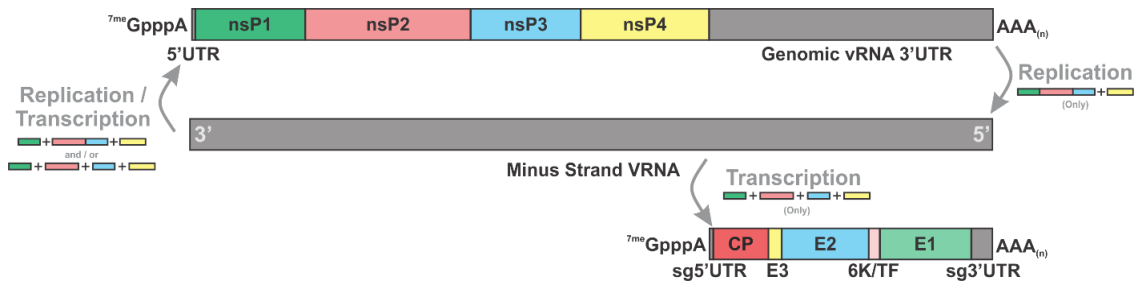


Figure 1.1- Schematic of the Genomic Organization of Alphaviruses

A schematic of the alphaviral RNAs with the Genomic RNA on top, the minus TNA in the middle, and the subgenomic RNA on bottom. The replication complex necessary for generation of each strand of RNA is depicted on the side by showing the cleavage stage of P123. Colors coordinate to the genomic map with nsP1 being green, nsP2 pink, nsP3 light blue, and nsP4 yellow.

Overview of Viral Lifecycle

An *Alphavirus* particle is ~70nm in size, and on the outside of the viral envelope are 80 trimers of the E1/E2 glycoprotein heterodimer for a total of 240 copies of the E1 and E2 glycoproteins[47-50]. The glycoproteins are inserted in a host-derived membrane layer and attached to a nucleocapsid core (NC) composed of 240 copies of capsid protein (CP) that holds a single copy of the genomic RNA. While the minimal infectious unit of the viral particle is the viral RNA, all viral components contribute towards infectivity and are essential to viral infection.

The first step of the viral life cycle is receptor-mediated endocytosis (Fig, 1.2 [51]). On the surface of the *Alphavirus* virion, there are trimer complexes of the E1 and E2 glycoproteins. E1 begins by binding to attachment factors such as heparin sulfate, then E2 is responsible for binding to a variety of receptors dependent on the individual *Alphavirus* species including proteins like Mxra8, Laminin receptor, VLDLR, and ApoER2 [52-54]. Once attached to a receptor the virus is internalized by clathrin-mediated endocytosis to an endosome [55, 56]. From the early endosome to late endosome transition, there is membrane fusion mediated by E1 forming pores facilitated by the lowering pH of the maturing endosome[57-59]. Once the E1 pore is formed in the endosomal membrane this allows for the exchange of protons and various ions such as Na⁺, K⁺, and Ca²⁺ [60, 61]. The fusion of the membranes allows for the release of the NC from the endosome and the proton exchange causes an area of low pH around the endosome thought to help initiate NC disassembly [62].

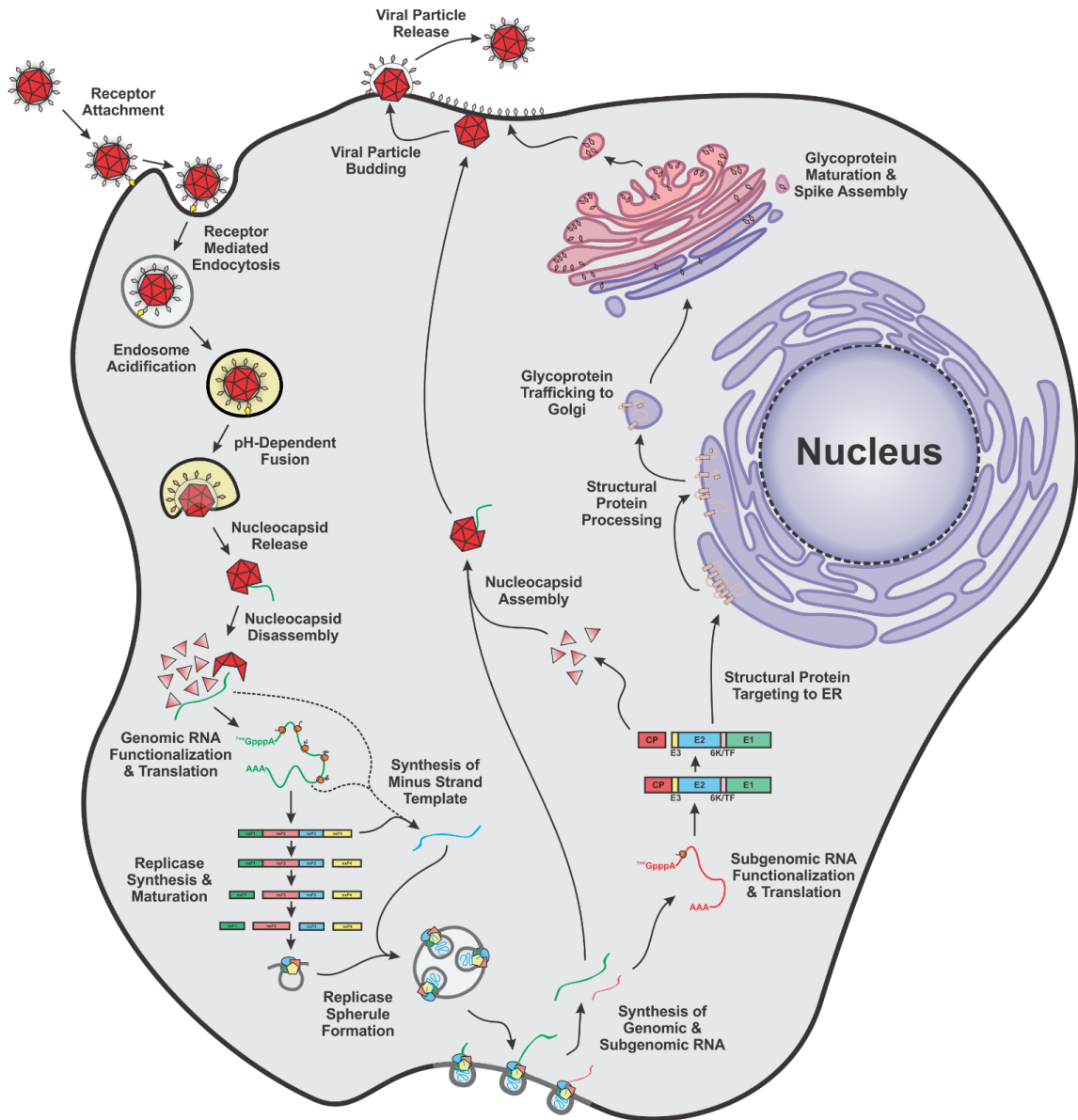


Figure 1.2- The *Alphavirus* Lifecycle

A Schematic of the *Alphavirus* lifecycle depicting major events including, endocytosis, nucleocapsid disassembly, viral replication, particle assembly and budding¹.

¹ Figure adapted from Westcott et. al *Dancing with the Devil: A Review of the Importance of Host RNA-Binding Proteins to Alphaviral RNAs during Infection* Viruses 2023 volume 15 no. 1

After the nucleocapsid core reaches the cytosol the CP of the nucleocapsid core interacts with 60s ribosomal RNAs, this facilitates the release of the genomic RNA into the cytosol [63]. As alphaviruses are positive-sense RNA viruses, once the viral genome is released into the cytosol, it can be directly picked up by ribosomes and begin the translation of viral nonstructural gene products. Early in infection, the non-structural proteins (nsP) are produced from the viral genome to form the viral replicase complex. The first three non-structural proteins, nsP1, nsP2, and nsP3, are formed as a polyprotein named P123 [64]. The nsP2 protein has protease activity it uses to sequentially cleave nsP1 and nsP3 from P123 making three independent proteins [65]. The RNA-dependent RNA-Polymerase, nsP4 is then translated and along with either P123, or the four individual nsPs, nsP4 forms the replication complex. The replicase complex P123 + nsP4 is responsible for production of negative sense RNA; and once P123 is processed into individual nsP the replication complex of nsP1, nsP2, nsP3, and nsP4 is responsible for production of genomic and sub-genomic RNA.

The later stages of cellular infection starts to see the production of a second positive-sense RNA, the sub-genomic RNA, which is co-linear with the genomic RNA and is comprised of the sequence of the 3' end of the genomic RNA. The sub-genomic RNA is responsible for the translation of the structural proteins, CP, E3, E2, 6K/TF, and E1. Much like the nonstructural polyprotein P123, the structural proteins are translated as a polyprotein consisting of all structural proteins except for TF which is only translated from a transcriptional frame shift resulting in a truncated protein product lacking E1 [66]. The nascent polyprotein is cleaved by a

protease domain in CP which frees the CP leaving it in the cytosol so that the remaining polyprotein can be trafficked to the endoplasmic reticulum (ER) for the expression and maturation of the glycoproteins [44]. While in the ER glycoproteins E2 and E1 form heterodimers and undergo post-translational modifications including glycosylation and palmitoylation before being trafficked to the Golgi and ultimately to the cell membrane where the E1/E2 dimers trimerize and form functional *Alphavirus* glycoproteins ready for budding into a new viral particle [66-68]. Once the glycoproteins are on the cell membrane the encapsidated viral RNA genome can bind to the cytosolic tail of E2 and buds out as a new viral particle [69-71].

Current approaches for antivirals towards alphaviruses have focused heavily on targeting the nsPs and halting viral replication with nucleosides. While there are still no approved antivirals for use against alphaviruses there have been promising candidates that are still being evaluated for efficacy in restricting *Alphavirus* infection. The nsP2 and 4 are prime targets for their roles in helicase activity and RNA polymerase and have shown have their functionality limited by drugs such as sofosbuvir and ML336 [72-74].

Nonstructural Proteins

The nsP1 Protein

As mentioned above, nsP1 is originally translated as part of the polyprotein P123. The role of nsP1 is to act as the capping enzyme for the RNA strands being produced by the replication complex. It possesses a guanylyltransferase domain and a methyltransferase domain that work to attach a Type-0 7meGppA cap structure to the 5' end of both genomic and sub-genomic RNA [65]. It has been shown that not every strand of the viral RNA is capped by nsP1, and that these noncapped RNAs play a role in infection and are somehow necessary for pathogenesis [75-78].

The nsP1 protein also has been shown to associate with lipid membranes initially via an amphipathic helix structure, and later via palmitoylation, and functions as the pore for the replication spherule [79]. Replication spherules can be found at either the cell membrane or ER depending on the species of *Alphavirus*. To form the spherule twelve nsP1 form a ring structure, and are then, at specific cysteine residues, palmitoylated to allow for a strong attachment to the lipid membrane [80, 81]. The spherule allows for an isolated site that allows the small molecules necessary for RNA synthesis to enter but prevents dsRNA sensor proteins from detecting the dsRNA replication intermediates. Recent cryo-electron microscopy and X-ray crystallography has shown the stoichiometry of the spherule complex as 12:1:1 of nsP1 to nsP2 and nsP4 indicating that while there are 12 nsP1s in a spherule only one of them is associated with nsP2 and nsP4 for replication [82].

The nsP2 Protein

The nsP2 protein has a variety of functions attributed to it, each of which are critical to alphaviral replication and infection. As previously mentioned, nsP2 contains a protease domain in its C-terminus and is responsible for the cleavage and maturation of P123 into the individual nsP1, 2, and 3 proteins [83]. Cleavage of nsP1 from 2 can be done in cis fashion but the cleavage of 3 from 2 can only be done in trans fashion causing a temporal regulation of how quickly the nsP 1, 2, 3, 4 replicase can be formed [84]. The protease domain has been shown to be crucial for viral replication as enzymatically inactive nsP2 results in an attenuated virus unable to have viral RNA synthesis [85]. The N-terminal domain of the nsP2 protein exhibits helicase activity necessary for unwinding RNA secondary structures formed during replication [86]. The N-terminus also contains a triphosphatase motif responsible for the removal of a phosphate group from the 5' end making an RNA diphosphate able to interact with and be capped by nsP1 [87].

Outside of replication, nsP2 has also been shown to play a pivotal role in host shutdown mechanisms for arthritic alphaviruses [88]. The nsP2 of these viruses contains a nuclear localization signal (NLS) and ~50% of all produced nsP2 can be found in the nucleus. Once translocated to the nucleus, nsP2 degrades RPB1, an essential subunit of RNA Polymerase II [89]. This prevents RNA synthesis resulting in the loss of host gene transcription. SINV with the P726G mutation in nsP2 lacks host translational shutdown, and as a result limits cellular death and viral replication as the host is able to continue macromolecular synthesis

[90]. This mutant SINV has become invaluable in studying the *Alphavirus* lifecycle and molecular interactions with host proteins due to the lack of cytotoxicity.

The nsP3 Protein

While the other nsPs of alphaviruses have been well studied and comprehensively defined, the nsp3 protein has until very recently been more poorly described. It has been shown to be necessary for the production of negative-strand RNA as well as sub-genomic RNA, however the precise role(s) it plays during replication are enigmatic. The nsP3 contains three domains, the macro domain (Macro), the alphavirus-unique or zinc-binding domain (AUD), and the hypervariable domain (HVD) [65]. The C-terminus of nsP3 contains a degradation signal that regulates the steady-state expression level of the protein. The exact purpose of this signal is unknown, but it is hypothesized to be used to regulate the stoichiometry of nsP expression during replication [91]. The macro domain is a conserved domain across the alphaviruses and has a de-ADP-ribosylation activity that converts ADP-ribose¹-phosphate to ADP-ribose [92, 93]. ADP-ribosylation has been implicated to be a component of the antiviral response suggesting nsP3 plays a role in innate immune evasion [94, 95]. The AUD contains four cysteine residues that are absolutely conserved and have been shown to house a zinc ion [96]. Mutants in the AUD have shown defects in early RNA synthesis suggesting it plays a role in negative-strand production [97-99]. The HVD as the name suggests is highly variable across alphaviruses but it does contain common features and is thought to be an area of binding to host factors [100, 101].

The HVD gives nsP3 a unique property not seen in the other nsPs which is the capacity to undergo hyper-phosphorylation[101, 102]. Phosphorylation mutants have shown slightly different phenotypes depending on the viral species; for instance, for SINV and CHIKV phosphorylation was shown to be necessary for full virulence and replication, while in VEEV phosphorylation had limited effects on mammalian tissue culture replication but was impaired in invertebrate tissue culture [98, 103]. The HVD has also been shown to be a platform for the recruitment of host factors, including G3BP and FXR, which are essential proteins in initiating stress granule formation [91, 104-106]. These are essential interactions for alphaviruses and contribute to host shutdown mechanisms that enable viral replication and evasion of the innate immune response by disrupting cytoplasmic RNA granule function.

The nsP4 Protein

The nsP4 protein is the RNA-dependent RNA-Polymerase (RdRp) responsible for the reading of template RNA and synthesis for genomic, sub-genomic, and negative-sense RNA. The C-terminus is conserved with other RdRps found throughout all RNA viruses [107, 108]. Where it begins to differ is in the N-terminus which is thought to interact with nsP1 and help assemble the replication complex necessary for nsP4 functionality [82]. There is a tyrosine residue present in the N-terminus that makes nsP4 less stable, but mutation of this residue leads to lower production of RNA leaving its function unclear [109]. The nsP4 protein is also responsible for the poly-adenylation of the 3' end of positive-

sense RNA and lacks any proofreading activity leading to a high mutation rate[65, 110].

Structural Proteins

The Capsid Protein

The CP is a multifunctional protein but is most often recognized as being responsible for housing the genomic RNA in the virus particle as part of the nucleocapsid core. The *Alphavirus* CP is unique compared to other RNA virus capsids, in that it lacks the beta-sheet jelly roll confirmation typically found in positive-sense RNA viruses. Instead, structurally the CP resembles the host chymotrypsin serine protease, HtrA [111].

In a mature viral particle, there are 240 copies of CP arranged in a T=4 configuration giving the NC an icosahedral shape. Structurally, the CP can be divided into three domains, the N-terminus contains Region I (RI) and Region II (RII), and the C-terminus the Protease domain (Pro). It is the Pro domain, which spans amino acids 114-263, that gives CP its chymotrypsin-like structure as well as the proteolytic activity necessary to cleave itself off from the nascent structural polyprotein. While the Pro domain remains catalytically active prior to cleavage, the act of cleaving CP from pE2 leaves a tryptophan residue in the active site preventing any further proteolytic activity after release [112, 113]. The Pro domain is also responsible for forming the face of NC and for the interaction with E1 during particle assembly.

While the Pro domain is well conserved and structured, the remaining two domains, R1 and RII, are highly disorganized and at the amino acid level are poorly conserved across the *Alphavirus* genus. While the sequences for these two regions might not be strictly conserved, there is a general trend of a high local concentration of basic charged amino acids that is conserved across the genus. The RI domain, which spans amino acids 1-80, is responsible for the dimerization of CP during NC assembly in addition to associating with the cargo RNA via the phosphodiester backbone; and the RII domain, which spans residues 81-113, is responsible for RNA specificity and ensuring that genomic RNA is incorporated into NC [114-117]. The RII domain is also important for initiating viral gene expression, as it binds to the S60 rRNA of the host ribosome and recruits it to the site of incoming viral RNA [63, 118, 119]. For the encephalitic alphaviruses, the RII also contains an NLS used to import CP to the nuclear pore where it clogs nuclear trafficking and prevents the export of host mRNA [120]. This is a major contributor to the host shutdown mechanisms of encephalitic alphaviruses.

While CP structural roles including, viral assembly, budding, and genomic release, have been well documented, there has been neglect in the identification and studying of non-assembly roles that CP may play during infection, with the notable exception of encephalitic CP clogging nuclear pores as a mechanism of interfering with host gene expression. There is a growing body of evidence that CP is necessary throughout the viral lifecycle to help stabilize genomic RNA, as well as limit host immune detection. In a previous study by Sokoloski et al., non-assembly-related CP binding sites on genomic RNA were mutated and as a result,

the viral RNA had a lower half-life suggesting that CP plays a role in protecting viral RNA from host RNase pathways [121]. A study by Landers et al. (included here as chapter 3) performed an exploratory screen of potential CP host protein interactions which revealed the potential for CP to interact with various immune sensing and RNA degradation pathways suggesting that CP has a variety of functions outside of its primary role in viral structure. The potential roles of CP in enabling pathogenesis and how it contributes to the viral life cycle will be the focus of this dissertation.

The Glycoproteins

As mentioned earlier, the structural proteins are produced as a polyprotein from the sub-genomic RNA synthesized during late infection. The structural proteins are translated in the order of CP-pE2-6K/TF-E1 and the nascent CP contains a protease domain and cleaves itself from the growing polyprotein, as discussed above. Once CP is free from the structural polyprotein an N-terminal translocation signal on pE2 (the precursor to E2 and E3) is exposed and directs the growing protein to the ER [122, 123]. Once in the ER, the maturation process begins to produce the functional glycoproteins necessary for virus particle formation.

To begin the maturation of the remaining structural proteins, signal peptidases cleave sites present in 6K and E1 proteins leading to the cleavage of them away from pE2. E1 then forms a heterodimer complex with pE2 where the

E3 protein domain serves to stabilize the E1/E2 dimer during folding and maturation [124]. Once processed in the ER pE2/E1 complex is trafficked into the Golgi where furin protease cleaves E3 from E2 leaving a mature E1/E2 heterodimer that then migrates from the Golgi to the plasma membrane where it forms into a trimer of E1/E2 heterodimers and awaits a NC to attach and begin the budding process to form a new viral particle [125-127].

The E2 protein, as stated earlier, is the glycoprotein necessary for binding to a host cell receptor for viral uptake and can be divided into domains A, B, and C [128, 129]. Domains A and C contain a loop and are responsible for the dimerization with E1's fusion peptide. Domain B contains the receptor binding domain. Domain C is also the site of interaction with E3 during the pE2/E1 stage of glycoprotein maturation and for some alphaviruses the E3 protein may remain bound to this E2 domain after cleavage. The intracytoplasmic tail of E2 located at the C-terminus of the C-terminal domain is also important for interacting with a hydrophobic pocket found on the surface of NC which allows the glycoproteins and NC to bind and form in correct morphology with 240 copies of CP bound to 80 E1/E2 trimers.

The E1 glycoprotein, similar to E2, is divided into three domains but these are named I, II, and III, based on their distance from the N-terminus [128, 130]. The major function of E1 is to mediate membrane fusion after the virus has been taken up by the cell during receptor mediated endocytosis. Once the endosome acidifies the drop in pH causes E1 to dissociate from E2 and form an E1 homotrimer which simultaneously causes a fusion loop in domain II to be exposed

[131]. This conformation change brings the envelope membrane in reach of the endosome membrane to begin fusion allowing for the release of the NC into the cytosol. Domains I and III help align and direct the functions of domain II.

6K/TF

The 6K protein, as the name suggests, is a 6 kDa protein produced from the sub-genomic RNA. Mutations and deletions in 6K result in a variety of phenotypes, ranging from no differences in viral assembly to defects in glycoprotein maturation and virus budding depending on the virus used, as well as the particular cell culture model [132-134]. Altogether these data suggest that 6K has a variable amount of importance depending on the viral species as well as the host species. The 6K protein has also been shown to be a viroporin with cation-selective ion channel properties in overexpression experiments [135, 136]. These ion channels are thought to play a role in virus budding.

In addition to the abovementioned structural proteins there is an alternate protein called TF that is translated from a frameshift mutation in the 6K protein which results in a new stop codon before E1 can be produced [66]. The consequences of the stoichiometric difference in E1 and E2 production that occurs because of this is currently unknown, but the U6A codon motif that results in TF translation is absolutely conserved across the genus, indicating that it is crucial for the viral life cycle [68, 137]. The exact frequency in which TF is translated over 6K is uncertain but it's thought to be around 30%; however, the empirical rates tend

to vary amongst the alphaviral species [66]. The TF protein retains the viroporin properties of 6K and much of the protein is found in the ER, suggesting it could have a role in ion transfer in the ER during infection, a property not uncommon in viruses. It has also been shown that palmitoylation of TF is necessary to inhibit Type I Interferon (IFN) response as well as translocate TF to the plasma membrane [135, 136, 138].

Arthritic Infection Mouse Models

As mentioned earlier, alphaviruses can be divided based on the disease that manifests clinically during infection. The arthritic members such as SINV, SFV, and RRV can readily be modeled in vivo with mouse infections. To properly model the natural route of infection, mice are often inoculated with the virus in a rear footpad to mimic a mosquito bite. From the inoculation site, local fibroblast and macrophages become infected, resulting in the formation of measurable viremia ~24 hours post-infection as the virus spreads to various tissues including muscle and joint associated cells. From here pathogenesis begins and symptoms such as arthritis, tenosynovitis, and myositis start to appear. For an adult, immunocompetent mouse, symptoms begin to manifest 2-7 days post-infection (dpi) and persist for about 2 weeks post-infection [139, 140]. While the virus is cleared after those 2 weeks of primary acute infection, measurable amounts of viral RNA can be detected for up to 16 weeks post-infection in the joints [39, 141, 142]. While adult mice can recover from infection, neonatal mice succumb to lethal encephalitis regardless of the *Alphavirus* being tested; and the phenotypic

differences between the model systems are thought to be a result of neonates having a less developed immune system [143].

Arthritis caused in these models is driven by the immune response but the reliance on innate or adaptive varies between viruses. A study with RRV-infected Rag^{-/-} mice, which are deficient in B and T-cells, showed normal disease progression as wild-type (WT) mice [144]. On the other hand, the ablation of macrophages showed lower levels of inflammation resulting in less disease and tissue damage. In contrast, CHIKV infections of Rag^{-/-} mice as well as CD8 depleted mice showed a decrease in the amount of swelling and inflammation compared to a WT mouse infection [145]. Interestingly, while these mice did show lower levels of pathogenesis, they also have an increased viral burden as well as persistent viremia suggesting that while the adaptive immune system is responsible for some of the pathogenesis it is also necessary for efficient clearance of the virus.

Complement-mediated cell death, as well as antibody-dependent enhancement (ADE), have been shown to play a role in the development of pathogenic inflammation in RRV infections [146-148]. C3 is an essential protein in the complement system, and C3^{-/-} mice showed reduced signs of disease and tissue damage. Further studies showed that C3 contribution to inflammation is not related to an increase in the recruitment of macrophage or Natural Killer cells, but instead stimulates the activation of these cells through S100A9, S100A8, and IL-6. As mentioned earlier, one of the first steps to *Alphavirus* pathogenesis is to infect macrophages and in cases of reinfection, if sub-neutralizing levels of antibodies

are produced the antibodies will contribute to disease by increasing the virus uptake into macrophages by the Fcγ receptor to exacerbate disease. Collectively these data show that while the immune system plays a crucial role in the clearance of alphaviruses it is also exploited by the virus in several ways to contribute to pathogenesis and disease outcome.

Encephalitic Infection Mouse Models

While encephalitic models of infection exist using EEV, VEEV, etc. certain specific strains of SINV, such as AR86, are neurotropic in mouse models and are used as a robust model for mimicking encephalitic infections in a research setting. The use of the AR86 strain of SINV affords a greater level of biosafety, and a more robust molecular toolkit, relative to the other encephalitic alphaviruses. Like the arthritic infection, modeling encephalitic infection can be achieved through a rear foot pad injection on a mouse to simulate a mosquito bite. In addition, an intracranial injection model can be utilized where the virus is directly injected into the brain bypassing the need to become viremic and migrate into the brain if the virus is attenuated outside of the Central Nervous System (CNS). Footpad injection of neurotropic SINV in 4-week-old C57BL/6 mice follows a path of replication similar to that previously described for the arthritogenic infection, in that footpad then 1dpi measurable viremia occurs for ~24 hours. While viremic, the virus spreads to secondary tissues like quadricep muscles, lymph nodes, and finally the brain. The virus is in measurable amounts in the brain by 3-5 dpi, and mice succumb to infection in ~6 dpi [149]. Once in the brain observable clinical

symptoms include weakened grip strength, partial limb paralysis, or full limb paralysis. For intracranial injections, symptoms begin to show at 1 dpi and peak at 3 dpi with mice surviving for ~4 dpi. Much like arthritic mouse models the age of the mouse plays a role in these disease outcomes, neonatal mice to mice of 4 weeks old will succumb to infection [150]. At about 5 to 6 weeks of age mice infected with neurotropic SINV will still exhibit illness and have some measurable clinical symptoms, but they will recover from infection. This is due to neurons maturing and having higher levels of antiapoptotic factors as well as innate immune factors such as Bcl-2 and, IRF3 and 7, respectively [151-153].

Once in the brain, the primary cells infected by alphaviruses are the neurons. Replication occurs largely in the hippocampus and anterior horn of the spinal cord [154, 155]. This results in inflammation and encephalitis that leads to paralysis of one or more limbs. Viral-induced apoptosis is responsible for inflammation and is the main driver of tissue damage from infection. It has been shown that SINV-induced apoptosis is through caspase-mediated pathways, and that Bcl-2 and Bax overexpression inhibits this apoptosis and limits cellular death in tissue culture but does not prevent death of spinal cord motor neurons or limp paralysis suggesting these phenotypes have other contributing factors [156]. Apoptosis of the infected neurons leads to the release of pathogen-associated molecular patterns (PAMPs) and damage-associated molecular patterns (DAMPs). The release of PAMPs and DAMPs signals to the immune system and causes an influx of macrophages and T-cells to the brain. It is thought that these

cells become overstimulated and cause excessive damage to neuronal tissue further contributing to pathogenesis and neurological symptoms [156, 157].

Viral clearance from the brain happens in a nonlytic fashion and is driven by IFN γ produced by T-Cells in a JAK/STAT-dependent manner as well as antibody neutralization and clearance [158, 159]. Due to viral RNA persistence, antibodies are of extra importance as they ensure if any reactivation is to occur the newly generated virus can be rapidly neutralized [151, 159, 160]. Autophagy has also been shown to play a role in the nonlytic clearance of viruses from neurons [161]. The cellular adaptor protein p62 can bind to CHIKV CP and target it for autophagosomes presumably resulting in the limiting of viral particle assembly [162].

Evasion of Innate Immune Response

As alphaviruses are sensitive to Interferon Response Genes (ISGs), they must have mechanisms to either prevent the induction of ISGs or limit the ISG's ability to interact with viral components and inhibit replication / pathogenesis. The classic model by which this is accomplished is via the various ways alphaviruses shut down host transcription and translation. The primary mechanisms for this, as discussed above, include in arthritic virus nsP2 proteins translocating to the nucleus and causing degradation of the RNA Polymerase II subunit RBP1, and the CP from encephalitic viruses localizing to the nucleus to clog nuclear pores and preventing trafficking of mRNA from the nucleus. In addition to shutting off host

transcription, CHIKV nsP2 has been shown to inhibit JAK/STAT signaling which limits the induction of Type I and II IFNs [163]. While these methods work and help prevent ISG response they all rely on viral gene expression that is only found later during infection. This leaves an opening during early infection before viral gene expression that the host cell can recognize and respond to invaded viruses.

In addition to the prevention of host gene expression late during infection, cytoplasmic RNA bodies are targeted by the alphaviruses. Stress granules are formed during infections as a response to the phosphorylation of eIF2 α triggered by the unfolded protein response from an ER and the detection of dsRNA by PKR [164]. This prevents the translation of both viral and host proteins and results in cytoplasmic granules containing mRNA, initiation factors, and other mRNA-associated proteins thus sequestering the components necessary for translation. Alphaviruses prevent stress granule formation by nsP3 through two major methods, the first is the HVD of nsP3 binds to and sequesters G3BP1/2, critical factors for the initiation of stress granule formation [104]. The second method is through the Macro ADP-ribosylhydrolase activity which causes the disassembly of stress granules and aggregated proteins [92]. These functions work together to release the translation machinery back into the cytosol allowing for the continuation of viral gene product synthesis.

During structural gene synthesis, there is a high concentration of unfolded glycoproteins in the ER which triggers the Unfolded Protein Response (UPR). UPR leads to the activation of dsRNA-dependent protein kinase (PKR)- like ER kinase (PERK) to phosphorylate eIF2 α , this prevents eIF2 α from being recycled to an

active state bound to GTP necessary for translation [164]. The goal of this is to limit the amount of protein synthesis and thus lower the amount of stress in the ER while it folds host proteins; the loss of eIF2 α function also serves to limit the translation of viral proteins [165]. The UPR does not impact structural gene translation due to a hairpin loop in the sub-genomic RNA that stalls the ribosome on the start codon to help initiate translation.

So, while alphaviruses remain sensitive to ISGs the mechanism necessary to effectively translate them in response to infection gets shut down through a mixture of host and virus-derived pathways. There remains the question of how during early stages of infection before viral gene replication has had a chance to shut down the innate immune response, how do alphaviruses prevent detection by the innate immune system? A potential candidate for this could be the CP, as it is present in the cytosol after viral RNA the virus wouldn't have to wait for gene expression for CP to block the cytosolic sensors used to detection pathogens which will be discussed in the following chapter.

CHAPTER 2

TOLL-LIKE RECEPTOR INTRODUCTION

Toll-Like Receptor Overview

The Toll-Like Receptors (TLRs) are a family of Pathogen Recognition Receptors (PRRs). Their role is to bind to a wide array of pathogen-associated molecular patterns (PAMPs) to signal the initiation of an immune response to a microbial pathogen. In the specific contexts of a viral infection, they can respond to the presence of viral proteins or genetic materials and instigate the transcription of Type I IFNs leading the establishment of an antiviral state. TLRs can be found expressed on a wide variety of cells in various tissues but their highest expression is on antigen-presenting cells such as Dendritic cells and Macrophages, as well as B-cells; once an IFN response has been triggered neighboring cells start upregulating their TLR expression profiles as part of the establishment of an IFN-dependent antiviral state [166].

The innate immune system is composed of a variety of PRRs that can be divided by their subcellular localization as either cytosolic or membrane bound on internal and external faces of the cellular membranes. The cytosolic receptors include the RIG-I Like Receptors and Nod-like receptors that bind to intracellular RNAs that exhibit PAMPs such as 5' triphosphate moieties and branched dsRNAs, as well as the Aim-2 and cGAS receptors that bind to extra-nuclear DNA [167].

Importantly, due to their cytosolic localization these PRRs are unable to sample the extracellular environment to institute an innate immune response prior to infection. The TLR family of PRRs are membrane-bound and can be further divided into plasma membrane-associated (TLR 1, 2, 4-6, and 10) and endosome-associated TLRs (TLR 3, 7-9). Individually the TLRs are specific for certain types of PAMPs, but as a family they can respond to a wide arrange of PAMPs including, proteins, saccharides, lipids, and nucleic acids. This makes the TLRs a diverse and crucial group for the detection of foreign pathogens including, bacteria, fungi, and importantly viruses. Moreover, as the TLRs sense pathogens in an extracellular manner they enable host cells to respond to pathogens such as viruses prior to viral infection and replication.

The TLRs were the first PRRs discovered and as such are the most well-described and understood. Their functionality is highly conserved, with similar protein motifs being found in bacteria and plants, indicating that TLRs are an evolutionarily ancient system by which hosts may recognize and respond to foreign entities and pathogens [168-172]. The first identification of a TLR family member came from efforts examining the immune responses of *Drosophila*, where a protein named Toll, originally shown to play a role in embryonic development, was discovered to induce NF- κ B activation when a secreted protein named Spätzle (Spz) bound to the receptor as a ligand[173-175]. In the insect Toll system, PAMP detection and the subsequent response are separated by Spz proprotein activation by one or more cellular proteases. The Spz proprotein is cleaved extracellularly in response to various pathogens, and afterwards the proteolytically cleaved Spz

fragment binds to the extracellular domain of Toll to activate Pelle, the invertebrate homolog of IRAK1, which phosphorylates NF- κ B. As the name suggests, the vertebrate Toll-Like receptor is similar to Toll, but as the TLRs have continued to evolve along with vertebrates, the TLRs have lost their role in embryonic development. A major difference between the invertebrate and vertebrate orthologs is that vertebrate TLRs do not rely on Spz as a ligand to bind to TLRs for activation, and instead they can directly interact with PAMPs to initiate signaling.

TLR Structure, Trafficking, and Maturation / Activation

Structurally, the TLRs consist of three domains, first an extracellular Leucine Rich Repeat (LRR) ectodomain that functions to interact with PAMPs; second, a single-pass transmembrane domain which anchors the protein into a membrane; and finally, a cytoplasmic Toll/IL-1 receptor (TIR) domain that is responsible for the induction of a signaling cascade after ligand binding. Upon binding of a PAMP to the LRR, the TLR will form either a homodimer or heterodimer which brings their cytosolic TIR domains in range of each other to begin activation of a signaling cascade that recruits a TIR contain protein[176]. TIR-containing proteins involved in TLR signaling, and their functions are discussed below. The exact TIR proteins associated with the TLR TIR domains depend on the specific TLRs, as most have MyD88-related proteins with the notable exception of TLR3 having TRIF-related TIR proteins, and TLR4 having MyD88 or TRIF depending on location.

As TLRs are membrane bound, they are synthesized in the ER where TLRs destined for the endosome (TLRs, 3, 7, 8, and 9) bind to UNC93B1 for regulation and transport, although there is some evidence that suggests UNC93B1 could also be used by plasma membrane-associated TLRs like TLR5 [177, 178]. While in the ER, TLR folding is coordinated by heat shock proteins Glycoprotein 96 (gp96), and Protein Associated with TLR4 A (PRAT4A) [179, 180]. These chaperone proteins have been shown to play a role in the folding of all TLRs, except for TLR3. Once folded in the ER, the TLRs are then sorted out into Coat Protein complex II (COPII)-coated vesicles by various adapter proteins (AP) including AP1, 2, 3, and 4 [177, 181, 182]. The specific AP is thought to be dependent on the TLR; notably, UNC93B1 stays bound to the TLR and accompanies it to the Golgi apparatus. TLR7 has been shown to interact with AP4 and is directly trafficked to the Golgi from the ER; in contrast, TLR9 interacts with AP2 through UNC93B1's N-terminal region and is first trafficked to the plasma membrane before making its way to the Golgi [177]. Once in the Golgi, UNC93B1 ubiquitinates the TLR cytosolic tail marking it for endosomal packaging. Up to this point, the TLRs have been inactive and have not had a chance to accidentally respond to host RNA, but once in the endosome a combination of asparagine endopeptidase as well as cathepsins B, S, H, L, and K cleave part of the LRR domain leading to the activation the TLR [183-186]. At this time the mature TLR can form its final hetero- or homodimer conformation. Trafficking for TLR3 and TLR8 is not as well studied or understood as TLR7 and TLR9 but there is some evidence for TLR3 that once it enters the

Golgi, Tripartite motif-containing protein 3 (TRIM3) an E3 ligase, polyubiquitinates TLR3 marking it for ESCRT proteins to take it to endosomes [187].

The Functional Detection of PAMPs by TLRs

PAMPs and danger-associated molecular patterns (DAMPs) are the ligands that bind PRRs to initiate immune response signaling. As the name suggests PAMPs are derived from pathogens and tend to be molecular structures or patterns not found endogenously in host cells. PAMPs can include, lipopeptides, peptidoglycans, glycoproteins, lipopolysaccharides, as well as RNA and DNA. DAMPs on the other hand are derived from host cells that are damaged, they can be extracellular or intracellular derived proteins such as heparan sulfate or heat shock proteins. While PAMPs enable the detection of microbial pathogens, DAMPs allow a way for damaged or stressed cells to signal to others to initiate inflammation. Despite being categorically different from PAMPs, DAMPs bind to TLRs and similarly signal through TIR domains as PAMPs do.

To date there are 13 described mammalian TLRs with humans having 10 (TLR1-10) and mice having 12 (TLR1-9 & 11-13); with each TLR responding to a certain class of molecule with some overlaps creating redundancies in the TLR system; specific TLR ligands are detailed out in Table 2.1. To properly function, TLRs form a homodimer, or a heterodimer with a different TLR, and the nature and the type of TLRs involved in the dimerization can influence the PAMP that the receptor detects. As described earlier, the TLRs differ in regard to their membrane

localizations, as TLRs 1, 2, 4-6, and 10 are plasma membrane-associated, while 3 and 7-9, as well as the mouse TLRs 11-13, are endosomal-associated. While some plasma membrane-associated TLRs have been shown to respond to viral PAMPs, such as TLR4 responding to respiratory syncytial virus or TLR 2 to measles virus, cytomegalovirus, and herpes simplex virus through TLR engagement with their viral envelope glycoproteins, alphaviruses have only been shown to be detected by endosomal TLRs and as such these TLRs will be the primary focus of the remainder of this chapter[188-191].

TLR	PAMP	Source	Reference
TLR 1/2	Triacyl lipopeptides	Bacteria	[192]
TLR2	β -Glucan	Fungi	[193]
	Envelope Glycoproteins	Viruses	[194]
	Lipoproteins	Various	[195]
	Peptidoglycan	Bacteria	[196]
	Porins	Bacteria	[197]
	Zymosan	Fungi	[198]
TLR 2/6	Diacylted lipopeptides	Bacteria	[199]
	Lipoteichoic acid	Bacteria	[200]
	Glycoproteins	Viruses	[201]
TLR 3	Double-Stranded RNA	Viruses	[202]
	Poly(I:C)	Synthetic	[203]
TLR 4	Envelope Glycoproteins	Viruses	[188]
	Lipopolysaccharide	Bacteria	[204]
TLR 5	Flagellin	Bacteria	[205]
TLR 7	Single-stranded RNA	Viruses	[206]
TLR 8	Single-stranded RNA	Viruses	[206]
TLR 9	Unmethylated CpG DNA	Bacteria & Viruses	[206]
TLR 10	Unknown		

Table 2.1 TLR and their agonist A list of TLRs, the PAMP they respond to, and the source(s) for those PAMPs

Signaling Pathways

The signaling pathways for TLRs can be divided into two categories, Myeloid differentiation factor 88 (MyD88)-dependent and TIR-domain containing adaptor molecule (TRIF)-dependent. All TLRs except for TLR3 signal through the MyD88-dependent pathway; but there is also the notable exception that TLR4 can signal through both MyD88 and TRIF. A diagrammatic figure of TLR activation and signaling consequences can be found in Fig. 2.1.

To signal through these pathways, a complex of TIR-containing proteins must form on the TLRs' cytosolic tail; five known proteins act as TLR adapters, MyD88, TRIF, MyD88-adaptor like (MAL) also called TIR domain-containing adaptor protein (TIRAP), TRIF-related adaptor molecule (TRAM), and sterile α - and armadillo-motif-containing protein (SARM). Upon ligand binding to the receptor, one of these TIR-containing proteins will bind to the cytoplasmic tail of TLR and start to form a complex of proteins. The TIR domain of the TLR's tail is the determinant of which proteins will bind and which signaling pathways are ultimately used. For both pathways, SARM has been shown to act as a negative regulator [207, 208].

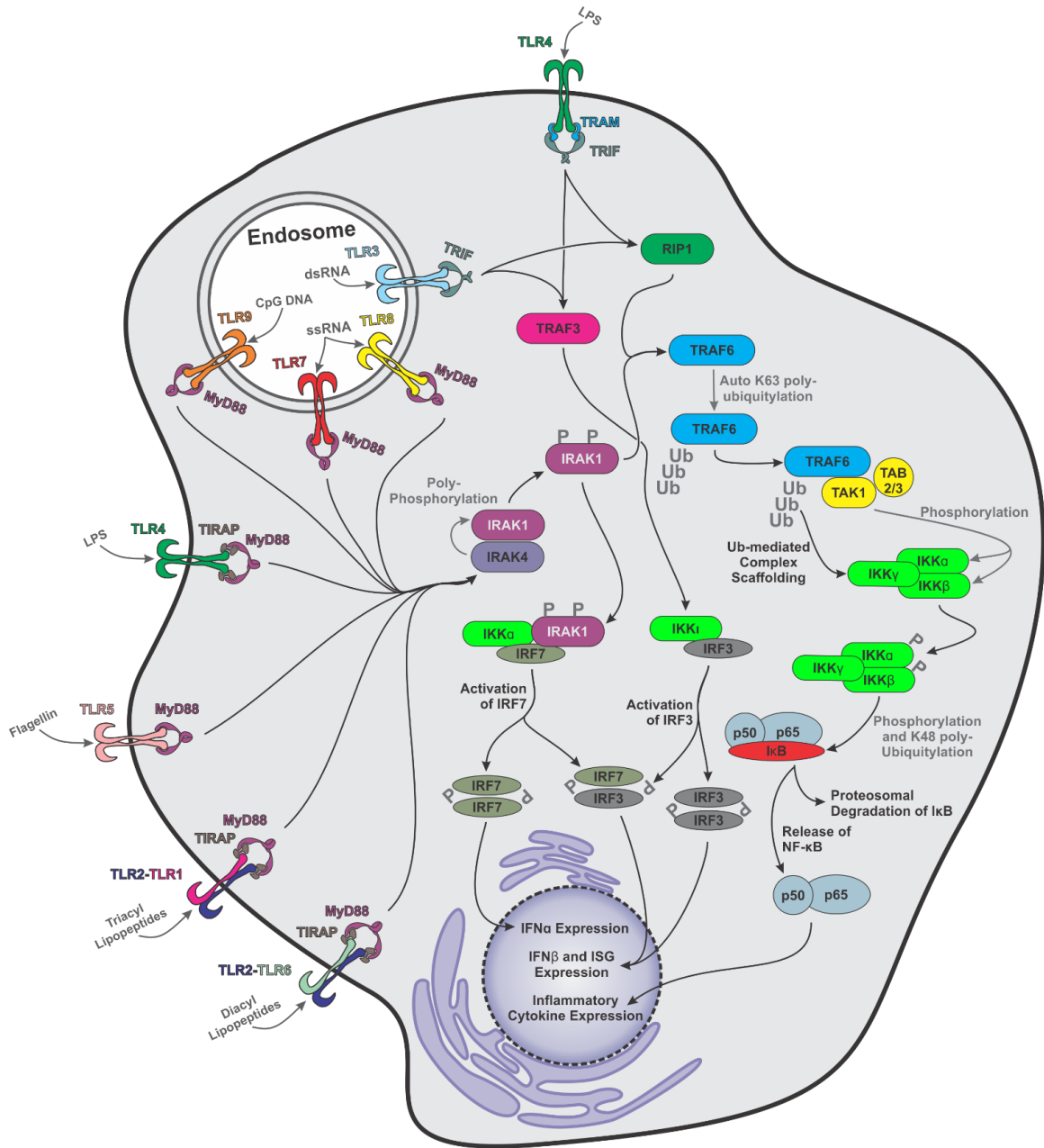


Figure 2.1- TLR Signaling

TLR localization and signaling through either MyD88 dependent pathways or TRIF dependent pathways and the associated activation of NF-κB, IRF7 or IF3. Individual proteins are labeled, as are known post-translational consequences of specific interactions.

MyD88-Dependent

As stated earlier, all TLRs except for TLR3 signal through the MyD88-dependent pathways. Upon binding to a ligand, the TIR domain recruits MyD88 to form a complex around the cytosolic tail called the Myddosome. Exceptions to this process include TLRs 2, 4, and 9, which first require MAL to bind to the TLR TIR endodomain before Myd88 can bind [209]. TIR domains present in both the TLR and MyD88 proteins mediate the interaction. On the basis of the available structural and biochemical evidence, it is thought that in total six copies of Myd88 come together when forming the Myddosome, with two copies bound the TIR domains from the TLR protein dimer, and then four more in a ring-like structure below those bound directly to the TIR domains[210]. On the Death Domain (DD) of Myd88 allows for the recruitment and interaction of another essential protein component of the Myddosome, the IL-1 receptor-associated kinase (IRAK) 4 protein. The complete Myddosome contains four copies of IRAK4, each interacting with the DD of a different MyD88 protein. As the name suggests IRAK4 is a kinase and is responsible for the phosphorylation of, IRAK1 during TLR signaling [211]. Upon recruitment to the Myddosome IRAK1 is first phosphorylated by IRAK4, this allows a series of autophosphorylation event resulting in conformational changes to fully activate IRAK1. Upon hyperphosphorylation, IRAK1 is released from the Myddosome into the cytosol where it can bind to tumor necrosis factor receptor-associated factor 6 (TRAF6) or IFN-regulatory factor 7 (IRF7) [212-214]. TRAF6 and IRF7 activate nuclear factor κ B (NF- κ B) and Type I IFN response, respectively, as is discussed in greater detail below.

TRIF-dependent

The other signaling cascade utilized by TLRs is the TRIF pathway. As stated previously, this is the only pathway that TLR3 can utilize, which is due to a mutation in the TIR domain binding loop that precludes MyD88 binding [215]. Upon TLR binding to a ligand, TRIF is recruited to the TIR domains of the cytosolic tail of TLR3; but for TLR4 to signal through TRIF first TRAM must bind to the TIR domain and serve as a bridge for the connection of TLR4 and TRIF [216]. Similar to MyD88-dependent signaling, the end goal for TRIF-dependent signaling is the activation of NF- κ B and IFN transcription factors, although in this case IRF3 is the targeted transcription factor instead of IRF7. To activate these pathways, TRIF recruits and activates TRAF3 and TRAF6[217-219].

NF- κ B Signaling During TLR Signaling

NF- κ B signaling can be broken down into canonical and noncanonical pathways. The canonical pathway plays a role in signaling for inflammation and immune responses, while the noncanonical pathway plays a role in B- and T-cell maturation and survival as well as lymphoid tissue development [220]. As TLRs activate the canonical pathway, that is what will be discussed in depth here.

TRAF6 is the factor responsible for the activation of NF- κ B for both the MyD88-dependent as well as TRIF-dependent TLR responses. Upon activation, TRAF6 polyubiquitinates itself at K63 by way of its E3 ubiquitin ligase domain [204,

221]. This ubiquitination event provides scaffolding for the assembly of the kinase complex necessary for activating NF- κ B. Specifically, the polyubiquitination of TRAF6 causes the recruitment of TGF-beta Activated Kinase (TAB2) which allows transforming growth factor beta-activated kinase 1 (TAK1) to be recruited and clustered together to initiate autophosphorylation [222, 223]. Once activated, TAK1 can phosphorylate the I κ B kinase (IKK) complex. IKK is composed of three subunits, IKK α , IKK β , and IKK γ (which is also referred to as NF- κ B essential modulator [NEMO]) [224-226]. IKK γ has no intrinsic catalytic function, but it can interact with the K63 polyubiquitin chain on TRAF6 putting IKK in the proximity of TAK1. Both IKK α and IKK β are phosphorylated by TAK1, but it has been shown that IKK β plays a more crucial role in the canonical NF- κ B pathway [227]. Once activated IKK can phosphorylate I κ B at two serine residues which causes ubiquitin tagging for degradation of the protein by the proteasome. Once I κ B is degraded, it releases the two subunits of NF- κ B, p50, and p65 (sometimes referred to as RelA) which were previously sequestered in the cytosol by I κ B. The newly freed NF- κ B protein complex is then able to translocate to the nucleus where it serves as a transcription factor for the stimulation of proinflammatory cytokine and chemokine expression.

Interferon Expression and Signaling After TLR Activation

The type-I IFNs (IFN α and IFN β) produced by the TLRs after PAMP detection serve as the innate immune system's primary response to viral infection. Type-I IFNs signal for the transcription of a wide array (>350) of IFN stimulated

gene (ISG) products which function to instill an antiviral state by inhibiting viral entry, replication, and escape [228]. A major advantage of the IFN system is that an infected cell that produces type-I IFN secretes it into its surroundings, allowing for neighboring cells to begin a protective ISG response before they get infected to help limit viral spread. This antiviral state means that viral infections must find a way to overcome type-I IFN signaling or prevent it from happening.

As stated above, TLRs activate expression of IFN through the work of transcription factors IRF7 and IRF3, which drive transcription of IFN and a small subset of ISGs. After PAMP detection, IRF7 is phosphorylated by IRAK1 from the MyD88-dependent TLRs [214]. IRF3 is phosphorylated by TANK binding kinase 1 (TBK1) and IKK ϵ , two kinases related to IKK [229]. TRAF associated NF- κ B activator (TANK) is recruited to the polyubiquitinated TRAF and serves as a platform for TBK1 and IKK ϵ where they are activated and able to phosphorylate IRF3.

Once phosphorylated, IRF3 and IRF7 can form homo- or heterodimers (if both active IRF3 and IR7 are present) and translocate to the nucleus where they bind to an interferon-sensitive response element (ISRE) promoter region to initiate the transcription of the Type I IFNs, IFN α and IFN β . These IFNs are secreted out of the cell where they can be picked up by IFN α receptor (IFNAR) to activate the JAK/STAT signaling pathway. Janus Kinase (JAK) is a family of kinases consisting of JAK 1, 2, 3, and TYK1. JAK1 and TYK1 can be found on the cytosolic tail of IFNAR, and upon ligand binding to the receptor, they undergo autophosphorylation. This activates them to phosphorylate the transcription factor,

signal transducer and activator of transcription (STAT) [230]. There are seven members of the STAT family, STAT 1, 2, 3, 4, 5A, 5B, and 6; and STAT1 and STAT2 are activated in response to Type I IFN stimulation and form a heterodimer once phosphorylated by JAK. STAT2 is constitutively associated with IRF9 and remains associated after phosphorylation and dimerization with STAT1. The IRF9 protein is what allows the STAT complex to bind to an ISRE and begin the transcription of ISGs to elicit an antiviral response [231, 232].

Toll-Like Receptors in Alphavirus Infections

As positive-sense RNA viruses, alphaviruses are capable of being readily identified by TLRs 7 and 8, and as they produce dsRNA during replication, like all RNA viruses, they can also be susceptible to TLR3 once viral replication has begun. Thus far alphaviruses have not been shown to trigger TLRs 2 or 4 so the body of work that has been done examining how alphaviruses are impacted by TLRs has focused on TLRs 3 and 7 in vertebrates.

With neurotropic SINV strains it has been shown that MyD88 and TLR7 are completely dispensable in regard to the host response to infection, as their absence results in no differences in mortality or viral burdens of infected mice. This same study also looked at the impact of TRIF mediated signaling, and showed that in the absence of TRIF, there was an increase in mortality but no significant changes to viral titers were measured in the brain or spinal cord. This suggests that TLR3 plays a role in controlling the disease, but not necessarily controlling

replication, and that TLR7 and MyD88 were not natively controlling SINV infection [233].

An earlier study where human bronchial epithelial cells were treated with polyinosinic acid: polycytidylic acid (Poly(I:C)), a known agonist of TLR3, one hour before infection with CHIKV showed an increase in IFN α and β production as well as the antiviral factors OAS, MxA, and APOBEC3G, negatively impacting CHIKV infection. Specifically, it was also observed that in Poly(I:C)-treated cells the development of cytopathic effect was delayed out to 48 hours, and viral RNA replication was lowered up to 72 hours during CHIKV infection [234]. These data show that alphaviruses can be susceptible to TLR3 signaling; however, these efforts stopped short of identifying whether TLR3 PAMPs were formed during infection, as priming of the pathway with exogenous Poly(I:C) was performed before infection.

Another study examining CHIKV infection showed that MyD88^{-/-} and TRIF^{-/-} mice suffered from increased viremia when compared to WT mice. But when they quantitatively assessed footpad swelling, a robust readout for joint-associated inflammation, the footpad swelling of MyD88^{-/-} mice was comparable to that of WT mice. In contrast, TRIF^{-/-} mice showed significantly more pronounced swelling relative to wild type mice. This observation led to the conclusion that while MyD88 signaling does seem to contribute to the immune response to CHIKV, TLR3/TRIF-related signaling was more important in terms of TLR PAMP detection [235].

A study with RRV showed that TLR7 was necessary to fight infection and that MyD88^{-/-} or TLR7^{-/-} mice exhibited exacerbated disease progression, severity,

increased tissue damage, and difficulties clearing the virus compared to WT mouse infections. Interestingly, inflammatory cell recruitment between TLR7^{-/-} and WT-infected mice showed no significant differences for innate immune cells, but a slight but significant difference in T-cell recruitment, suggesting that for RRV the TLR response is important later in infection when the adaptive immune response is starting to be activated [236].

Collectively the literature on the TLR response to alphaviruses shows a complex story that won't have one universal answer for all TLRs, or alphavirus, in terms of importance for controlling the infection. Regardless, as the impact of the TLRs is largely blunted across all alphaviral species, it is likely that all have some mechanism by which the potential impacts and consequences of the TLRs on alphaviral infection is mitigated. The variety in reported phenotypes suggests that there is something that has likely differentially evolved in alphaviruses, perhaps making some better than others for blocking either MyD88- or TRIF-dependent TLR responses. As our knowledge of alphavirus/TLR interactions grows and more is learned about which viruses inhibit which TLRs, there could be patterns to emerge as to which groups of alphaviruses or more dependent on inhibiting different TLRs.

Rationale

Like most viruses, alphaviruses are extremely susceptible to the effects of IFN and the ISGs produced from the innate immune response, and as such they must have methods to evade or prevent their induction during infection. Classically it has been thought that shutdown of host transcription and translation is responsible for preventing the induction IFN expression and the expression of ISGs. But as host macromolecular shutdown is something that doesn't start until later stages of infection, and is entirely dependent on viral gene expression, there remains a window during early infection when the virus is susceptible to PRRs inducing an IFN response. One of the classes of PRRs that can work early in infection are the TLRs, which as described earlier have been shown to have a mixed importance to controlling and clearing alphaviruses. This suggests that some alphaviruses have a method to limit or prevent PAMP detection by TLRs before viral gene expression has begun. Furthermore, if viral gene expression is required to blunt the host response to infection, host cells which are exposed to viral PAMPs, but not actively undergoing viral gene expression, are freely able to elicit a controlling innate immune response thereby limiting infection. As alphaviruses can readily replicate in immunocompetent hosts, there must be an additional evasion mechanism that is yet undescribed.

Looking at the viral lifecycle from a molecular perspective reveals what viral components are present within a cell from the early stages of infection. These viral particle components are the solitary copy of the viral genomic RNA, and 240 copies of the CP from the disassembled NC. From this, we hypothesized that CP could be

interacting with component(s) of the TLR signaling pathways preventing signaling and enabling the virus to remain undetected until later viral gene expression can shut down host transcription/translation.

To test this hypothesis we utilized a novel protein:protein interaction discovery method that utilizes a biotin ligase to tag protein interactants for purification and identification. From this, we found that IRAK1, a key kinase in MyD88-dependent TLR signaling interacted with several CPs from the *Alphavirus* genus (Chapter 3). Following this we were able to identify the necessary interacting domain on CP for the CP:IRAK1 and create a mutant virus with the CP:IRAK1 interaction ablated. This deficient IRAK1 interaction virus when infected in C57BL/6 mice showed no clinical symptoms of disease as well as failure to disseminate from the site of infection indicating that the CP:IRAK1 interaction is crucial for pathogenesis and the evasion of the innate immune response. The mutant virus also showed a robust activation of IFN- β when macrophages were infected (Chapter 4). Altogether, these data give insight into early infection host-pathogen interactions and how alphaviruses evade the immune system before they shut down host cellular processes in highly permissive cells. Furthermore, as this interaction is crucial for pathogenesis, it represents a potential mechanism to target for therapeutic interventions or vaccine developments.

CHAPTER 3

THE ALPHAVIRAL CAPSID PROTEIN INHIBITS IRAK1-DEPENDENT TLR SIGNALING²

Introduction

Alphaviruses are positive-sense RNA viruses which are primarily spread via vector-competent mosquito species [44]. Collectively, and often on a seasonal basis, the members of genus *Alphavirus* are responsible for local, regional, and global outbreaks of clinically severe illness [17, 237-248]. Alphaviruses may be broadly classified via their predominant symptomology as either arthritogenic or encephalitic. Arthritogenic alphaviruses, such as Sindbis virus (SINV; the prototypic alphavirus), Ross River virus (RRV), Semliki Forest virus (SFV), and Chikungunya virus (CHIKV), exhibit low mortality despite often causing febrile illness with debilitating multifocal arthritis [6, 8, 11, 14-16, 18, 249, 250]. In some instances, the multifocal arthritis may persist for several months to years past the resolution of the primary infection [6-8, 15, 251, 252]. In contrast to arthritogenic alphaviruses, encephalitic alphaviruses can exhibit significant mortality and life-altering neurological sequelae, primarily in young children and adolescents [22,

² This chapter adapted from work previously published in *Viruses* 2021, Volume 13, no. 3 with the same title under a Creative Commons Attribution (CC BY). Landers, V D. et al. *The Alphaviral Capsid Protein Inhibits IRAK1-Dependent TLR Signaling*. *Viruses* 2021 13(3)

24, 25, 253]. Despite the clear impact of alphaviruses on global human health and quality of life in developing and developed communities alike, there are no clinically proven antiviral therapeutics, or safe and effective vaccines to mitigate the public health threat posed by alphaviruses.

An infectious alphaviral particle is relatively simple in design. Measuring approximately 70 nm in diameter, an alphavirus particle features an RNA cargo surrounded by two concentric icosahedral protein layers divided by a host-derived lipid envelope [128, 254]. The viral glycoproteins E1 and E2 (and in some instances E3) are ordered in an icosahedral array projecting from the external surface of the viral envelope [128, 254]. Several copies of the viral 6K and TF proteins, precisely how many is unknown at this point, are associated with the viral envelope [137, 255]. The C-terminal endodomain of the E2 protein interacts with the viral capsid (CP) protein, which also forms an icosahedral structure which is symmetrically aligned with the viral glycoprotein spikes. The CP protein is the sole viral protein component of the nucleocapsid core and is the most abundant viral protein in the mature viral particle [44]. The alphaviral entry pathway initiates with the interaction of the host receptor with the viral E2 glycoprotein, resulting in the endocytosis of the viral particle, and culminates with the delivery of the nucleocapsid core to the host cytoplasm [44]. The nucleocapsid core then rapidly disassembles, releasing the CP protein from the viral genomic RNA, the latter of which interacts with host factors to engage the translational machinery to initiate the synthesis of the viral replicase complex.

While still becoming better understood at the molecular level, the fate of genomic RNA is straightforward. In contrast, despite being the predominant viral component released to the host cytoplasm, the role of the viral CP protein after entry is less understood. Prior work by the Sokoloski lab identified a series of non-assembly CP–RNA (naCP–RNA) interactions which functioned during the early stages of viral infection [121]. The disruption of the naCP–RNA interactions negatively impacted viral particle infectivity, which correlated with decreased viral RNA stability in cellular models of infection [121]. Collectively, these data led us to hypothesize that the alphaviral CP proteins which are delivered as part of the nucleocapsid core may function to influence the host cell environment after disassembly. We further postulated that the molecular activities of the CP protein are dependent on the formation of host–pathogen protein–protein interactions which impart new functionality to the CP protein complex, or disrupt the activities of the normal cellular protein complexes.

The above overarching hypotheses, and the absence of a comprehensive analysis of the alphaviral CP protein–protein interaction data in the knowledgebase, led us to examine the protein–protein interactions of the SINV CP protein using an innovative approach. Here we detail the use of an adapted BioID approach to identify the putative host–pathogen interactions of the SINV CP protein [256, 257]. This discovery approach led to the identification and validation of a novel alphaviral host–pathogen interaction—the interaction of the alphaviral CP protein with the host IRAK1 protein. The host IRAK1 protein is a critical component of the TLR and IL-1R signal transduction pathways, and thus the CP–

IRAK1 interaction may negatively impact the detection and response to TLR and IL1R ligand binding [258, 259]. Using a robust series of state-of-the-art model systems, we assessed the impact of the CP–IRAK1 on IRAK1-dependent signaling and found that the alphaviral CP protein was capable of significantly inhibiting IRAK1-dependent TLR signaling. Importantly, the SINV CP proteins delivered from viral particles during viral entry were sufficient to mask TLR agonist detection, regardless of viral particle infectivity. Taken together, the data presented in this study significantly contribute to the field by i) using an unbiased approach to identify putative CP–protein interactions, and ii) delineating a novel mechanism by which the host innate immune response is evaded during the earliest stages of alphaviral infection prior to viral gene expression.

Materials and Methods

Tissue Culture Cells

HEK293 (ATCC CRL-1573) and BHK-21 (ATCC CCL-10) cells were cultured in Minimal Essential Media (MEM; Cellgro Mediatech, Inc, Manassas, VA USA), supplemented with 10% Fetal Bovine Serum (FBS; Corning, Corning, NY USA), 1x Penicillin/Streptomycin (Pen/Strep; Corning, Corning, NY USA), 1x Non-Essential Amino Acids (NEAA; Corning, Corning, NY USA), and l-glutamine (Corning, Corning, NY USA). HEK293-derived reporter cells, namely HEK-Blue hTLR3, HEK-Blue hTLR4, and HEK-Blue hTLR7 (Invivogen, San Diego, CA USA), were cultured in Dulbecco's Modified Eagle Medium (DMEM; Corning, Corning,

NY USA) supplemented with 4.5 g/L glucose, 10% FBS, 1× Pen/Strep, and 1× Normocin (Invivogen, San Diego, CA USA). To maintain genetic homogeneity, the HEK-Blue tissue culture cells were maintained at low passage number and supplemented with the appropriate selection antibiotics on alternating passages to maintain genomic integrity (as indicated by Invivogen's instructions per each cell line). All cell lines were cultured in humidified tissue culture incubators at 37 °C in the presence of 5.0% CO₂.

Plasmids

The vertebrate expression plasmids for the BioID2 screen were independently constructed, but based off those previously utilized by Kim et al., 2016 [256]. Specifically, the pBioID2-Only, and pSINVCP-BioID2 plasmids were generated via the Gibson Assembly of DNA fragments encoding a cMyc-tagged BioID2 biotin ligase and the CP protein from SINV (strain AR86) into the pCDNA3.1/Zeo(+) expression vector. To enhance the stability of the SINV CP-BioID2 fusion protein, the protease activity of the alphaviral CP proteins was eliminated by the mutation of an essential active residue required for protease activity [260].

The vertebrate expression plasmids utilized in the Nanoluc BiMolecular Complementation studies described here were independently constructed, but based on those previously identified by Mo et al., 2017 [261]. Briefly, the Nanoluc protein was subdivided into two complementing fragments followed by a poly-

glycine linker. N67, which consisted of the *N*-terminal 67 amino acids of the Nanoluc protein, and C67, which consists of the remaining amino acid residues, were subcloned via Gibson Assembly reactions into the vertebrate expression vector pCDNA3.1/Zeo(+). The resulting plasmids, pSplit.Nanoluc.N67 and pSplit.Nanoluc.C67, were then used in further Gibson Assembly reactions to create the plasmids used in this study. Briefly, these included pSplit.Nanoluc.N67.huIRAK1, which included the full-length human IRAK1 ORF, and the pSplit.Nanoluc.C67.SINV CP; RRV CP; EEE CP; VEE CP; CHIKV CP; and YFV CP plasmids which contained the full-length ORFs of the respective alphaviral or flaviviral capsid proteins. As above, to ensure the stability of the Nanoluc fragment fusion proteins, the protease activity of the alphaviral CP proteins was eliminated by the mutation of an essential enzymatically active residue required for protease activity [260]. Control plasmids including the BiID2 ORF in lieu of either the IRAK1 or the CP proteins were generated as non-specific controls.

To express the native SINV CP protein in a context outside of SINV infection, a vertebrate expression plasmid encoding the wild-type SINV CP protein and a mCherry reporter was generated via Gibson Assembly into the pCDNA3.1/Zeo(+) vector. Specifically, the native ORFs of the SINV CP protein and E3 protein were fused to an mCherry ORF fragment to generate pEXPR.SINVCp.mCherry, which upon transfection into a cell will direct the synthesis of a CP-E3-mCherry polyprotein which is processed into CP and E3-mCherry via the native protease activity of the SINV CP protein.

All DNA fragments for the generation of the clones above were synthesized by Genscript (GenScript USA Inc., Piscataway, NJ USA) and assembled using the Gibson Assembly mastermix available from Synthetic Genomics, Inc. (Codex DNA Inc., San Diego, CA USA) according to the manufacturer's instructions. All plasmids were verified by sequencing prior to their use in these studies. Specific plasmid information, including details regarding the restriction enzymes used for their construction; antibiotic resistance markers and bacterial growth conditions; and complete plasmid sequences, are available upon direct request.

All plasmids were cultured overnight in *E. coli* DH5 α (or comparable) bacteria under antibiotic selection and purified via miniprep or midiprep purification kits (Omega Bio-Tek Inc., Norcross, GA USA). The purified plasmid DNA was phenol chloroform extracted twice to remove any trace endotoxin or bacterial proteins from the plasmid preparations.

Generation and Preparation of SINV

This study utilized p389_{P726G}, a Toto1101-derived SINV strain which encodes an EGFP reporter protein fused to the nsP3 gene [262], and a point mutation in the nsP2 protein which abrogates the inhibition of cellular transcription (P726G) [263]. The corresponding infectious clone of this SINV construct was generated via site-directed mutagenesis of the p389 infectious clone. This particular strain was chosen as it enables the rapid visual confirmation of viral infection and allows for continued cellular transcription during infections of highly

permissive tissue culture cells. Infectious viral stocks were generated via the electroporation of in vitro transcribed RNA into BHK-21 cells, as previously described [76]. Briefly, $\sim 3 \times 10^6$ BHK-21 cells were electroporated with 10 μg of in vitro transcribed RNA using a single pulse at 1.5 kV, 25 mA, and 200 Ω . After the total infection of the monolayer (as determined by EGFP signal), the tissue culture supernatants were harvested and titered to determine the number of EGFP positive focus-forming units per ml using standard plaque assays.

For the studies utilizing non-infectious SINV particles, the aforementioned SINV reporter mutant virus was inactivated via UV irradiation [77, 264]. Briefly, 1 ml of virus stock was aliquoted into one well of a 24-well plate, on ice, and irradiated by exposure to 260 nm UV light in a Stratalinker for 5 min. The virus was promptly used, and any remaining inoculum was discarded. The verification of UV inactivation was accomplished via the visualization of no EGFP signal in inoculated BHK-21 cell monolayers after 24 h of infection.

TLR Agonists and Other Receptor Ligands

All agonists and recombinant protein ligands were diluted in pyrogen-, endotoxin-, and nuclease-free phosphate-buffered saline, or distilled water, as indicated below. The reconstituted agonists/ligands were aliquoted into single-use tubes and stored at $-80\text{ }^\circ\text{C}$ until use. The HEK293 TLR3 cells used in this study were stimulated with high-molecular-weight poly(I:C) (Invivogen, San Diego, CA USA) diluted in 1x PBS. Prior to use, the poly(I:C) was heated to $75\text{ }^\circ\text{C}$ and allowed

to slow cool to room temperature to anneal the poly(I) and poly(C) RNA strands into dsRNA. The HEK293 TLR4 cells were stimulated with Kdo2-lipid A (Avanti Polar lipids) diluted in sterile nuclease free distilled water. Prior to use, the Kdo2-lipid A was sonicated to ensure a homogenous solution prior to aliquoting and storage. The HEK293 TLR7 cells were stimulated with CL307 (Invivogen, San Diego, CA USA) diluted in sterile nuclease free distilled water. All of the HEK293 cells utilized in this study expressed native levels of TNFR receptors and were naturally responsive to stimulation with recombinant hTNF α (R&D Systems Inc., Minneapolis, MN USA).

The Identification of SINV CP Protein–Protein Interactions

To identify the protein–protein interactions of the SINV CP protein, we utilized a modified method derived from the previously reported BioID screens [256, 257, 265, 266]. Per purification, approximately 2×10^6 HEK293 cells were cultured as 80% confluent monolayers under normal conditions prior to transfection with either pBioID2-Only, or pSINVCB-BioID2. Four hours after transfection, the tissue culture medium was replaced with fresh whole growth medium supplemented with 1 μ M biotin. After a 24 h labeling incubation period, the tissue culture cells were washed with 1xPBS, and whole-cell lysates were generated via the addition of Lysis Buffer (50 mM Tris, pH 7.6; 500 mM NaCl; 0.4% Sodium Dodecyl Sulfate (SDS); 1 mM DiThioThreitol (DTT); and 2.0% Triton X-100). The whole-cell lysates were vortexed and frozen to ensure complete lysis, and the lysates were stored at -80 °C until ready for further use.

To verify that the BioID2 biotin ligase was working during our discovery approach, and to confirm that the biotin labeling was specific, we assessed the whole-cell lysates using SDS-PAGE and Western Blotting techniques. Briefly, equal amounts of whole-cell lysates were resolved via 8% SDS-PAGE and blotted to PVDF membranes. The blotted proteins were then probed for protein biotinylation using streptavidin-HRP, or with anti-cMyc monoclonal antibodies to detect the individual expressed BioID2 fusion proteins.

To purify the biotinylated host proteins, the whole-cell lysates were thawed on ice prior to being vigorously vortexed and clarified via centrifugation at 16,000× *g* for 5 min. The clarified whole-cell lysates were transferred to a fresh microfuge tube and incubated with magnetic streptavidin beads for one hour at room temperature on a rotisserie mixer. After binding, the supernatant was removed and discarded, and the magnetic beads were washed 5 times to remove unbound proteins and non-specific contaminants. The bound proteins were then released from the streptavidin resin via resuspension in 6× Laemmli buffer and a 15 min incubation at 95 °C.

The eluted proteins were transferred to a fresh microfuge tube and precipitated with 100% (w/v) TriChloroacetic Acid (TCA) at a ratio of 1:4 (TCA:Sample). After vortexing, the samples were incubated on ice for 10 min to allow complete precipitation of the macromolecules in the solution. The precipitated proteins were pelleted via 5 min of centrifugation at 14,000× *g*, and the supernatant was decanted into an appropriate waste container. The protein

pellet was washed three times with ice cold acetone, and the pellet was dried by incubating the microfuge tube at 95 °C for 5 min to drive off excess acetone.

The dried samples were resuspended in a minimal volume of 200 mM triethylammonium bicarbonate solution (pH 8.5) and reduced via the addition of 25 mM DTT stock solution to a final concentration of 5 mM. The samples were incubated at 65 °C for 30 min, prior to the addition of Iodoacetamide to a final concentration of 10 mM and further incubation at room temperature in the dark for a period of 30 min. The alkylated samples were digested via the addition of 0.1 µg of mass spec grade trypsin and incubation at 37 °C for 30 min. After the primary digestion period, a second bolus of 0.1 µg of trypsin was added, and the samples were further digested overnight at 37 °C. After digestion, the samples were dried in a SpeedVac and stored at -80 °C.

The Identification of Putative SINV Capsid Interactions by Mass Spectrometry

Prior to liquid chromatography and mass spectrometry, the dried samples were dissolved in 20 µl of 2% (v/v) acetonitrile and 0.1% (v/v) formic acid, and 2 µl of each sample was analyzed further. The columns used for liquid chromatography separation were an Acclaim PepMap 100 75 µm × 2 cm, nanoViper (C18, 3 µm, 100 Å) trap, and an Acclaim PepMap RSLC 75µm × 50 cm, nanoViper (C18, 2 µm, 100 Å) separating column heated at 50 °C. An EASY-nLC 1000 UHPLC system was used with solvents A = 2% (v/v) acetonitrile/0.1% (v/v) formic acid, and B = 80% (v/v) acetonitrile/0.1% (v/v) formic acid. Following injection onto the trap, the

sample was separated with a 165 min linear gradient from 0% to 55% B at 250 nL/min, followed by a 5 min linear gradient from 55% to 95% B with a flow ramp from 250 to 300 nL/min, and lastly a 10 min wash with 95% B at 300 nL/min. A 40 mm stainless steel emitter was coupled to the outlet of the separating column. A Nanospray Flex source was used to position the end of the emitter near the ion transfer capillary of the mass spectrometer. The ion transfer capillary temperature was set at 225 °C, and the spray voltage at 1.75 kV.

An Orbitrap Elite ETD mass spectrometer was used to collect data from the LC eluate. An Nth-Order Double Play was created in Xcalibur v2.2. Scan event one obtained an FTMS MS1 scan (normal mass range, 240,000 resolution, full scan type, positive polarity, profile data type) for the range 300–2000 m/z. Scan event two obtained ITMS MS2 scans (normal mass range, rapid scan rate, centroid data type) on up to twenty peaks that had a minimum signal threshold of 5000 counts from scan event one. Either the lock mass option was enabled (0% lock mass abundance) or RAW files were recalibrated offline in Xcalibur v2.2 using the 371.101236 m/z polysiloxane peak as an internal calibrant.

Proteome Discoverer v1.4.1.14 was used to analyze the data. The 9/27/2018 version of the UniprotKB reviewed reference proteome canonical and isoform Homo sapiens sequences (Proteome ID UP000005640) concatenated with BiOLD2 and SINV capsid BiOLD2 sequences was used in the Mascot v2.5.1 and SequestHT searches. The enzyme specified was trypsin (maximum two missed cleavages with inhibition by P) with Carbamidomethyl(C) as a static modification and Oxidation(M), Biotin(K) as dynamic. Fragment tolerance was 1.0

Da (monoisotopic) and parent tolerance was 50 ppm (monoisotopic). A Target Decoy PSM Validator node was included in the Proteome Discoverer workflow.

The result files from Proteome Discoverer were loaded into Scaffold Q+S v4.4.5. Scaffold was used to calculate the false discovery rate using the Scaffold Local FDR and Protein Prophet algorithms. Peptides were accepted if the identification had a probability greater than 99.9% and a parent mass error within 10 ppm. Proteins were accepted if they had a probability greater than 99.9% and at least two peptides. Proteins were grouped into clusters to satisfy the parsimony principle.

The host proteins identified by the BioID2 approach were assigned as specific or non-specific on the basis of their relative detection in the BioID2-CP or BioID2 Control mass spectrometry data sets. To reduce the introduction of bias in the data sets, any relative peptide quantification data were disregarded, and proteins were considered duly identified if uniquely assignable peptides were detected.

Bioinformatic/Ontological Analyses of Putative SINV CP Protein–Protein Interactions

To identify whether or not the host proteins identified by the BioID2 discovery approach were subject to unintentional bias on the basis of their relative protein abundance in the host proteome, we compared the relative protein

abundances of the non-specific and SINV CP-specific data sets to the HEK293 proteome [267].

The 19 host factors identified by the SINV capsid BioID2 discovery approach as specific to the SINV CP protein were examined using the STRING analysis (version 11.0) algorithm to detect the presence of protein–protein interaction networks [268]. The parameters used to define the presence or absence of interaction networking included gene fusion, co-occurrence, experiments, databases, and text mining, and the confidence level was set to medium. The confidence/strength of interactions between individual host factors were scaled (arbitrarily by STRINGS version 11.0) and indicated via line weight between interconnected nodes, with higher weight indicating greater confidence.

In addition to the identification/visualization of interaction networks, the 19 putatively identified interactants were examined ontologically using DAVID to identify enriched cellular component, molecular function, and biological process ontological groups [269, 270]. Due to the relatively small number of host proteins in the specific group, the fold enrichment, and relative statistical significances of any identified ontological groups exhibited considerable range (as noted in the text).

The entire BioID2 data sets and ontological analyses are available as supplemental data files (see Supplemental File S1 in the accompanying supplemental materials).

Nanoluciferase-Based BiMolecular Complementation Analysis (Nanoluc BiMC)

To validate the interaction between IRAK1 and SINV CP, we utilized an innovative BiMC approach to overcome the non-specific interaction of the CP proteins with purification resins [261]. In these experiments, HEK293 cells were seeded into flat white-bottomed 96-well plates at a density of 1.25×10^4 cells per well. After an overnight incubation period, the cells were co-transfected with pSplit.Nanoluc.C67 plasmids encoding either an alphaviral CP protein or the BioID2 protein as a control, and the corresponding pSplit.Nanoluc.N67 plasmid encoding the human IRAK1 protein using Lipofectamine 3000 (Invitrogen, Thermo Fisher Scientific, Waltham, MA USA). Specific transfection conditions for the Nanoluc BiMC assay consisted of 50 ng of each expression plasmid to achieve a total of 0.1 μ g of DNA. The cells were transfected in whole growth media and incubated for a period of 48 h under normal conditions prior to the assessment of Nanoluc complementation via the quantitative detection of Nanoluc activity via live-cell NanoGlo reagents.

Briefly, to measure the levels of Nanoluc activity the growth medium was gently removed and replaced with 100 μ L of Optimem media (Thermo Fisher Scientific, Waltham, MA USA). Immediately after the addition of the Optimem media, NanoGlo live-cell assay (Promega, Madison, WI USA) reagents were prepared fresh as according to the manufacturer's instructions, and rapidly added to each well. The plate was briefly rocked by hand to ensure the Nanoglo reagent and cell culture media were well mixed prior to the detection of luminescence in a Synergy H1 microplate reader.

Quantitative Analysis of TLR, IL1R, and TNFR Signaling

Aside from the obvious differences in regards to the agonists/ligands being utilized, the overall experimental approaches used to determine the impact of the CP–IRAK1 interaction were identical. For all assays, the HEK293-derived reporter cell lines were cultured to ~75% confluence in a 96-well format in whole media lacking antibiotic selection prior to being experimentally treated and assessed as follows.

To determine the impact of the SINV CP protein on IRAK1-dependent signaling, the HEK293-derived reporter cell monolayers were transfected with expression plasmids encoding either the BioID2 control plasmid or a SINV CP-E3-mCherry fusion protein capable of producing the native full-length SINV CP protein after cleavage from the C-terminal E3-mCherry fusion protein. At 24 h post transfection, the supernatant was removed and replaced with whole growth medium supplemented with the indicated receptor agonists/ligands, and the cells were returned to the incubator for a period of 16 h. After the agonist/ligand activation period, the tissue culture supernatants were harvested and assayed as described below.

To determine the impact of SINV infection on IRAK1-dependent signaling, the HEK293-derived reporter cell monolayers were either mock infected or infected with SINV_{P726G} at an MOI of 10 PFU/cell. Twelve hours post infection, the tissue culture media was removed and replaced with fresh pre-warmed whole growth

medium supplemented with the indicated receptor agonists/ligands, and the tissue culture cells were returned to the incubator and incubated under normal conditions for a period of 16 h. After the agonist/ligand activation period, the tissue culture supernatants were harvested and assayed as below.

To determine the impact of SINV co-exposure on IRAK1-dependent signaling, we modified the above approach. Specifically, the HEK293-derived reporter cell monolayers were either mock infected or infected with SINV_{P726G} at an MOI of 10 PFU/cell in media supplemented with the aforementioned receptor agonists/ligands for a period of 1 h at 37 °C in a 5.0% CO₂ tissue culture incubator. After the co-exposure period, the treatment media was removed and the monolayers gently washed with pre-warmed whole growth medium to remove residual virus/ligand. A minimal volume of whole growth medium was added to the cell monolayers, and the cells were incubated for 16 h prior to harvesting the tissue culture supernatants for assaying.

To define whether or not SINV replication/gene expression was required for the inhibition of IRAK1-dependent signaling, the co-exposure experiment described above was performed identically with the exception that UV inactivated SINV particles were utilized. Similarly, to determine whether delivery of the nucleocapsid core to the host cytoplasm was required for the disruption of IRAK1-dependent signaling, the aforescribed co-exposure experiments utilizing infectious SINV were performed in the presence of whole growth medium supplemented with 40 μM ammonium chloride to block the final steps of the viral entry pathway by preventing acidification of the endosome.

For all of the experimental approaches described above, the harvested tissue culture supernatants were immediately quantitatively assayed for the presence of Secreted Embryonic Alkaline Phosphatase via the use of QuantiBlue detection medium (Invivogen, San Diego, CA USA). Briefly, in a sterile clear-bottomed 96-well plate, 20 μ L of cell-free tissue culture supernatant was added to 180 μ L of QuantiBlue detection reagent and the solutions were mixed by gentle pipetting. Afterwards, the 96-well plate was incubated at 37 °C in a plate reader, and absorbance readings at 620 nm were taken regularly for a period of three hours, or until the A620 nm curves of the highest agonist concentrations indicated saturation of the limit of detection. The A620 nm readings from pre-saturation time points were comparatively assessed to determine agonist/ligand detection via the level of NF κ B activation as determined by the SEAP assay colorimetric readout.

The quantitative analysis of signal transduction, as per NF κ B activation, was determined by comparing the SEAP activity of the control and experimental conditions over the agonist dose range after the subtraction of non-agonist-treated wells [271, 272]. Specifically, the control agonist treatment with the highest level of relative SEAP activity within the given dose range was standardized to 100%, and all other wells were normalized accordingly to determine their relative SEAP activity to the identified maximum observed value. The quantitative data obtained from multiple biological replicates for a given dose concentration were averaged and plotted with respect to agonist concentration. Non-linear regression analysis of the data, via GraphPad Prism 7.0.2 using the log(agonist) vs. response variable slope (four parameters) non-linear curve fit function, was used to determine the

activation profiles in response to agonist treatment, and the 95% confidence intervals of the data. In addition, the agonist concentrations at which the control and experimental treatments reached 50% maximal activity ($EC_{50_{MAX}}$) were determined using these non-linear regression calculations.

Statistical Analyses

The quantitative data reported in this study represent the means of at least 5 biological replicates from at least two independent viral stocks, or DNA plasmid preparations, as specifically indicated in the figure legends. The error bars for any given quantitative value represent the standard deviations of the means. The statistical analysis of comparative samples was accomplished using variable bootstrapping, as previously described [76]. Any p -values for a given data set were determined via one-way ANOVA analyses and reconfirmed using Student's t -test as a post hoc analysis. Bioinformatics analyses were completed using the standard analyses of the STRING analysis (version 11.0) and DAVID gene ontology informatics suites, as described in the text.

Results

The Discovery of Novel Sindbis Virus Capsid Protein–Protein Interactions

Previous work from our lab demonstrated that the SINV CP protein binds to the SINV viral genomic RNA at discrete interaction sites to accomplish non-

assembly associated roles during infection. Further characterizations indicated that when the non-assembly SINV CP–RNA interactions were disrupted the incoming genomic vRNAs had significantly decreased half-lives relative to wild-type SINV RNAs [121]. This led to the speculation that the non-assembly CP–RNA interactions were involved in the regulation of viral genomic RNA stability early during infection following the disassembly of the nucleocapsid core. Nonetheless, we postulated that the SINV CP protein was unlikely capable of directly mediating RNA stability by itself; and thus, we set out to define the extent to which the SINV CP protein engaged with host factors via protein–protein interactions.

To overcome the challenges associated with working with the alphaviral CP proteins, we adapted the BioID2 discovery approach to identify SINV CP host interactions in an unbiased manner [256, 257, 265]. In this approach, the expression of BioID2 fusion proteins in the presence of excess biotin results in the labeling of protein interactants, allowing for subsequent affinity purification and identification via mass spectrometry. As depicted in Figure 3.1A, we fused the coding region of the promiscuous BioID2 biotin ligase to the C-terminus of the SINV CP protein in a mammalian expression plasmid, thereby enabling the ectopic expression of a BioID2-CP fusion protein after the transfection of the BioID2-SINV CP expression plasmid in to HEK293 cells.

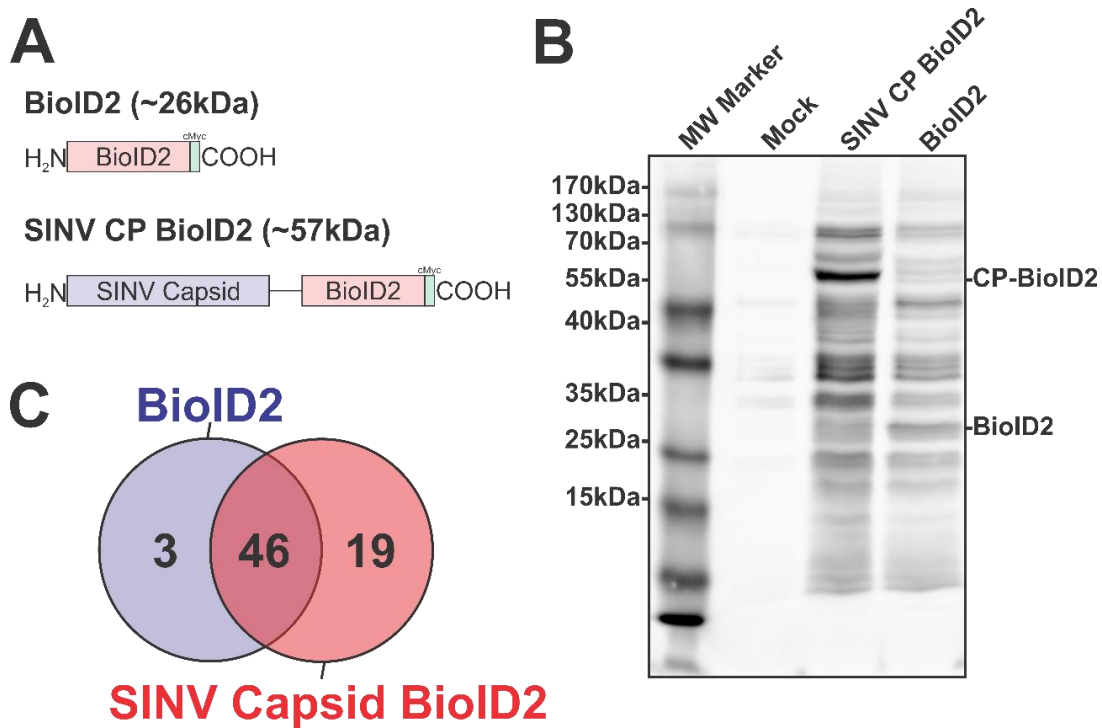


Figure 3.1- The Identification of the Host–Pathogen Interactions of the SINV Capsid Protein

(A) A diagram of the BioID2 fusion proteins expressed in 293HEK cells via plasmid transfection. Individual domains are labeled above. The line in the SINV CP BioID2 construct represents a poly-glycine linker, and the green box represents a cMyc tag. (B) A representative blot of 293HEK cell lysates after the BioID2 approach. Briefly, transfected or control transfected cells were cultured in the presence of excess biotin prior to the generation of whole-cell lysates. Equal protein amounts were resolved using SDS-PAGE, and subsequently probed for protein biotinylation using streptavidin-HRP. (C) A Venn diagram of the host proteins identified by mass spectrometry after the BioID2 approach designated the host factors as either non-specific or specific to BioID2 transfection/purification.

To test the functionality of the BioID2 biotin ligase after fusion to the SINV CP protein, whole-cell lysates were generated from HEK293 cells transfected with either the BioID2-CP or BioID2-Control expression plasmids, or mock transfected, following incubation in the presence of excess biotin. Equal amounts of whole-cell lysate were resolved via SDS-PAGE and transferred to PVDF prior to being probed for protein biotinylation using HRP-conjugated streptavidin (Figure 3.1B). As shown by the presence of readily detectable protein species in the BioID2-CP and the BioID2-Control lanes, and the relative absence of signal in the mock-treated lane, the BioID2 biotin ligase was functional when fused to the SINV CP protein. Importantly, the overall labeling patterns of the BioID2-CP and BioID2-Control lanes exhibited unique profiles relative to one another, suggesting that the fusion of the CP protein to the BioID2 biotin ligase resulted in the specific labeling of putative CP interactants. Subsequent Western blotting with anti-Myc tag monoclonal antibodies revealed that the major protein species in either BioID2-containing transfection condition were the ectopically expressed BioID2 fusion proteins themselves and confirmed that none of the other high-molecular-weight species were BioID2-CP truncation products.

As the functionality of the BioID2-CP fusion approach had been confirmed, we next wanted to identify the host factors which engaged with the SINV CP protein during BioID2-CP expression. To this end, we transfected the aforementioned BioID2 expression plasmids into HEK293 cells and generated whole-cell lysates on a preparative scale for identification of putative interactants by mass spectrometry. As briefly described above, the biotinylated protein species from

BioID2-CP and BioID2-Control whole-cell extracts were purified using streptavidin resin prior to the development of trypsin digested peptide libraries for high sensitivity mass spectrometry.

In total, the two independent BioID2-CP data sets had a total of 85 and 90 unique proteins identified; whereas the BioID2-Only control had 59 and 79 unique proteins identified. Comparative analysis of the mass spectrometric data arising from two independent BioID2-CP and BioID2-Control purifications was used to identify and assign interaction specificity to putative interactants. To ensure a high degree of rigor during the discovery approach in order to be assigned as a SINV CP protein interactant a given host protein had to be detected in both of the SINV CP data sets, and absent in either of the BioID2-Control data sets. Similarly, in order to be considered a “genuine” non-specific BioID2 interactant, a given host protein had to be reproducibly detected in both BioID2-Control data sets. As shown in Figure 1C, these comparative analyses revealed that a total of 68 proteins were assignable as identified interactants. Of these, 46 were identified as common between the BioID2-CP and BioID2-control, and 3 were present solely in the BioID2-Control samples, leaving 19 proteins unique to BioID2-CP (Figure 3.1C).

Altogether, these data confirm that the BioID2 approach represents a means by which the host–pathogen interactions of the alphaviral CP proteins may be elucidated in a manner unrestricted by cross-linking or co-translational labeling kinetics. These efforts have led to the identification of 19 putative CP–protein interactions.

Ontological Analyses Reveal Novel Host–Pathogen Interactions

While the BioID2-CP screen led to the identification of novel SINV CP protein–protein interactions, interaction discovery screens are often subject to type-I errors. To determine the likelihood of a putative interactant being from a genuine CP–protein interaction and not the simple function of protein abundance, we compared the data obtained from the control and SINV CP BioID2 purifications with the relative protein abundances of the HEK293 proteome [267]. This analysis, while not directly evidentiary, enables a qualitative assessment of purity by identifying whether or not a set of interactants (or an individual interactant) may be over-represented on the simple basis of protein abundance. As presented in Figure 3.2A, the host factors detected and assigned as specific to the SINV CP conditions generally were of lower relative protein abundance than those identified and assigned as non-specific interactants. Nonetheless, several of the SINV CP-specific host proteins were comparable to the non-specific interactants in regards to their arbitrary abundances in the proteome.

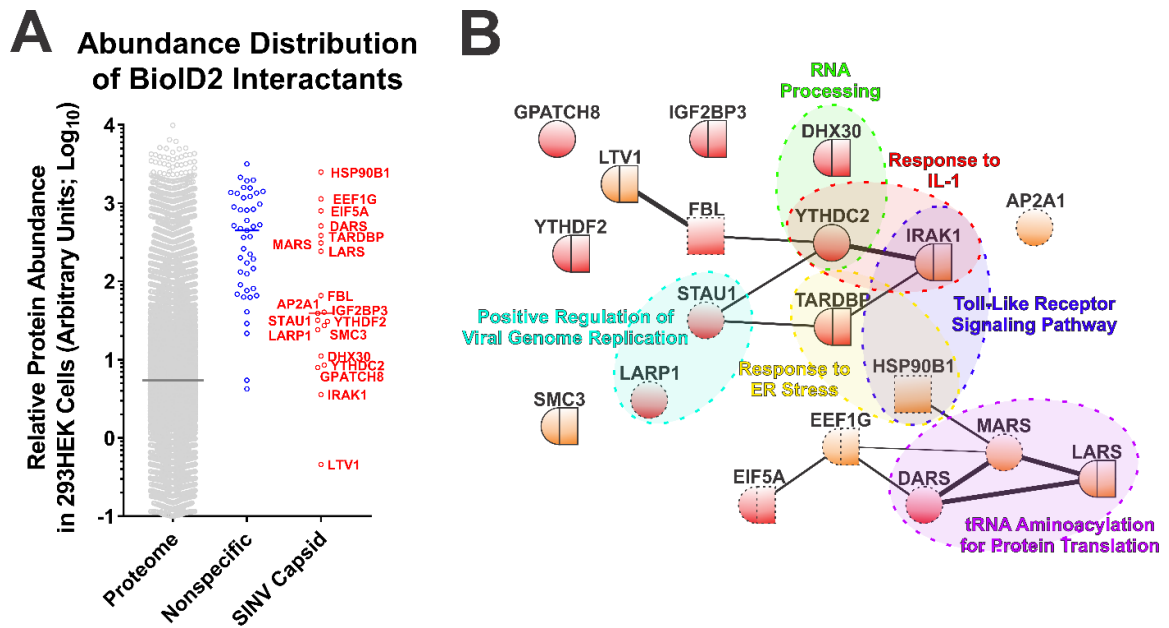


Figure 3.2- Ontological Analysis of the SINV CP–Protein Interactants Reveals Novel Host–Pathogen Interfaces

(A) Comparative analysis of arbitrary protein abundances of the host proteome (293HEK), and the non-specific and CP-specific interactants identified via the BioID2 approach. The lines represent the median abundance, and the CP-specific interactants are indicated next to their corresponding data point. (B) A STRINGs network map of the CP-specific interactants. The color and styling of the individual nodes indicates the properties and ontological category of the corresponding protein: round = cytoplasmic localization; square = nuclear localization; round/square = shuttling protein, or found in both compartments; red = RNA-associated protein; dashed outline = membrane associated. The weight of the linear connections between the individual nodes is indicative of the relative strength/confidence of the interaction. Molecular function ontological groups, as described in depth in the text, are highlighted in a color-coded manner.

The 19 host factors detected during the above SINV CP BioID2 discovery approach were examined via the STRING protein–protein interaction network and functional enrichment analysis tool to identify common interaction networks and molecular/biological function ontologies [268, 273]. As shown in Figure 3.2B, STRING analysis (version 11.0) revealed that several of the CP protein interactants exhibited protein–protein interactions with each other independent of the CP protein, suggesting possible indirect labeling of protein complexes. Nevertheless, the group of CP interactants at large was overall devoid of extensive interrelatedness, providing an indication that the SINV CP protein interacts with host factors in a largely specific manner. Ontological analyses provided further insight into the biological functions of the SINV CP interactants. As depicted in Figure 2B, analysis of cellular component ontology revealed that the putative interactants were associated with the cytosol (GO:0005829), the cytoplasm (GO:0005737), membranes (GO:0016020), and the nucleus (GO:0005634) to statistically significant degrees (all with p -values < 0.05 , and all surviving post hoc Bonferroni analyses). However, the fold enrichments were ranged modestly from 2 to 4-fold. Analysis of molecular function indicated enrichment of the poly(A) RNA binding (GO:0044822), protein binding (GO:0005515), RNA binding (GO:0003723), ATP binding (GO:0005524), mRNA 3'-UTR binding (GO:0003730), and nucleic acid binding (GO:0003676) ontological groups. As with the analysis of cellular component ontology, each of the aforementioned groups were statistically significant by Fisher's exact test (p -values < 0.05) and survived Bonferroni post hoc analyses (with the exception of mRNA 3'-UTR binding and nucleic acid

binding), and enrichment ranged from 1.8 to 10-fold amongst the FDR correction survivors.

Additionally, as highlighted in Figure 3.2B, several functional clusters were identifiable amongst the putative interactants identified by the BioID2-CP screen. Notable clusters of biological function with significant enrichment (> 15-fold) include the Positive Regulation of Viral Genome Replication (GO:0045070), RNA Processing (GO:0006396), Response to ER Stress (GO:0034976), tRNA Aminoacylation for Protein Translation (GO:0006418), Response to IL-1 (GO:0070555), and Toll-Like Receptor Signaling Pathway (GO:0002224). While the biological process GO terms listed had considerable enrichment, and initial statistical significance by Fisher's exact test (with the exception of Response to ER Stress, and RNA Processing where the *p*-values were greater than the statistical threshold of 0.05), all GO clusters succumbed to false discovery rate adjustments (likely due to the relatively few numbers of proteins in each group).

The above data indicate that the SINV CP protein is associated with a number of cytosolic RNA- and protein-binding proteins; however, these data do not indicate a singular extensive/monolithic role for the SINV CP protein in any particular cellular process outside of infection. The association of the CP protein with host factors involved in the stability of cellular RNAs is consistent with the aforementioned non-assembly roles of the SINV CP protein during infection.

The detection of the host IRAK1 protein as a putative CP–protein interaction significantly drew our attention due to the critical roles of the IRAK1 protein in TLR and IL1R signaling [258, 259]. Previous studies have demonstrated that the host

TLRs contribute to the control of alphaviral infection, as MyD88^{-/-} mice exhibited enhanced viremia and viral dissemination relative to wild-type controls [235, 274]. Similarly, TLR7^{-/-} mice exhibit increased pathology and viral burdens during alphaviral infections [275]. As such, given the impact of the TLRs on alphaviral infection, we focused our efforts on evaluating the CP-IRAK1 interaction at a greater level of molecular and biological depth.

The SINV CP-IRAK1 Interaction Is Genuine, and the CP-IRAK1 Interaction Is Conserved across the Genus Alphavirus

To confirm the results of the BioID experiments, we utilized a BiMolecular Complementation (BiMC) approach that utilized two fragments of the Nanoluc reporter [261]. Accordingly, the N terminal BiMC fragment of Nanoluc was fused to the human IRAK1 protein, and the complementary C-terminal fragment was fused to either the SINV, Chikungunya virus (CHIKV), Ross River virus (RRV), Venezuelan Equine Encephalitis virus (VEEV), Eastern Equine Encephalitis virus (EEEV), or Yellow Fever virus (YFV) capsid proteins, or the BioID2 protein as a control. To confirm and independently validate the observations of the BioID2 discovery approach, HEK293 cells were co-transfected with N-terminal Nanoluc IRAK1 plasmid and one of the above-mentioned complementary C-terminal expression plasmids. Forty-eight hours post transfection, the cells were treated with NanoGlo live-cell reagent and assayed for luminescence in a plate reader. As shown in Figure 3.3, co-expression of the IRAK1 and SINV capsid Nanoluc BiMC proteins resulted in significantly increased Nanoluc activity relative to the control

reactions, with an approximately 12-fold difference between the two experimental conditions. Similarly, co-expression of the Nanoluc-IRAK1 protein with the other alphavirus CP proteins also significantly restored Nanoluc activity relative to the control. Specifically, the new world alphaviruses VEEV and EEEV demonstrated the highest BiMC activity with the human IRAK1 protein, exhibiting approximately 22-fold and 20-fold greater signal than control reactions, respectively. The CP proteins of the Old-World alphaviruses RRV and CHIKV exhibited similar BiMC profiles to SINV, with greater than 10-fold Nanoluc activity relative to control reactions.

Therefore, the CP–IRAK1 interaction is genuine and is conserved amongst multiple members of the genus *Alphavirus*. While the consequences of this interaction cannot be directly inferred from these data, we hypothesized a scenario in which the functionality of the IRAK1 protein was compromised by the CP–IRAK1 interaction. Given the importance of the IRAK1 protein to TLR and IL-1 signaling, the host's capacity to respond to viral infection would be significantly perturbed if the CP–IRAK1 interaction suppressed the capacity of the IRAK1 protein to function.

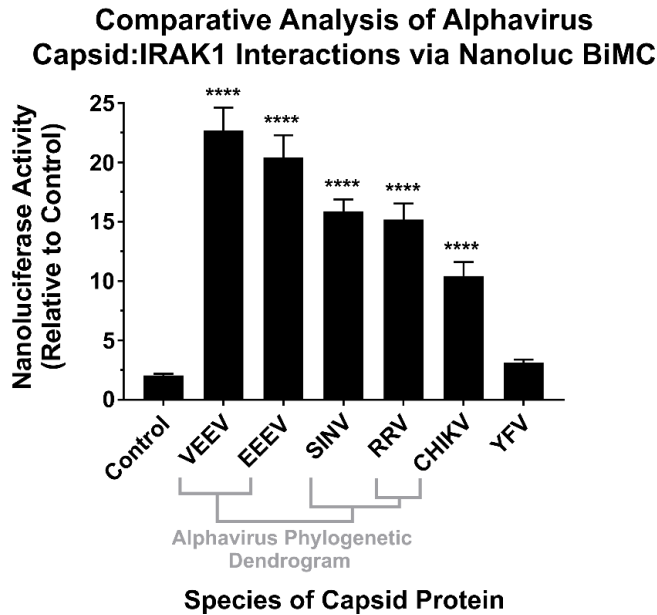


Figure 3.3- The CP–IRAK1 Interaction Is Genuine, and Widely Conserved across the Genus *Alphavirus*

The interaction of the alphaviral CP proteins with the host IRAK1 protein was assessed using Nanoluc-based BiMolecular Complementation (BiMC). The luminescent intensity of the CP–IRAK1 BiMC conditions was compared relative to those of control reactions lacking an interacting pair of Nanoluc fragments. Quantitative data shown is the mean of at least five biological replicates, with the error bar the standard deviation of the means. Statistical significance relative to the control reactions, with a p -value of $< 0.0001 = ****$, was determined by one-way ANOVA analysis. Below the X axis is a phylogenetic dendrogram of CP amino acid relatedness amongst select members of the genus *Alphavirus*.

The Sindbis Capsid Protein Is Sufficient to Inhibit IRAK1-Dependent Signaling

Following the validation of the SINV CP–IRAK1 interaction using BiMC, we hypothesized that the CP–IRAK1 interaction might be a means by which alphaviruses interfere with IRAK1-dependent signaling during infection to evade the induction of an antiviral innate immune response early during infection. To test this hypothesis, we utilized a series of robust/highly tractable tissue culture model systems which have been previously demonstrated to be effective in quantitatively assessing TLR activation [271, 272, 276-279]. Thus, we examined the impact of the SINV CP protein on IRAK1-dependent and independent signaling events using a series of 293HEK-based reporter cell lines which express Secreted Alkaline Phosphatase (SEAP) upon stimulation of TLRs 3, 4, and 7, or the TNF α receptor, via an NF κ B/AP1-responsive promoter. TLR3 and TNF α receptor were chosen as controls for generalized NF κ B/AP1-responsiveness as their signaling pathways are IRAK1-independent. In addition, TLR4 was chosen for these evaluations as it is a TLR dependent on IRAK1 signaling, but is not triggered by alphaviral infection or the presence of alphavirus PAMPs; thus, through the use of TLR4 we are able to examine the impact of IRAK1-dependent signaling without any potential confounding effects of viral PAMP sensing, as TLR4 stimulation is dependent on the addition of exogenous LPS. In contrast, TLR7 was selected for specific evaluation as it has been shown to be able to respond to alphaviral PAMPs, and hence, is likely to demonstrate the importance of IRAK1-dependent signaling during viral infection.

Concisely, the aforementioned 293HEK reporter cell lines were transfected with mammalian expression vectors encoding either the SINV CP protein or the Biold2 protein. Twenty-four hours post transfection the culture medium was replaced, and the cells were treated with agonists appropriate for each target receptor over a broad dose range in half-log dilution steps. The agonist/ligand-treated cells were allowed to further incubate for 16 h post treatment (hpt) prior to the colorimetric assessment of SEAP activity in a plate reader (Figure 3.4A). As shown in Figure 3.4B, the ectopic expression of the SINV CP protein negatively impacted TLR7 signaling to a dramatic extent, as evidenced by a near complete loss of TLR activation over the CL307 agonist dose range examined relative to control treated cells. Similarly, albeit to a lesser extent, ectopic expression of the SINV CP protein negatively impacted TLR4 signaling, as evidenced by reduced maximal activation, and the amount of Kdo2-lipid A agonist required to reach an equivalent $EC_{50_{MAX}}$ response of the control cells was increased by > 10-fold (Figure 4C).

To control for the possibility that the SINV CP protein was non-specifically interfering with cellular signaling and/or NFkB transcriptional activation, we examined the dose responsiveness of two IRAK1-independent signaling pathways after stimulation with their cognate receptor ligands during ectopic expression of the SINV CP protein. The TLR3 receptor is functionally unique amongst the TLRs in that it induces NFkB-mediated gene expression in an IRAK1-independent manner [280]. Hence, to determine whether the SINV CP protein non-specifically inhibited NFkB-mediated gene expression, we examined the dose responsiveness

of TLR3 reporter cells to high-molecular-weight poly(I:C). Consistent with our hypothesis that the SINV CP protein interferes with TLR signaling in an IRAK1-dependent manner, the dose responsiveness of TLR3 was unaffected by the SINV CP protein (Figure 3.4D). Nonetheless, to further demonstrate that IRAK1-independent signaling and NF κ B responsive transcription were not non-specifically perturbed in each of the cellular reporter systems utilized in this study, we examined the dose responsiveness of TNF α receptor (TNFR) to recombinant TNF α in each of the aforementioned cell lines during SINV infection. As depicted by the data in Figure 3.4E, the SINV CP protein did not pointedly interfere with TNRR signaling, as evidenced by similar EC₅₀_{MAX} values despite statistically significant but quantitatively modest differences at the high concentrations.

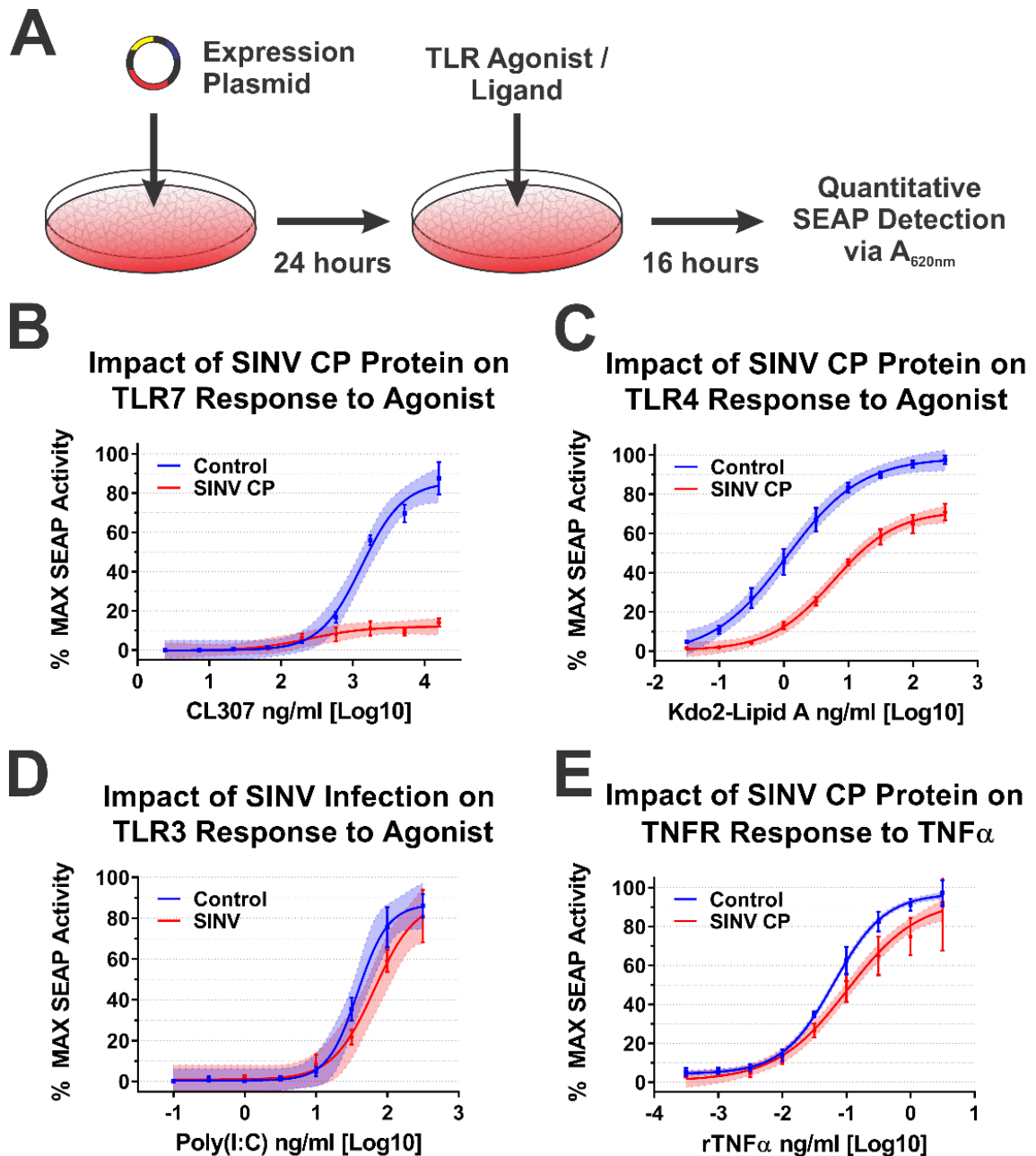


Figure 3.4- The SINV Capsid Protein Inhibits IRAK1-Dependent Signaling in a Specific Manner.

(A) A diagram of the experimental approach used to test the capacity of the SINV CP protein to inhibit IRAK1-dependent signaling in a specific manner. Comparison of the curves in each panel reveals the impact of SINV CP protein

expression on (B) TLR7 activation by CL307, (C) TLR4 activation by Kdo2-lipid A, (D) TLR3 activation by poly(I:C), and (E) TNFR activation by rTNF α . In all graphs, cells receiving control transfections prior to agonist treatment are represented by blue lines and data points, and those receiving the SINV CP protein expression plasmid are represented by red lines and data points. All quantitative data shown are the minimum of six independent biological replicates conducted over several days with at least two independent plasmid preparations. Quantitative data shown are the means of the biological replicates, and the error bars represent the standard deviation of the means. The connecting line represents a non-linear regression of the underlying data, and the shaded region indicates the 95% confidence interval of the non-linear regression. Thus, data points where the shaded regions do not intersect are statistically significant by at least a p -value of <0.05 , as determined by ANOVA analysis.

However, these data may be driven by increased signal variation at the higher concentrations of rTNF α . Thus, the inhibitory effects observed for IRAK1-dependent signaling events are specific and not due to simple disruption of intracellular signaling or the inhibition of transcription/translation.

As our BiMC studies indicated that multiple alphaviral CP protein species interact with IRAK1, we sought to determine whether they impacted TLR7 activation. For simplicity, we focused our efforts on the Old-World alphaviral species as their respective CP proteins are not known to negatively impact host transcription [281]. As shown in Figure 3.5, the ectopic expression of the CP proteins of CHIKV, RRV, and SFV all negatively impacted the capacity of the TLR7 receptor to respond to CL307 agonist treatment.

Altogether, the data presented in Figures 3.4 and 3.5 indicate that the alphaviral CP protein is sufficient and directly capable of inhibiting IRAK1-dependent signaling in a highly specific manner, strongly supporting our hypothesis that the CP–IRAK1 interaction represents a means by which the host innate immune response may be evaded during infection. The data presented in Figures 3.3 and 3.5 are supportive of the conclusion that the CP–IRAK1 interaction is functionally conserved amongst several members of the genus. Nonetheless, the ectopic expression of the SINV CP protein likely does not directly mimic the levels of alphaviral CP protein generated during natural infections, or those delivered by the incoming viral particles.

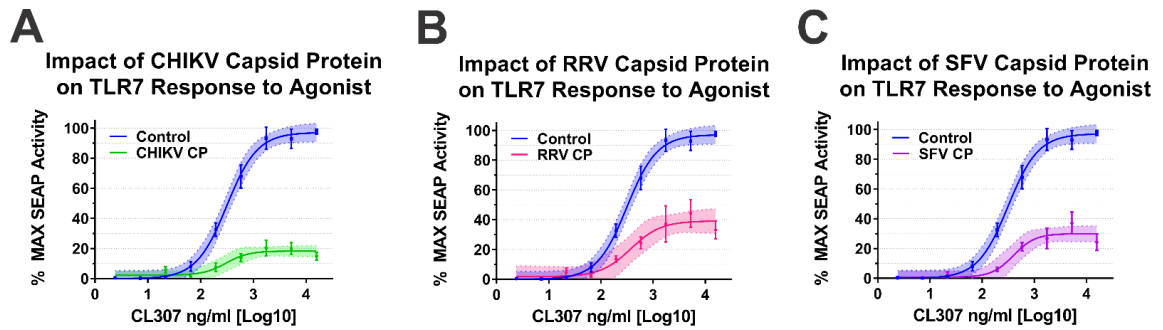


Figure 3.5- Old-World Alphavirus Capsid Proteins Inhibit IRAK1-Dependent TLR7 Signaling

Comparison of the curves in each panel above reveals the impact of the Old World Alphaviral CP proteins expression on TLR7 activation by CL307. Specifically, the impact of ectopic expression of (A) CHIKV CP protein, (B) RRV CP protein, and (C) SFV CP proteins were assayed identically to that described for Figure 4. Quantitative data shown are the means of the biological replicates, and the error bars represent the standard deviation of the means. The connecting line represents a non-linear regression of the underlying data, and the shaded region indicates the 95% confidence interval of the non-linear regression. Thus, data points where the shaded regions do not intersect are statistically significant by at least a p -value of < 0.05 , as determined by ANOVA analysis.

Sindbis Virus Infection Impairs IRAK1-Dependent Signaling in Tissue Culture Model Systems

While the data presented in Figures 3.4 and 3.5 were highly supportive of our initial hypothesis that the SINV CP–IRAK1 interaction represents a means by which alphaviruses may evade the induction of the host innate immune response via the disruption of IRAK1-dependent signaling, the conditions assayed above do not mimic those of genuine viral infection. Indeed, the ectopic expression of the alphaviral CP proteins likely results in the overestimation of the impact of the interaction as the intracellular levels of the CP protein are likely to be in far excess of those observed during infection. To this end, we sought to define the impact of the SINV CP protein in a model system where the CP protein was derived from bona fide infectious events.

Because a hallmark of alphaviral infection in highly permissive cells is the shutoff of host macromolecular synthesis, we employed a previously established approach which utilizes a SINV mutant that does not shut down host transcription, specifically the P726G point mutant of the SINV nsP2 protein, to enable SEAP activation in response to agonist treatment [263].

To test the impact of the SINV CP protein on IRAK1-dependent signaling during SINV infection, we infected the battery of 293HEK-derived TLR reporter cells described above with a Toto1101-derived SINV GFP reporter strain that included the nsP2 P726G mutation at an MOI of 10 PFU/cell. The use of the transcriptional shutoff deficient P726G mutant was important to the quantitative and qualitative assessment of the CP:IRAK1 interaction, as this mutant enabled a

robust cellular transcriptional response to be assessed after infection. Thus, unlike infections involving wildtype SINV which would have reduced or muted reporter gene expression, the P726G mutant allowed for the specific examination of the impact of the CP protein on transcriptional activation. Moreover, the use of the P726G mutant eliminates the possibility that cell death from host transcriptional shutdown would confound the underlying data through either host cell loss or the release of non-viral PAMPs which may activate reporter gene expression. The total infection of the cell monolayer was confirmed via GFP fluorescence, and 12 h post infection (hpi) the culture medium was replaced, and the cells were treated with agonists appropriate for each target receptor over as described above. The agonist/ligand-treated cells were further incubated for 16 h post treatment (hpt) prior to the colorimetric assessment of SEAP activity in a plate reader (Figure 3.6A).

Consistent with the data presented above, SINV infection significantly impaired IRAK1-dependent signaling events, as demonstrated by decreased maximal activation and dose responsiveness to agonist treatment for SINV infected cells relative to mock infected controls. Specifically, as shown in Figure 3.6B, TLR7 maximal activation and dose responsiveness were reduced by 2-fold, and ~50-fold, respectively. TLR4 activation was similarly impacted, as TLR4 reporter cells infected with SINV exhibited a ~2-fold decrease in maximal activation relative to mock infected cells, and the amount of Kdo2-lipid A agonist required to reach an equivalent $EC_{50_{MAX}}$ response to that of the control cells was increased by ~12-fold (Figure 3.6C).

To further support our conclusion that the observed inhibition of IRAK1-dependent TLR signaling was specific, we, as before, assessed TLR3 and TNFR dose responsiveness in our SINV infection model system. As observed above during the ectopic expression of the SINV CP protein, SINV infection did not affect the IRAK1-independent signaling events of TLR3 (Figure 3.6D). Once again, modest but statistically significant effects were observed in regards to TNFR stimulation during SINV infection.

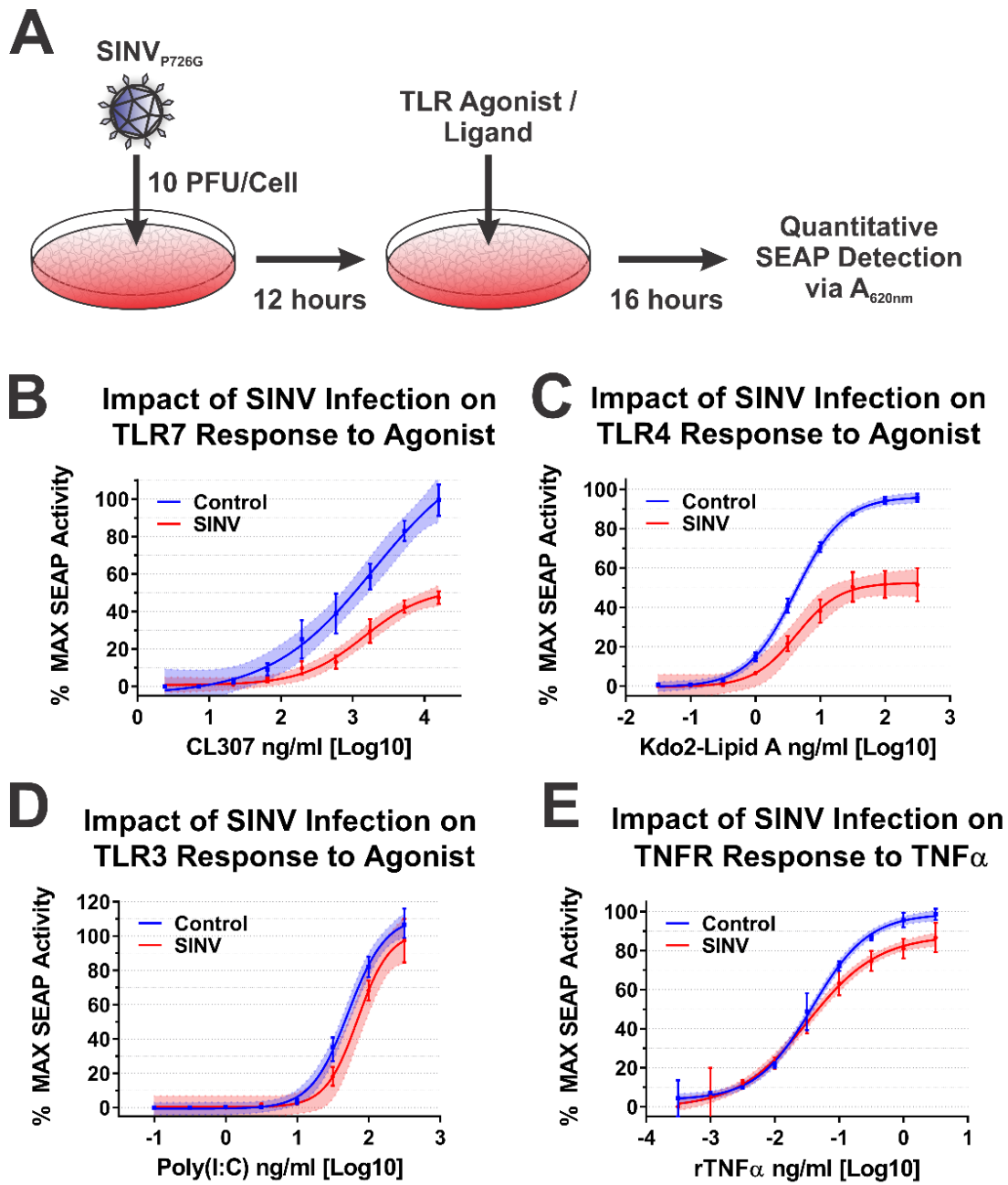


Figure 3.6- The SINV Infection Inhibits IRAK1-Dependent TLR Signaling

(A) A diagram of the experimental approach used to test the capacity of SINV_{P726G} to inhibit IRAK1-dependent signaling in a specific manner during infection. Comparison of the curves in each panel reveals the impact of SINV

infection on (B) TLR7 activation by CL307, (C) TLR4 activation by Kdo2-lipid A, (D) TLR3 activation by poly(I:C), and (E) TNFR activation by rTNF α . In all graphs, cells mock infected prior to agonist treatment are represented by blue lines and data points, and those receiving infectious SINV_{P726G} represented by red lines and data points. All quantitative data shown are the minimum of six independent biological replicates conducted over several days with at least two independent SINV preparations. Quantitative data shown are the means of the biological replicates, and the error bars represent the standard deviation of the means. The connecting line represents a non-linear regression of the underlying data, and the shaded region indicates the 95% confidence interval of the non-linear regression. Thus, data points where the shaded regions do not intersect are statistically significant by at least a p -value of < 0.05 , as determined by ANOVA analysis.

Collectively, the data presented here show that IRAK1-dependent TLR7 and TLR4 signaling is markedly inhibited during SINV infection, while the IRAK1-independent signaling events of TLR3 and the TNF α receptor were unaffected by SINV infection. These observations largely agree with our previous model system which utilized ectopically expressed CP proteins. However, the magnitude of impact on TLR7 signaling is less striking during infection. Whether this is due strictly to CP expression levels, or an accumulating effect on IRAK1-dependent signaling is unclear at this time.

SINV Infection Impairs IRAK1-Dependent Signaling during Viral Particle/TLR7 Agonist Co-Exposure

During alphaviral infection, there are two stages in which the CP protein may affect host IRAK1-dependent signaling—immediately upon entry to a new host cell when local areas of high CP protein concentrations are formed during nucleocapsid disassembly, or later during infection when the synthesis of new CP protein has commenced [44]. From the data obtained from the ectopic expression studies above, we are able to conclude that the synthesis of CP protein is capable of inhibiting IRAK1-dependent signaling events. Similarly, the quantities of CP protein synthesized during SINV infection are also capable of interfering with IRAK1-dependent TLR signaling. Accordingly, we may reasonably conclude that, in addition to the numerous other changes to the cellular environment, IRAK1-dependent signaling during the later stages of infection is impacted by the SINV CP protein. However, the above data do not indicate whether or not IRAK1-

dependent signaling is perturbed by the delivery of SINV CP protein to the cytoplasm of the target cell during viral entry. To test whether the SINV CP protein can negatively impact IRAK1-dependent signaling in an entry model of infection, we utilized a co-exposure system to assess the dose responsiveness of the TLR7 receptor in the presence of SINV particles (Figure 3.7A).

As demonstrated by the data in Figure 3.7B, co-exposure of TLR7 reporter cells with SINV particles and the TLR7 agonist CL307 elicited reduced maximal activation and reduced dose responsiveness by approximately 10-fold relative to control cells which were mock infected during co-exposure. Thus, the SINV CP protein delivered as part of the nucleocapsid core is capable of diminishing the IRAK1-dependent sensing of ssRNA PAMPs during the early stages of infection. It should be noted that the overall reduction in maximal activation was lessened relative to systems with continual CP expression (as in Figures 3.4–3.6).

As before, we utilized TLR3 as a means by which the specificity of the inhibition of IRAK1-dependent signaling could be assessed during a co-exposure approach. As shown in Figure 3.7C, co-exposure of poly(I:C) and infectious SINV particles did not impact the capacity of the cells to sense and respond to TLR3 agonist. These data in conjunction with that described above further secure the conclusion that the SINV CP protein specifically inhibits IRAK1-dependent signaling during infection.

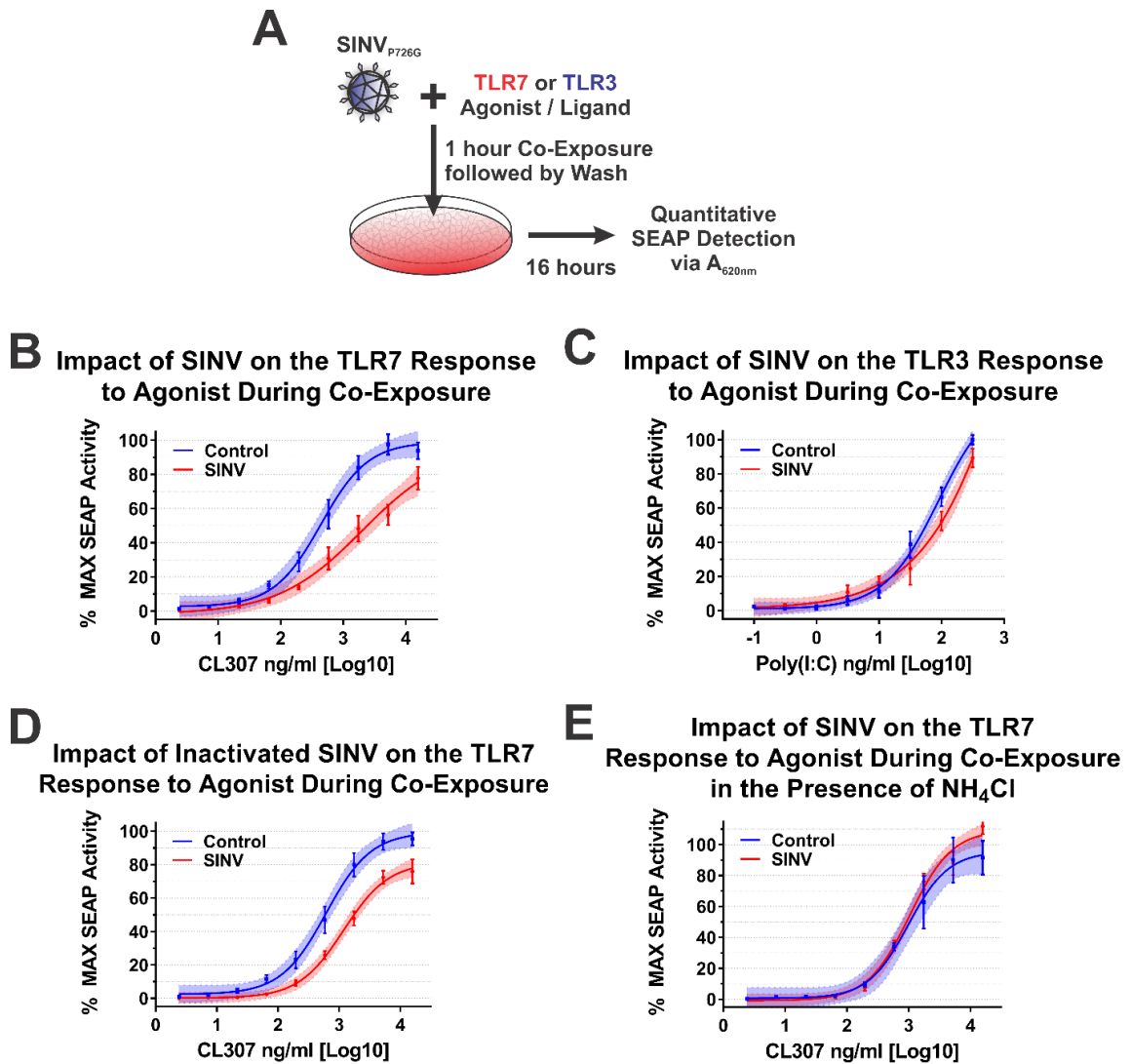


Figure 3.7- The SINV Capsid Protein Delivered by Incoming Infectious and Non-Infectious Particles Is Sufficient to Inhibit IRAK1-Dependent TLR Signaling

(A) A representative diagram of the co-exposure systems used to assess the impact of the incoming SINV CP proteins derived from particles. Specific differences between the experimental designs are noted in the title of each graph. Comparison of the curves in each panel reveals the impact of the CP-IRAK1

interaction on agonist co-exposure during (B) delivery of the SINV CP protein from infectious particles in the presence of the TLR7 agonist CL307, (C) delivery of the SINV CP protein from infectious particles in the presence of the TLR3 agonist poly(I:C), (D) delivery of the SINV CP protein from UV inactivated particles in the presence of the TLR7 agonist CL307, and (E) the effect of viral entry inhibitors on the sensing of CL307 by TLR7. In all graphs, mock infected cells are represented by blue lines and data points, and those receiving SINV viral particles are represented by red lines and data points. All quantitative data shown are the minimum of six independent biological replicates conducted over several days with at least two independent SINV preparations. Quantitative data shown are the means of the biological replicates, and the error bars represent the standard deviation of the means. The connecting line represents a non-linear regression of the underlying data, and the shaded region indicates the 95% confidence interval of the non-linear regression. Thus, data points where the shaded regions do not intersect are statistically significant by at least a p -value of <0.05 , as determined by ANOVA analysis.

Careful consideration of the co-exposure approach identifies the possibility that nascent synthesis of the SINV CP protein may be negatively impacting the capacity of the TLR7 reporter cells to respond to agonist exposure. To control for this possibility and assess the specific impact of the incoming viral CP proteins, we redesigned the co-exposure system to utilize UV-inactivated viral particles which are incapable of initiating viral replication, and by extension incapable of de novo expression of the CP protein from the subgenomic RNA. In this system, any effect noted on IRAK1-dependent signaling must be due to components of the incoming viral particles. As shown in Figure 3.7D, co-exposure of UV-inactivated SINV CP particles and CL307 similarly resulted in decreased TLR7 sensing relative to mock infected co-exposure controls. Hence, the incoming viral CP proteins delivered from non-infectious viral particles are capable of inhibiting IRAK1-dependent signaling.

Finally, in order to demonstrate that cytoplasmic entry of the SINV CP protein was required for the inhibition of the IRAK1-dependent TLR7 signaling process, we further modified the infectious co-exposure system to include the presence of ammonium chloride, a lysosomotropic salt which prevents the acidification of the endosome during maturation thereby preventing the entry of viral particles [282, 283]. Microscopic visualization of the treated cells confirmed the functionality of the ammonium chloride block to viral entry via the lack of GFP expression. Notably, in this system no deficiency in IRAK1-dependent signaling was observed (Figure 3.7E). Therefore, these data demonstrate that endosomal acidification and the completion of the viral entry pathway leading to the release of

the CP protein to the cytoplasm is required for the inhibition of IRAK1-dependent signaling.

Collectively, these data provide further evidence in support of our initial hypothesis and delineate the impacts of the CP–IRAK1 interaction on IRAK1-dependent signaling during viral entry. Moreover, these data indicate that the fusion of the viral envelope, and presumably the release of the nucleocapsid core into the cytoplasm, is required for the inhibitory effects of the incoming SINV CP protein.

Discussion

Defining the SINV Protein–Protein Interaction Network

Here we present our efforts using an innovative BioID2 discovery approach to identify novel host–pathogen interactions of the alphaviral CP protein in tissue culture models of infection. Prior to this study, the identification of alphaviral CP protein host–pathogen interactions were limited in scope; and to our knowledge, the unbiased discovery of CP protein–protein interactions was absent from the knowledgebase. The most in depth characterizations of alphaviral CP protein–protein interactions involve those of the VEEV CP protein, which has been shown to interact with elements of the nuclear import/export machinery, and host kinases during infection [281, 284-288]. The lack of unbiased discovery efforts in the knowledgebase is likely due to the molecular nature of the alphaviral CP protein, which unfortunately exhibits a high degree of promiscuous binding to commercially

available purification resins. The net effect is the substantial precipitation of the alphaviral CP proteins in the absence of target-specific antibodies unless highly stringent binding and wash conditions are used [121]. The harsh wash conditions necessitate the formation of cross-linked complexes prior to purification, as the wash conditions identified through the literature are likely to be incompatible with the purification of native protein–protein interaction complexes. As cross-linking methods form a molecular “snap shot” of the cellular environment, protein–protein interactions which are comparatively rare, temporally regulated, or fleeting in nature are likely to be underrepresented or absent during detection.

To overcome the challenges associated with alphaviral CP protein–protein interaction discovery, we utilized the BioID2 discovery approach. The covalent addition of a biotin moiety to host factors that come in close proximity to the alphaviral CP proteins enables their subsequent purification under rigorous conditions [256, 257]. A key advantage of this approach is that the BioID2 biotin ligase is capable of tagging host protein interactants whose interactions may be exceedingly rare, or those which may be highly transient, as the biotin tag durably remains after the interaction event for subsequent purification.

As reported by our data above, several host–pathogen interactions were identified via the SINV CP-BioID2 discovery screen. Whether or not these are genuine interactants remains to be determined experimentally; however, we believe these interactions to be bona fide CP–protein interactions for several reasons. First, the lack of extensive intrinsic protein–protein interactions amongst the identified interactants is reflective of the close-proximity requirement of the

biotin labeling event during the BioID2 screen. Further evidence of specificity can be obtained from the observations that host proteins with RNA-binding domains, such as RNA-Recognition Motifs (RRMs), KH-type, and Zinc-fingers, are absent from the interactant list, suggesting that the associations of the CP protein with these factors is not simply due to non-specific interactions bridged by an RNA molecule. These observations, coupled with the fact that the BioID2-CP interactants are not biased towards high abundance proteins, provide further evidence that the putative CP–protein interactions are likely to be genuine and functionally meaningful to alphaviral biology.

Review of the putative interactants reveals several of particular interest for future validation and assessment. Amongst these are several host factors involved in the regulation of RNA stability or function, including LARP1, IGF2BP3, TARDBP, STAU1, the N6-methyladenosine readers (m6A) YTHDC2 and YTHDF2, and the Zinc-finger antiviral protein (ZAP)-associated DHX30. It is unclear as to whether the CP interaction serves to deter the interaction of these host factors with the viral genomic RNAs by creating a protective swarm around the incoming genome, or whether they aid in the attraction of beneficial factors to the viral genome via the maintenance of the naCP–RNA interactions after disassembly of the nucleocapsid core. Similarly, it is unknown at this time whether these interactions prevent or disrupt the RNA:Protein and, or protein–protein interactions of the putative interactants.

Thus, whether these interactions are specifically pro- or antiviral is unknown at this time, and further experimentation is merited. Nonetheless, we are able to

provide several predictions/hypotheses based on the defined roles of the aforementioned host factors. LARP1 is known to bind to mRNAs with a 5' Terminal Oligopyrimidine Motif (5' TOP) to prevent the association of eIF4E with the 5' cap structure [289-293]. Therefore, the CP–LARP1 interaction may serve to prevent LARP1 from assembling on the viral RNA to prevent its translation. The interactions of IGF2BP3 with a given mRNA are associated with enhanced RNA stability, therefore this interaction may be an instance where the recruitment of the protein to the viral RNA is beneficial to the viral genome [294, 295]. STAU1, or Staufen1, is a component of the Staufen-Mediated Decay (SMD) pathway, which is a highly regulated RNA surveillance pathway which competes with the Nonsense-Mediated Decay (NMD) pathway [296]. As alphaviruses have been previously identified as prime targets for NMD, but are apparently resistant to its effects, the interaction of the CP protein with STAU1 may represent a means by which the NMD pathway is evaded during infection [297]. We hypothesize that the CP–STAU1 interaction, if genuine, may represent a mechanism by which the naCP–RNA interactions serve to stabilize the incoming viral genomic RNAs [121]. The association of TARDBP with an RNA has been reported to attract elements of the cellular deadenylase machinery, specifically Caf1, to enhance the RNA decay in a target specific manner [298]. Consequently, the CP–TARDBP interaction may be another component of the alphaviral RNA's capacity to resist deadenylation during infection [299, 300]. The m6A-associated proteins YTHDF2 and YTHDC2 contribute to the regulation of RNA stability by recruiting the deadenylation machinery, and the 5'→3' exonuclease XRN1, respectively [301-306]. As such, the

CP protein may represent a means by which the stability of the incoming viral genomic RNA is further supported. Finally, DHX30 is known to associate and regulate the activity of ZAP [307]. Importantly, ZAP has been previously demonstrated to restrict RNA virus infection, including alphaviral infections [308-311]. As above, the CP–DHX30 interaction may be a means by which the virus can evade antiviral effectors in the inhospitable cellular environment until later stages of infection when the host cell has been effectively co-opted for viral replication.

The Host IRAK1 Protein Is a Conserved Interactant of the Alphaviral CP Proteins

Our BiMC experiments demonstrate that the CP–IRAK1 interaction was genuine and not an artefact of the BioID2 discovery approach, and that this particular host–pathogen interaction was conserved across several members of the genus *Alphavirus*. Interestingly, the BiMC data implied that the interaction may be the strongest with the CP proteins of the two encephalitic alphaviruses tested—VEEV and EEEV. While not explicitly tested, the CP protein of Western Equine Encephalitis virus (WEEV) may be reasonably presumed to share the IRAK1 interaction as it is highly similar to that of EEEV. Despite showing significant complementation, the three arthritic alphaviruses tested in this study—SINV, RRV, and CHIKV—showed somewhat reduced BiMC activity relative to encephalitic alphaviruses. The precise implications of this trend are unknown, and further biochemical assessment is warranted prior to concluding that the CP–IRAK1 interaction of the encephalitic CP proteins are indeed superior to those of the

arthritogenic viruses. Regardless, these data indicate that the CP–IRAK1 interaction is conserved.

Comparisons of the alphaviral CP proteins provides few details as to the identity of the necessary and sufficient interaction domains required for the CP–IRAK1 interaction. Broadly speaking the alphaviral CP protein may be subdivided into two domains—a largely disordered positively charged *N*-terminal region, and a *C*-terminal protease domain [131]. The *N*-terminal domain of alphaviruses exhibits considerable sequence divergence outside of unifying characteristic of being highly poly-basic. The *N*-terminal regions of several alphaviruses have been described in more detail, and often regions associated with nucleic acid binding, CP dimerization, and packaging specificity are noted [112, 114, 115, 117, 312-317]. For several alphaviruses, most notably VEEV, distinct motifs important to the biology of the CP protein have been identified [120, 284]. In contrast to the *N*-terminal domain, the *C*-terminal protease domain is largely conserved amongst the members of the genus [111, 131]. The data above suggest that the interaction may be mediated by a conserved aspect of the alphaviral CP proteins, which would seemingly implicate the *C*-terminal protease domain. Nonetheless, it is equally likely, perhaps if not more so, that the interaction is mediated by the *N*-terminal domain as this domain is known to facilitate other intermolecular interactions involving the alphaviral capsid proteins. Work designed to delineate the necessary and sufficient CP–IRAK1 interaction determinants are ongoing within the Sokoloski lab. Importantly, such experiments may lead to the creation of interaction deficient

viruses, by which the importance of the CP–IRAK1 interaction on viral replication/pathogenesis may be assessed.

The CP–IRAK1 Interaction Negatively Impacts the Detection of TLR Ligands

Taken together, our data demonstrate the importance of the interaction between the alphaviral CP and IRAK1 proteins on IRAK1-dependent signaling in a cellular model of infection. Indeed, from the data shown in Figures 4–7, we can reasonably conclude that the SINV CP protein inhibits IRAK1-dependent signaling in a highly specific manner. Nonetheless, the precise mechanism how this occurs is unclear currently. We hypothesize that the CP–IRAK1 interaction serves to disrupt downstream IRAK1 protein–protein interactions or preclude the phosphorylation/activation of IRAK1 [258, 259].

Our data indicate that the SINV CP protein reduces the dose responsiveness of IRAK1-dependent TLRs during ectopic expression and infections of tissue culture models. We posit that the alphaviral CP protein serves to enable the evasion of the host innate immune response by masking the detection of PAMPs via the interruption of the IRAK1-dependent signaling cascade concurrent with the viral entry events and prior to viral gene expression (Figure 3.8). Importantly, our data indicate that the CP proteins delivered from incoming viral particles, regardless of their infectious potential, were capable of inhibiting TLR7. Therefore, the CP protein is capable of masking PAMP detection in permissive cells, and in non-permissive cells which are exposed to CP protein

without viral gene expression. The magnitude of effect is clearly linked to the level of CP protein present in the system, as greater effects were observed in the presence of ongoing CP protein synthesis. Therefore, in addition to be an early mechanism by which the sensing of viral PAMPs by the IRAK1-dependent TLRs may be manipulated, ongoing CP protein expression represents a means by which IRAK1-dependent processes are blunted during the later stages of infection.

The overarching impact of this phenomenon is the evasion of the direct and collateral activation of an innate immune response without the need for prior intracellular viral gene expression [281, 284, 318-320]. It is likely that this evasion mechanism is highly important to viral replication and dissemination, as alphaviruses are exceptionally sensitive to the effects of type-I IFNs [90, 321]. Thus, while alphaviruses have evolved several mechanisms by which the innate immune response may be limited during intracellular replication, the fact that these evasion mechanisms require the accumulation of viral proteins via ongoing viral gene expression creates the necessity of an earlier evasion mechanism to preserve the permissibility of the host environment. We hypothesize that the CP–IRAK1 interaction represents such a mechanism.

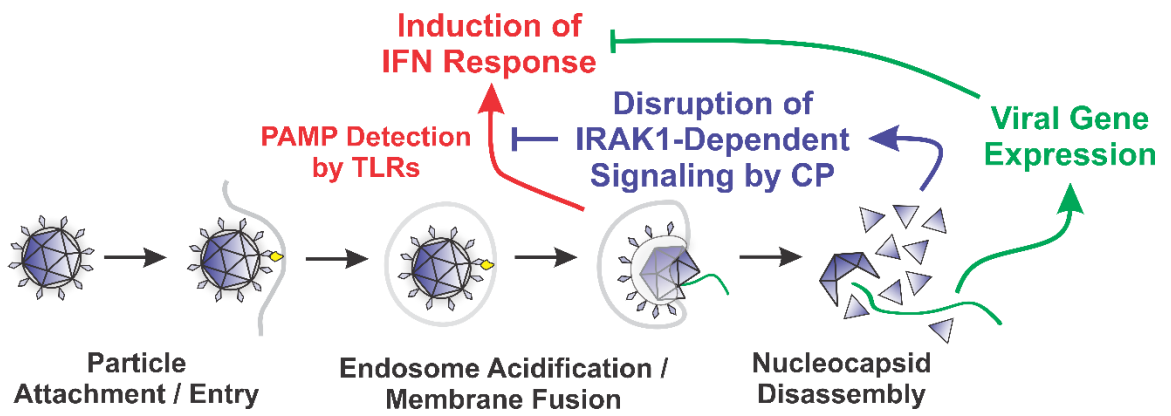


Figure 3.8- A Diagram of the Roles of the Nucleocapsid Components Early during Infection

Potential Ramifications of the CP–IRAK1 Interaction beyond TLR Evasion—The Disruption of IL-1 Signaling

The host IRAK1 kinase is functionally important to cellular signaling events unrelated to the direct sensing of PAMPs. The IRAK1 protein, as can be deduced from its full name—the Interleukin-1 Receptor-Associated Kinase 1—is integrally involved in the sensing of ligands via the IL1R receptor. As the data shown in this study indicate that IRAK1-dependent signaling events are disrupted by the Old World alphaviral CP proteins, we hypothesize that IL1R signaling events may be similarly affected during alphaviral infection, and preliminary efforts confirm that this hypothesis is likely true.

As IL-1 is a key mediator of the host inflammatory response, interfering with IL1R signaling may have profound impacts on the establishment and resolution of the inflammatory response [322-324]. IL-1 has been identified as integral to the formation of arthritis and encephalitis in both infectious and non-infectious settings [325, 326]. It should be noted that elevated levels of IL-1 are associated with severe alphaviral disease [141, 327-329].

During inflammation, the activity/impact of IL-1 is controlled by balancing IL1R signaling through the expression of IL-1, IL-1 responsive genes, and IL1R-antagonists (IL1RAs). As the CP–IRAK1 interaction effectively mutes IRAK1-dependent signaling via an intracellular mechanism, the signals received by the binding of IL-1 to IL1R may not be effectively transduced leading to altered gene expression in cells exposed to CP protein. Importantly, the data shown in this study demonstrate that a permissive infection is not required for the perturbation of

IRAK1-dependent signaling, suggesting that bystander cells which are not actively infected may exhibit disrupted signaling profiles. Accordingly, further investigation into the impact of the CP–IRAK1 interaction on IL-1 signaling and host inflammation and pathology is needed.

Conclusions

Here we have reported the use of an innovative approach to identify the protein–protein interactions of the SINV CP protein. In addition to identifying novel CP–protein interactions, we utilized state-of-the-art model systems to define the interaction of the SINV CP protein with the host IRAK1 protein. Importantly, the CP–IRAK1 interaction negatively impacted the capacity of IRAK1-dependent signaling to occur. While viral entry was required for CP protein-mediated signaling interference, the CP proteins delivered by the incoming viral particles were sufficient to significantly mask TLR7 sensing regardless of their infectious potential. Thus, the CP–IRAK1 interaction masks IRAK1-dependent signaling in permissive and non-permissive cells alike. Taken together, the data presented in this study significantly contribute to the field by i) establishing the use of a robust discovery approach to identify alphaviral CP–protein interactions, and ii) delineating a novel mechanism by which the host innate immune system is evaded during the earliest intracellular stages of the alphaviral lifecycle.

CHAPTER 4

CAPSID PROTEIN MEDIATED EVASION OF IRAK1-DEPENDENT SIGNALING IS ESSENTIAL TO SINDBIS VIRUS NEUROINVASION AND VIRULENCE

Synopsis

Alphaviruses are arthropod-borne, single-stranded positive-sense RNA viruses that are recognized as rapidly emerging pathogens. Despite being exquisitely sensitive to the effects of the innate immune response alphaviruses can readily replicate, disseminate, and induce pathogenesis in immunologically competent hosts. Nonetheless, how alphaviruses evade the induction of an innate immune response prior to viral gene expression, or in non-permissive infections, is unknown. Previously we reported the identification of a novel host/pathogen interaction between the viral Capsid (CP) protein and the host IRAK1 protein. The CP/IRAK1 interaction was determined to negatively impact IRAK1-dependent PAMP detection *in vitro*, however, the precise importance of the CP/IRAK1 interaction to alphaviral infection remained unknown. Here we detail the identification of the CP/IRAK1 interaction determinants of the Sindbis virus (SINV) CP protein and examine the importance of the interaction to alphaviral infection and pathogenesis *in vivo* using an interaction deficient mutant of the model neurotropic strain of SINV. Importantly, these interaction determinants are highly conserved across multiple Old-World alphaviruses, including Ross River virus

(RRV), Mayaro virus (MAYV), Chikungunya virus (CHIKV), and Semliki Forest virus (SFV). In the absence of a functional CP/IRAK1 interaction SINV replication is significantly restricted and fails to disseminate from the primary site of inoculation due to the induction of a robust type-I Interferon response. Altogether these data indicate that the evasion of IRAK1-dependent signaling is critical to overcoming the host innate immune response and the *in vivo* data presented here demonstrate the importance of the CP/IRAK1 interaction to neurovirulence and pathogenesis.

Introduction

Alphaviruses are rapidly emerging arthropod-borne positive-sense RNA viral pathogens with a significant capacity to cause severe illness in otherwise healthy individuals [44]. The clinical diseases caused by alphaviruses are divided into two categories, those which cause febrile arthritis, and those which cause encephalitis. The arthritogenic alphaviruses, including Sindbis virus (SINV); Chikungunya virus (CHIKV); and Ross River virus (RRV), cause moderate to severe multi-joint febrile arthritis in otherwise healthy individuals [6, 8, 11, 14-16, 18, 249, 250]. Unfortunately, arthritis caused by these viruses has the potential to develop into chronic arthritis which may persist or worsen over a period of several months, or years, after the resolution of acute infection [6-8, 15, 251, 252]. This prolonged chronic disease results in a long-term reduction of quality of life due to ongoing disability and limited use of affected joints. The encephalitic alphaviruses, which include members such as Western Equine Encephalitis virus (WEEV);

Venezuelan Equine Encephalitis virus (VEEV); and Eastern Equine Encephalitis virus (EEEV), have the capacity to cause viral encephalitis in young and elderly patients [22, 24, 25, 253]. Despite being comparatively rare clinically, these viruses exhibit high morbidity as they can cause severe encephalitis that may result in the death of the infected individual. Furthermore, individuals that survive clinical alphaviral encephalitis often experience life-long cognitive impairments. Due to their capacity to cause severe disease in otherwise healthy individuals, the lack of safe and effective therapeutics or vaccines for the treatment or prevention of alphaviral infection, and the rapid expansion of competent vector mosquito geographic range, the alphaviruses are recognized as emerging health concerns [17, 237-248]. Accordingly, research that defines alphaviral pathogenesis is critical to the development of innovative mitigation strategies by which the burdens of alphaviral disease may be alleviated.

The alphaviruses are exceptionally sensitive to the host innate immune system and are readily controlled by the antiviral effects of the type-I interferon (IFN) response [330-333]. To overcome host restriction of viral replication, the alphaviruses have evolved means by which the host innate immune response may be limited to enable viral replication and spread. The evasion of the innate immune response by the alphaviruses has been thought to be predominantly driven by the shutoff of host macromolecular synthesis, which effectively precludes the production of IFN, and interferon-stimulated genes (ISGs) [281]. However, the shutoff of host macromolecular synthesis brought about by transcriptional and translational repression requires viral gene expression and does not occur in

earnest until mid- to late infection in highly permissive models of alphaviral infection [321]. The delayed circumvention of the host response and the necessity for viral gene expression constitutes a window of opportunity for the host to detect and elicit a controlling innate immune response to infection in permissive and nonpermissive cell hosts. A major mechanism by which the cellular host may detect and respond to viral infection are the Toll-like Receptors (TLRs) which sense Pathogen Associated Molecular Patterns (PAMPs) including viral nucleic acids [334]. Nonetheless, prior studies have revealed that the TLRs have a minimal role during alphaviral infection, suggesting that the capacity of the host to sense viral infection via TLR-dependent mechanisms is greatly reduced during infection; however, the precise mechanisms as to how this occurs, especially in nonpermissive cells exposed to alphaviral PAMPs (as they lack the host shutoff afforded by viral gene expression), is unknown[233].

Recently our lab defined the host/pathogen Protein:Protein interactions of the Sindbis virus (SINV) Capsid (CP) protein utilizing an innovative BioID approach [335]. These efforts demonstrated that the alphaviral CP protein interacts with the host Interleukin-1 Receptor Associated Kinase 1 (IRAK1) protein. The identification and validation of the CP/IRAK1 interaction was notable, as the IRAK1 protein plays a key role in the signaling pathways of all TLRs (with the notable exception of TLR3) [204]. Further assessments using *in vitro* models of alphaviral infection revealed that the CP/IRAK1 interaction inhibits IRAK1-dependent signaling in a highly specific manner. Importantly, it was found that the CP proteins delivered by the disassembly of the incoming nucleocapsid cores were sufficient

to perturb IRAK1-dependent signaling, and even the CP proteins derived from non-infectious viral particles were capable of repressing IRAK1-dependent sensing of PAMPs. Altogether these data provided a potential explanation as to why TLRs failed to significantly contribute to the restriction of alphaviral infections in knockout mice, in that IRAK1-dependent TLR sensing may already be inhibited during alphaviral infection and that loss of TLR sensing provides no specific additional contribution to replication/infection.

While our previous efforts have demonstrated the capacity of the CP/IRAK1 interaction to negatively affect host PAMP sensing via IRAK1-dependent signaling pathways in cellular models of infection, the precise importance and biological impact of the interaction to alphaviral infection and pathogenesis *in vivo* has yet to be described. Here we present data obtained by way of leveraging a nanoluciferase-based Bi-molecular complementation (BiMC) approach to determine the necessary and sufficient CP/IRAK1 interaction determinants of the SINV CP protein. The knowledge gained from these efforts led to the development of a mutant virus unable to inhibit IRAK1-dependent signaling, allowing us to test the importance of the CP/IRAK1 interaction in both *in vitro* and *in vivo* settings. From these efforts, we conclude that the CP/IRAK1 interaction is crucially important for viral replication and dissemination as mutants lacking in the CP/IRAK1 interaction are severely limited by the induction of type-I IFNs. The elicitation of the host innate immune response, as per the effects of IFN, is achieved by way of an IRAK1- and Myd88-dependent mechanism, such as TLR sensing of viral PAMPs.

Methods

Tissue Culture Cells

BHK-21 (ATCC CCL-10, VA, USA) and HEK293 (ATCC CRL-1573, VA, USA) cells were cultured in Minimal Essential Media (MEM; Cellgro, NY, USA), supplemented with 10% Fetal Bovine Serum (FBS; Corning, 35-010-CV, NY, USA), 1x Penicillin/Streptomycin (Pen/Strep; Corning, 30-002-CI, NY, USA), 1x Non-essential Amino Acids (NEAA; Corning, 25-025-CI, NY, USA), and L-glutamine (Corning, 25-005-CI, NY, USA). HEK293-derived reporter cells, HEK-Blue hTLR7 (Invivogen, hkb-hltr7, CA, USA), were cultured in Dulbecco's Modified Eagle Medium (DMEM; Corning, 10-017-CV, NY, USA) supplemented with 4.5 g/L glucose, 10% FBS, 1x Pen/Strep, and 1x Normocin (Invivogen, ant-nr-1, CA, USA). HEK-Blue cells were kept at low passage numbers to maintain genetic homogeneity and given selection antibiotics every other passage to maintain genomic integrity. Immortalized wild-type C57Bl/6-derived (NR-9456, BEI resources, VA, USA), and C57Bl/6 congenic MyD88^{-/-} macrophages (NR-15633, BEI resources, VA, USA) were maintained in DMEM supplemented with 4.5 g/L glucose, 10% FBS (Corning), 2mM L-glutamine (Corning), 1mM Sodium Pyruvate (Corning, 25-000-CI, NY USA), and 10ug/ml ciprofloxacin (Corning, 61-277-RF).

All cells were cultured in a humidified incubator at 37°C in the presence of 5% CO₂, and passaged according to standard practices for each cell line.

Expression Plasmid Construction

The nanoluciferase BiMolecular Complementation expression plasmids used in this study were generated through site-directed mutagenesis or Gibson Assembly, using the previously described parental pSplit.Nanoluc.C67.SINV CP plasmid or the pSplit.Nanoluc.C67 plasmid, as described in detail below [261, 335].

The development of SINV CP truncation mutants were developed utilized site-directed mutagenesis via the Q5 Site-Directed Mutagenesis Kit (NEB, E0554S, MA, USA) to excise the individual domains of the CP individually in a stepwise fashion to generate a full battery of mutant constructs. The deletions of the individual domains were accomplished using primers- C67.SINV.DRI.F (5'-AAGCCTAAGAAGCCCAAGAC-3') and C67.SINV.DRI.R (5'-CATGCCGCTTCCACCTCC-3') for the deletion of the RI domain to generate pSplit.Nanoluc.C67.SINV.ΔRI; C67.SINV.DRIandII.F (5'-AGACTGTTGACGTGAAGAACG-3') and C67.SINV.DRIandII.R (5'-CATGCCGCTTCCACCTCC-3') for the deletion of the RI and RII domains to generate pSplit.Nanoluc.C67.SINV.ΔRI/RII; C67.SINV.DPRO.F (5'-TAACTTAAGCTTGGTACCGAG-3') and C67.SINV.DPRO.R (5'-TCTGTGCGCTTCCAGCTT-3') for the deletion of the Protease domain to generate pSplit.Nanoluc.C67.SINV.ΔPRO. The nanoluciferase BiMC expression constructs consisting of the RI and RII domains in isolation were generated by site-directed mutagenesis and via- C67.SINV.DRI.F and C67.SINV.DRI.R site-directed mutagenesis of the pSplit.Nanoluc.C67.SINV.ΔPRO plasmid to generate the RII-only construct pSplit.Nanoluc.C67.SINV.RII; and to generate the pSplit.Nanoluc.C67.SINV.RI construct primers C67.SINV.D2andPRO.F (5'-

TAACTTAAGCTTGGTACCGAGCTC-3') and C67.SINV.D2andPRO.R (5'-AGGAGGCTGCTTAGGGGC-3') were used to modify the parental pSplit.Nanoluc.C67.SINV CP plasmid. All reactions were performed according to the manufacturer's instructions.

The nanoluciferase BiMC expression plasmid encoding the RII fragments of the CP proteins of Ross River (RRV), Mayaro (MAYV), Chikungunya (CHIKV), and Semliki Forest (SFV), were cloned into the original pSplit.Nanoluc.C67 plasmid using Gibson Assembly approaches. All synthetic DNA fragments for these efforts were obtained from Genewiz (NJ, USA) and the restriction enzyme SfoI (NEB, R0606S, MA, USA) was used for the Gibson Assembly reaction. All DNA fragments used in this study were generated by GeneScript (NJ, USA) and assembled using the Gibson Assembly mastermix available from Synthetic Genomics, Inc. (GA1100-10, CA, USA) according to the manufacturer's instructions.

All plasmids were cultured overnight in *E. coli* DH5 α (or comparable) bacteria under antibiotic selection. Plasmids were purified by miniprep or midiprep purification kits (Omega Bio-Tek, D6943-02, D6904-04, GA, USA).

Nanoluc-based BiMolecular Complementation Analysis (Nanoluc BiMC)

NanolucBiMC was performed as previously described. Briefly, HEK293 cells were seeded into a flat white bottom 96 well plate at a density of 1.25×10^4 cells per well. After overnight incubation wells were transfected with

pSplit.Nanoluc.N67 and one of the pSplit.Nanoluc.C67 constructs using lipofectamine 3000 (Invitrogen, L3000001, MA, USA). A total of 0.1µg of DNA was transfected consisting of 50ng of each construct. After allowing to transfected cells to incubate for 48 hours under normal growth conditions the media was carefully removed and replaced with 100ul of Optimem (Gibco, 31985070, MA, USA) supplemented with Furimazine (AOBIOUS, AOB36539, MA, USA) at a concentration of 10µm. The reactions were briefly incubated for two minutes at room temperature prior to the measurement of luminescence activity via a Synergy H1 microplate reader (BioTek, VT, USA).

Generation and Preparation of SINV

This study utilized a series of SINV infectious clones, including p389, a Toto1101-derived SINV strain with a GFP reporter in the nsP3 protein; p389_{P726G}, a derivative of p389 that includes a point mutation in the nsP2 protein known to prevent the cessation of host gene expression[89]; and the AR86 neurotropic strain. For all strains referred to as SINV.ΔRII, the derivative mutant was generated by Gibson assembly using the corresponding fragment lacking amino acids 81 to 95 of the SINV CP protein. The restriction enzyme sites used to generate the ΔRII clones were HpaI and ZraI for the p389-derived mutants or BstBI and StuI for the AR86 clones. Synthetic DNA fragments containing the regions of interest for Toto1101 and AR86 were obtained from Genscript (NJ, USA), and Genewiz (NJ, USA), respectively.

The use of two strains of SINV was intentional, with the AR86 strain being utilized for *in vivo* studies as well as the macrophage studies, whereas the Toto1101-derived strain was used for all other studies. Infectious viral stocks were generated as previously described [76]. Briefly, RNA transcripts were generated *in vitro* then 10µg were electroporated into $\sim 3 \times 10^6$ BHK-21 cells using a single pulse at 1.5kV, 25mA, and 200Ω. Viral titers were determined by way of standard plaque assays in BHK-21 cells.

Analysis of SINV Mutant Growth Kinetics

The growth kinetics SINV.WT and the SINV.ΔR11 mutant were assessed using one-step growth kinetic assays involving BHK-21 cells cultured in 12-well tissue culture dishes. Briefly, confluent monolayers of BHK-21 cells were infected with either SINV.WT or SINV.ΔR11 at an MOI of 5 infectious units per cell. After a one-hour adsorption period, the inoculum was removed, and the cell monolayers were extensively washed with 1x PBS (Corning, 21-040-CMR, NY, USA) prior to the addition of whole medium supplemented with 25mM HEPES (gibco, 15630080, MA, USA) to enable the use of an automated liquid handling system lacking a CO₂ atmosphere. The infected cells were incubated at 37°C, and gently mixed prior to the harvesting of the tissue culture supernatants. The cell supernatant was collected at the indicated times post-infection and stored at 4°C, and fresh media was added to the cell monolayers.

Viral titers were determined using standard plaque assays using BHK-21 cells overlaid with 2% Avicel (in whole media). After a 30-hour incubation period, the cell monolayers were fixed with 3.7% formaldehyde (diluted in 1x PBS), and the plaques were enumerated following crystal violet staining.

Quantitative Analysis of TLR7 Dose Responsiveness

To define the impact of the individual alphaviral CP protein domains on IRAK1-dependent TLR7 signaling, HEK-Blue hTLR7 cells cultured to 75% confluence were transfected with the aforementioned CP protein expression plasmids. Transfection conditions were identical to those described above for the nanoluciferase BiMC assays, with the exception that the IRAK1 encoding plasmid was omitted in lieu of increased SINV CP expression plasmids. After a 24-hour incubation period, the supernatant was carefully removed and replaced with whole media supplemented with the TLR7-specific agonist CL307 (Invivogen, tlr1-c307, CA, USA) at the indicated concentrations prior to returning the cell to incubate under normal conditions. At 16 hours post-treatment, 20ul samples of the supernatant were carefully removed and transferred to a new 96-well containing 180ul of HEK-Blue Detection media (Invivogen, hb-det2, CA, USA) and after careful mixing the plate was quantitatively assessed for SEAP expression via colorimetric assay.

The quantitative detection of IRAK1-dependent TLR7 signaling was accomplished by incubating the above detection plate at 37°C in a plate reader

while regularly taking absorbance readings at 620nm for a period of three hours, or until the absorbance curves of the highest concentration of agonist reached saturation. Readings from pre-saturation time points were comparatively assessed to determine agonist detection with respect to concentration.

Briefly, the quantitative analysis of TLR7 signal transduction was determined by comparing the measurable SEAP activity of the control and experimental conditions over the CL307 agonist dose range after the subtraction of non-agonist-treated wells. The control agonist treatment with the highest level of SEAP activity was then standardized to 100%, and all other wells within an experimental replicate were normalized accordingly to determine their relative activity. The quantitative data from multiple biological replicates for a given dose were then averaged and plotted with respect to agonist concentration. Non-linear regression analyses of the data, via GraphPad Prism 7.0.2, using the log(agonist) vs. response variable slope (four parameters) non-linear curve fit function, was used to determine the activation profiles and 95% confidence intervals of the data. The concentrations of agonist required to reach 50% of maximal activity of control-treated reactions ($EC_{50_{MAX}}$) were determined using these non-linear regression equations.

To determine the impact of SINV.WT and SINV. Δ R11 infections on IRAK1-dependent TLR7 signaling a similar approach to that described above was utilized, with the notable exception being that the experimental conditions involved SINV p389^{P726G}-derived infections at an MOI of 10 infectious units per cell. Quantitative analysis of TLR7 signaling was identical to that described above.

Mouse Experiments

Four-week-old C57BL/6 mice were obtained from Jackson Laboratory (ME, USA) and acclimated in UofL vivarium facilities for a period of no less than 48 hours. For the footpad infection model, the mice were infected via rear foot pad injection with either 10,000 PFU of SINV.WT or SINV. Δ RII, or mock-infected, in a final volume of 10uL using a 30G syringe after sedation via isoflurane inhalation (502017, Vet One, ID, USA). The mice were returned to their cages and monitored to ensure recovery after isoflurane anesthesia, and the mice were monitored daily for weight gain/loss and the development of neurological disease. Individual animal weights were monitored with respect to time, and the development of neurological disease was scored on a 5-point scale as follows- 0, no signs of overt disease and normal behavioral activity; 1, abnormal trunk curl, grip, or tail weakness (1 of 3); 2, abnormal trunk curl, grip, or tail weakness (2 of 3); 3, absent trunk curl, lack of gripping, tail paralysis; 4, pronounced dragging of one or more limbs; 5, hind or fore limb paralysis. The Intracranial infection (IC) model was largely identical to that described above, with the major exception being that the virus inoculum was directly delivered to the left-brain hemisphere via a 30G syringe to a depth of 3mm. Recovery after IC injection was prolonged relative to that of the footpad model; however, all mice recovered after a period of no more than 30 seconds.

Once mice reached endpoint criteria (clinical score of 4 or 5 or 20% weight loss), or at the designated time for tissue collection, the mice were euthanized via isoflurane inhalation overdose followed by cervical dislocation or by thoracotomy and the collection of vital tissues. Tissues collected for virological and biological

analysis were rapidly frozen and stored at -80°C, and/or preserved in 10% formalin for later use. Serum was collected using blood collection tubes containing heparin sulfate, and brief centrifugation prior to aliquoting.

For the detection of infectious virus loads *in vivo*, harvested tissues were first homogenized by bead beating using a Bead Ruptor 4 (Omni International, 25-010, GA, USA) in a standardized volume of 1xPBS. After brief centrifugation to clarify the lysates, the supernatant was transferred to a fresh tube and viral loads were assessed using TCID₅₀ assays in a 384-well format. The results of which were then converted to PFU per unit volume/mass by way of calibrated TCID₅₀ assays using standardized samples.

Animal Ethics and Research

This study was performed under strict accordance with the recommendations described in the *Guide for the Care and Use of Laboratory Animals* of the National Institutes of Health. This protocol was approved by the Institutional Animal Care and Use Committee of the University of Louisville. Anesthesia was used for any manipulations that could result in pain or distress.

Transcriptomic Analysis of Infected Brain Tissue

Transcriptomic analyses were conducted in parallel to the virological analyses described above, with the notable exception that the tissues were solubilized in TRIzol (Invitrogen, 15596026, MA, USA) rather than 1xPBS. Total

RNA was extracted from the tissue lysates using the Direct-zol-96 MagBead RNA extraction kit (Zymo Research, R2102, CA, USA) per manufacturer's instructions using a KingFisher Duo Prime Purification System (ThermoFisher Scientific, MA, USA). The resulting purified total RNAs were then used as the input materials for the synthesis of cDNA libraries for next-generation sequencing.

Libraries for next-generation sequencing were prepared using the NEBNext Ultra RNA Library Prep kit (NEB #E7530L, MA, USA) according to the manufacturer's instructions using NEBNext Multiplex Oligos for Illumina Index primer sets #1 and #4. Information regarding specific samples and their indices may be found in the Supplemental Data accompanying this manuscript. Libraries were quantified by Qubit Flex Fluorometry using the Qubit 1X dsDNA HS Assay Kit (ThermoFisher, Cat. No. Q33231, MA, USA). The average Fragment length of each sample was assessed using an Agilent Fragment Analyzer 5200, utilizing either the Standard Sensitivity Next Generation Sequencing kit, or the High Sensitivity Next Generation Sequencing Kit, depending on the mass as determined by the Qubit assay. Equimolar amounts of each sample were pooled, and the mass of the pool was quantified by Qubit using a 1X dsDNA HS assay kit. The Qubit concentration reading and the average fragment length were used to determine molar concentration for loading. The library and PhiX standards were diluted using the standard normalization method following the manufacturer's directions. The total volume of the library was 20 μ L at 750 pM, with 2% PhiX spike in. Further denaturing and dilution of the library to 75pM is done on the instrument (NextSeq

2000). Sequencing was performed on a NextSeq 2000 using a P3 200-cycle reagent kit with a P3 flow cell.

The raw FastQ sequence data was downloaded from Basespace and trimmed using Fastqc and Trimmomatic prior to alignment to the *Mus musculus* genome via STAR. Differential expression analysis was performed using Cuffdiff2 and DESeq2. For the Cuffdiff2 analysis, Cuffnorm was used to produce FPKM (Fragments Per Kilobase Million) normalized counts. The counts were then filtered to include only genes with minimum expression of one FPKM in three or more samples and an average expression of at least one FPKM. For the DESeq2 analysis, raw read counts were obtained from the STAR aligned bam format files using HTSeq version 0.10.0. The raw counts were normalized using the Relative Log Expression (RLE) method and then filtered to exclude genes with fewer than 10 counts across the samples.

The raw unprocessed next-generation sequencing data associated with this study has been deposited to the appropriate repository. Processed data tables listing the differential transcriptomic data obtained during these studies may be found in the Supplemental Data Files associated with this manuscript.

Ontological Analysis of Next-Generation Sequencing Data

The data obtained from the next-generation sequencing of IC-infected whole mouse brain homogenates were processed to identify enriched Biological Process Ontological categories using standard approaches. Briefly, the differential

transcriptomics data for the SINV.WT vs Mock Infected and SINV. Δ RII vs Mock Infected data sets were parsed into lists of up-regulated and down-regulated transcripts which fit a criterion of >2-fold enrichment relative to Mock and a corrected p-Value of < 0.05. This resulted in the identification of 1388 up-regulated and 352 down-regulated genes for the SINV.WT vs Mock Infected data set; and 1004 up-regulated and 1234 down-regulated for the SINV. Δ RII vs Mock Infected data set. These lists were assessed using DAVID to identify enriched Biological Process ontological groups. The biological process ontological groups enriched for the parsed data sets were compared across the SINV.WT and SINV. Δ RII conditions to identify common and unique enrichment categories. In all cases, the ontological enrichment data was reassessed using Revigo to eliminate redundancy amongst the enrichments and group the enriched biological process ontological categories into simplified parent ontological groups to aid comparative analysis.

Full ontological tables and accompanying quantitative information may be found in the Supplemental Data Files associated with this manuscript.

Quantification of IFN β Expression in Macrophages

C57BL/6-derived macrophages were seeded into a 24-well plate. After growing to 80% confluency, they were mock infected (via PBS) or infected with equal particle numbers of either SINV.WT or SINV. Δ RII or 1 hour with occasional shaking. After the 1-hour absorption period, the media was carefully removed, and

the cells were washed 1x with PBS to remove any unattached virus prior to the replacement of the media and further incubation. After a 3-hour incubation period, the media was again carefully removed, and the cells were washed with 1x PBS and then harvested via the addition of TRIzol and stored at -80°C. Analyses of MyD88^{-/-} macrophages were identical to that described above for wild-type macrophages. To determine the specificity to which IRAK1-dependent signaling contributed to IFN β expression after SINV infection wild type macrophages were co-incubated in the presence of the IRAK1 kinase inhibitor JHX-119-01 (MedChemExpress, HY-103017, NJ, USA) at a concentration of 20mM.

Total RNA was extracted from the TRIzol containing samples using Direct-zol-96 MagBead RNA extraction kit (Zymo Research) per manufacturer's instructions using a KingFisher Duo Prime Purification System (ThermoFisher Scientific). The extracted total RNA was then used as the input materials for cDNA synthesis via Reverse Transcriptions using OneScript Plus Reverse Transcriptase (AbmGood, G237, BC, Canada) as per the manufacturer's instructions. The resulting cDNA was used as the input materials for qRT-PCR using PerfeCTa SYBR Green FastMix (Quantabio, 95074-250, MA, USA) to detect the levels of IFN β mRNA expression relative to the control gene GUSB. The relative quantities of mouse IFN β RNA, as per the $\Delta\Delta C_t$ method, were detected using primers Mus.IFN β .F (5'-AAGAGTTACACTGCCTTTGCCATC-3') and Mus.IFN β .R (5'-CACTGTCTGCTGGTGGAGTTCATC-3') with the mouse GusB housekeeping gene being detected using Mus.GusB.Fi (5'-GGAGGTA CTTCAGCTCTGTGAC-3') and Mus.GusB.Ri (5'-TGCCGAAGTGACTCGTTGCCAA-3').

Statistical Analysis

All quantitative data shown are from a minimum of three independent biological replicates, unless more replicates are specifically stated. All *in vivo* data involved the use of two independent preparations of viral inoculum to control for prep-to-prep effects. In all cases, the data shown represents the quantitative mean with the error bars representing the standard deviation of the means. Quantitative data obtained from *in vivo* experiments are represented by the geometric means and their respective errors. Where appropriate, the statistical analysis of ratios was performed using variable bootstrapping, as previously described [76]. Pairwise statistical analyses were conducted using unpaired Student's t-tests, with a minimum threshold p-value of < 0.05 being accepted as statistically significant. The statistical interpretation of next-generation sequence and ontological enrichment data relied on the use of Bonferroni corrections

Results

The CP/IRAK1 Interaction is Mediated by Domain RII of the Alphaviral Capsid Protein

As we have previously demonstrated that the alphaviral CP protein interacts with the host IRAK1 protein, we sought to determine the necessary and sufficient interaction determinants of the CP protein to better understand the interaction with the long-term goal of developing interaction-deficient viruses. The alphaviral CP protein contains three functional domains. The first N-terminal domain, the RI

domain, is a polybasic and proline-rich domain that is responsible for RNA packaging into the nucleocapsid core, presumably by electrostatic interactions between the polybasic residues of the CP protein and the negative phosphodiester backbone of the RNA cargo [114]. The second domain, the RII domain, is responsible for vRNA specificity when packaging the RNA cargo into the nucleocapsid core, and the release of the RNA cargo during disassembly [115, 116, 312, 336]. Finally, the third domain, the C-terminal Protease domain, bears similarity to the host protease HTRA, and is responsible for cleaving the CP protein off the structural polypeptide which consists of the remaining structural genes synthesized during viral structural protein expression [111, 337, 338]. In addition to the functional protease activity, the Protease domain is also responsible for forming the bulk of the structure of the nucleocapsid cores via interprotein interactions, and responsible, at least in part, for the assembly and release of infectious particles via an interaction with the cytosolic tail of E2 [338-341].

To define the interaction determinants, the previously described SINV CP nanoluciferase BiMolecular Complementation (BiMC) system was used to assess a series of mutant SINV CP truncation constructs, resulting in the creation of a panel of SINV CP constructs with deletions of one or two domains in a stepwise fashion (as shown in Fig. 4.1A). This approach allows for the qualitative and quantitative assessment of the CP/IRAK1 interaction via luminescence detection, as nanoluciferase activity is restored via BiMC when, and only if, a cognate SINV CP protein truncation mutant is capable of interacting with the corresponding IRAK1 BiMC construct.

As shown in Fig. 4.1B, the SINV CP/IRAK1 interaction is mediated by specific determinants within the N-terminus of the SINV CP protein. The RI domain was dispensable to the CP/IRAK1 interaction as the deletion of the RI domain (as per the Δ RI mutant) increased the BiMC of nanoluciferase by approximately two-fold relative to the full-length SINV CP protein (as per WT SINV). Nonetheless, extending the Δ RI truncation mutant to include the RII domain, as per the Δ RI/II mutant, resulted in the near complete loss of BiMC. Together these data strongly implicate the RII domain as the primary interaction determinant. Nonetheless, from these data, it remained possible that the Protease domain contributed to the interaction, as the Δ RI construct exhibited increased BiMC relative to full-length SINV CP protein. To determine whether the Protease domain contributed to the CP/IRAK1 interaction the capacity of a SINV CP protein construct lacking the Protease domain (as per Δ Pro) to engage in BiMC with IRAK1 was evaluated. As shown by Fig. 4.1B, the deletion of the protease domain resulted in no significant change in BiMC activity compared to full-length CP protein, indicating that the protease domain does not contribute substantially to the interaction with IRAK1. Lastly, to confirm the specifics of the individual contributions of the N-terminal domains to the CP/IRAK1 interaction the above efforts were followed up with constructs expressing either the RI or RII domains in isolation. As shown in Fig. 1B, the CP/IRAK1 interaction was entirely dependent on residues in the RII domain, and the RI domain, in its entirety, was dispensable to the CP/IRAK1 interaction (as per RI and RII constructs, respectively).

As the above data indicates that the RII domain of the SINV CP protein was the sole essential IRAK1 interaction determinant, we sought to determine whether the capacity of the RII domain to instigate the CP/IRAK1 interaction was functionally conserved across multiple arthritogenic *Alphavirus* species. To this end, nanoluciferase BiMC constructs encoding the isolated RII domains of Ross River (RRV), Mayaro (MAYV), Chikungunya (CHIKV), and Semliki Forest (SFV) were assessed for their capacity to interact with IRAK1 and restore nanoluciferase activity via BiMC. As shown in Figure 4.1C, all aforementioned arthritogenic alphavirus RII domains were capable of restoring nanoluciferase activity via IRAK1 BiMC relative to the control condition.

Collectively, these data indicate that the RII domain of the SINV CP protein contains the necessary and sufficient CP/IRAK1 interaction determinants; and that the conservation of the RII domains' capacity to elicit the CP/IRAK1 interaction is indicative of not only the importance of the CP/IRAK1 relationship but also the ubiquitous nature of this interaction amongst the arthritogenic alphaviruses. More importantly, identifying the elements of the SINV CP protein responsible for the CP/IRAK1 interaction enables the further evaluation of the repression of IRAK1-dependent signaling via the development of SINV CP mutants.

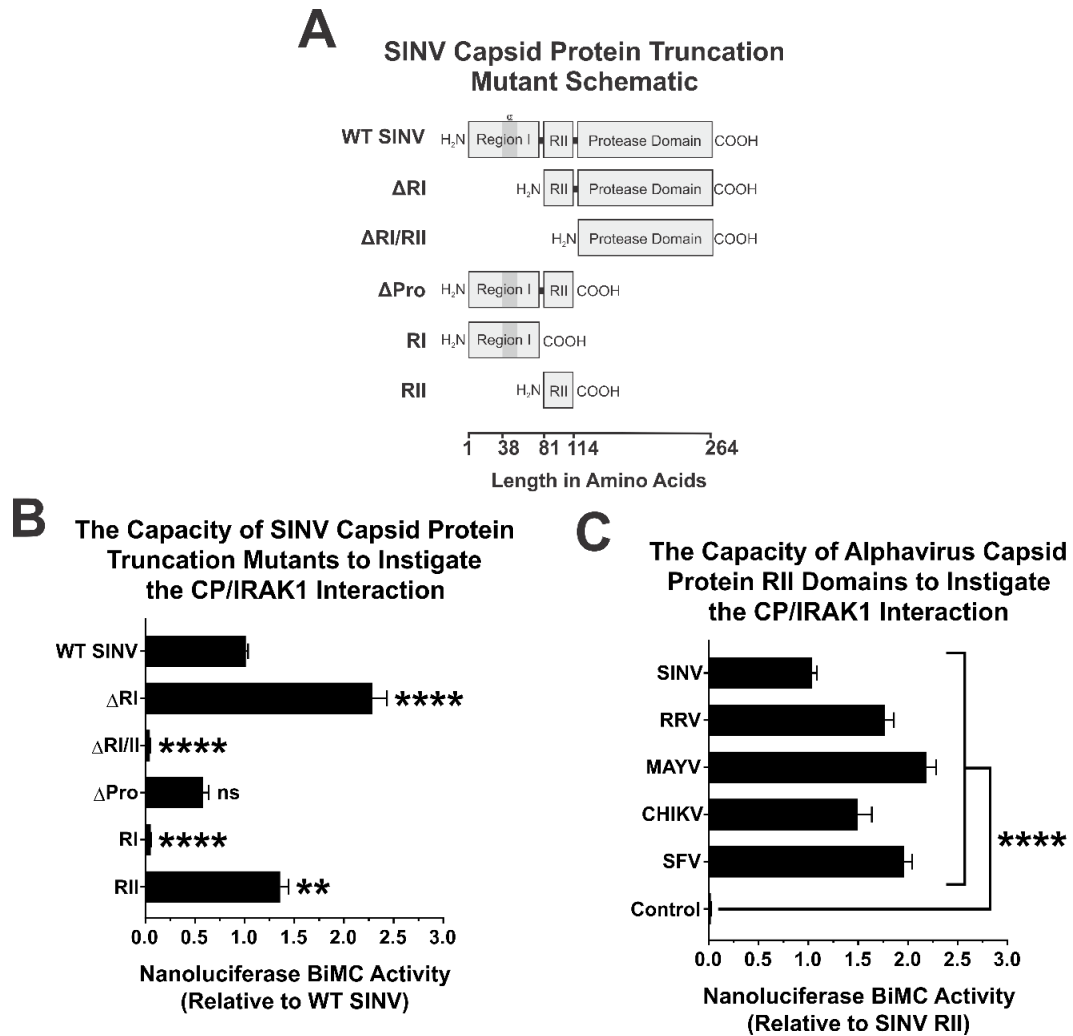


Figure 4.1- Functional Mapping of Capsid to IRAK1 Interaction

(A) Using nanoluc BiMC a series of truncated CP expression plasmids was developed to map the interaction of IRAK1. (B) From these mutants it was found that RII domain is necessary to facilitate interaction with IRAK1. (C) RII fragments from several Alphaviruses were tested and showed that RII is conserved as the interaction site for IRAK1.

The SINV RII Domain is Insufficient to Impart Total Loss of Signaling

After determining that residues in the RII domain were the primary CP/IRAK1 interaction determinant, we set out to determine if the RII domain alone was sufficient for the disruption of IRAK1-dependent signaling activity; or alternatively, if the consequences of the CP/IRAK1 interaction were dependent on the whole CP protein or a subset of CP protein domains. To accomplish this, the aforementioned SINV CP truncation mutants were evaluated for their capacity to interfere with IRAK1-dependent signaling in a tissue culture reporter model system. Specifically, a HEK293-derived TLR7-responsive reporter cell line that expresses Secreted Embryonic Alkaline Phosphatase (SEAP) when stimulated with the TLR7-specific agonist CL307 was used to determine the contributions of the SINV CP protein domains by way of assessing the maximal activation and dose-responsiveness of the TLR7 receptor after agonist treatment in the presence and absence of SINV CP protein [271, 272, 276-279, 342-347].

To define the specific contributions of the individual SINV CP domains, the TLR7 reporter cells were transfected with the SINV CP protein truncation mutants and treated with the TLR7-specific agonist CL307 over a broad dose range to trigger TLR7 activation in a quantifiable manner. As previously demonstrated, the transfection of an expression plasmid encoding full-length wild-type SINV CP protein caused a substantial reduction in IRAK1-dependent TLR signaling, as evidenced by significantly reduced maximum SEAP production/activity and a significant shift in dose responsiveness as evidenced by the EC₅₀_{MAX} (as shown in Fig. 4.2A). As BiMC identified the RII domain as containing the primary

interaction determinant, the assessment of the capacity of the RII domain (in isolation) to inhibit IRAK1-dependent signaling was prioritized. As shown in Fig. 4.2B, the expression of the RII domain alone was sufficient to repress IRAK1-dependent signaling; however, the overall effects were muted relative to those observed with the full-length SINV CP protein. Specifically, expression of the RII domain elicited a minor decrease to maximal activation levels, and a ~5-fold shift of the amount of agonist required to reach $EC_{50_{MAX}}$. While these differences are biologically significant, they fall far short of the near-total inhibition of TLR7 signaling observed with the expression of the full-length CP protein. Thus, to define whether other domains of the SINV CP protein contribute to the repression of IRAK1-dependent signaling, these efforts were expanded to include the other truncation mutants that include the RII domain. Interestingly, the inclusion of either the RI domain or the Protease domain alongside the RII domain did not result in increased suppression of IRAK1-dependent signaling (as per Figs. 4.2C and D, respectively). Consistent with this observation is the fact that neither the RI domain nor the Protease domain individually contributed to the repression of IRAK1-dependent signaling (Fig 4.3).

Taken together these data agree with the above BiMC analyses and demonstrate that elements of the RII domain are necessary for both the interaction with IRAK1 and the inhibition of IRAK1-dependent signaling. Interestingly, while the RI and Protease domains do not contribute towards facilitating the CP/IRAK1 interaction, the presence of both domains was necessary for the exceptionally robust repression of IRAK1-dependent TLR signaling by the SINV CP protein.

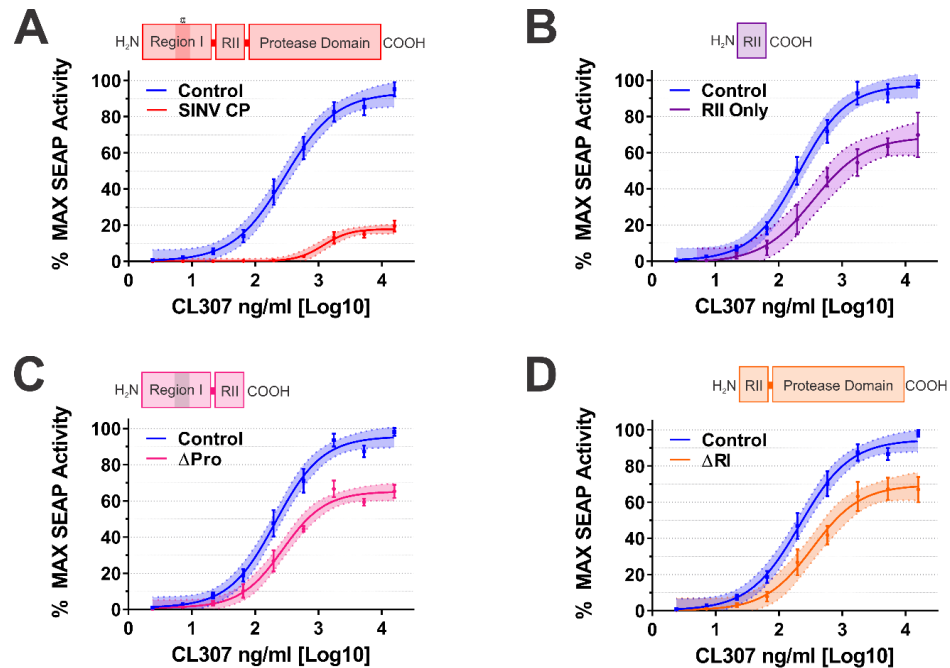


Figure 4.2- Functional Analysis of Different Capsid Fragments to Block IRAK1 Related Signaling

(A) In SEAP reporter cells that respond to the TLR7 agonist CL307 full-length CP shows almost complete inhibition of SEAP production indicating TLR response is disrupted. (B) RII only expression plasmid shows a modest but significant decrease in TLR activity. (C&D) Deletion of the protease domain or RII did not ablate the reduction in TLR activity, but it was recovered compared to full-length CP.

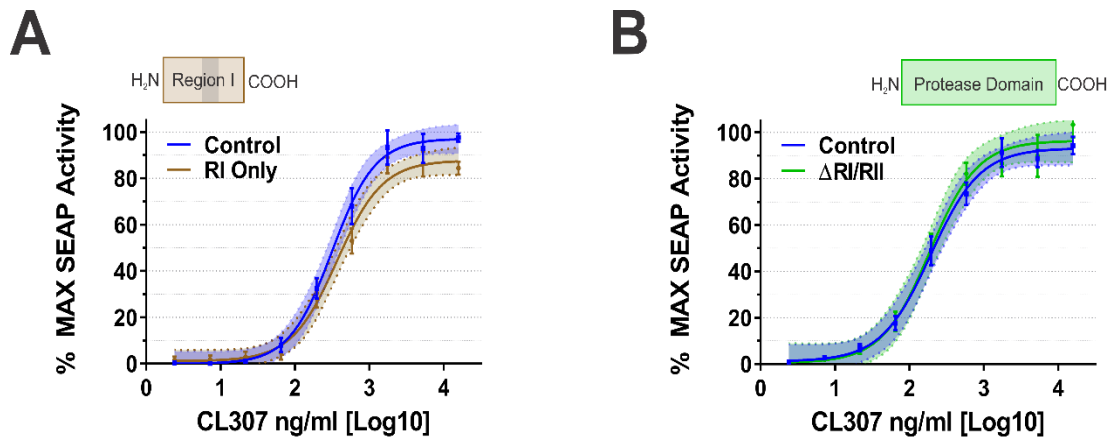


Figure 4.3 RI and Protease Domain are Incapable of Repressing TLR Activity

TLR 7 reporter cells transfected with either RI (A) or Protease Domain (B) on their own showed no inhibition of TLR activity.

Mutation of the RII Domain of the SINV CP Protein Ablates the Inhibition of IRAK1-Dependent Signaling

The identification of the necessary and sufficient CP/IRAK1 interaction determinants enables the use of a reverse genetics approach to develop CP/IRAK1 interaction deficient viruses by which the significance of the interaction to infection and pathogenesis could be assessed. Nonetheless, the RII domain has several important roles during alphaviral infection, and thus the capacity to make mutations is constrained by alphaviral biology. Prior examinations of the SINV RII domain have demonstrated that the leading 15 amino acids of the domain are dispensable for viral replication and assembly in highly permissive tissue culture cell models of infection [348]. Armed with this knowledge a SINV CP deletion mutant lacking amino acids 81 through 95, SINV.ΔRII, was generated using existing Toto1101 and AR86 infectious clones (Fig. 4.4A).

As the RII domain has been previously identified to mediate several critical structural aspects of alphaviral infection, the one-step growth kinetics of the SINV.ΔRII mutant were evaluated in BHK-21 cells which are highly permissive to alphaviral infection. As demonstrated by the data in Fig. 4.4B, the SINV.ΔRII mutant exhibited no over-defects relative to wild-type SINV AR86, reaffirming the prior observations that these residues were unessential in highly permissive models of infection. Similar observations were made using Toto1101-derived SINV.ΔRII mutants.

After confirming that SINV.ΔRII mutant virus had no defects regarding replication and growth kinetics, we next sought to demonstrate that this deletion

was sufficient to restore IRAK1-dependent signaling activity during infection. To this end, IRAK1-dependent signaling was assessed in TLR7 reporter cells which had been either mock infected or infected with either SINV.WT or SINV.ΔRII. As shown in Fig. 4.4C, IRAK1-dependent signaling remains largely intact during SINV.ΔRII infections, as the concentration of TLR7 agonist required to reach EC50_{MAX} during SINV.ΔRII infection was indistinguishable from that of mock-infected cells. Curiously, despite a complete restoration of dose-responsiveness, the maximal activation observed during SINV.ΔRII infection was consistently reduced by approximately 20% relative to the control. While not currently understood, the reduction in maximal activation appears to be specific to SINV infections, as the exogenous expression of a SINV CP protein mutant where the region of interest has been replaced with alanine residues fails to negatively impact IRAK1-dependent signaling (Fig 4.4).

From these data, we conclude that the repression of IRAK1-dependent signaling is dependent on residues within the N-terminal region of the RII domain, and that the repression of IRAK1-dependent signaling can be relieved by breaking the interaction between CP and IRAK1 through mutation of the SINV CP protein. Furthermore, these data indicate that the CP/IRAK1 interaction deficient mutant virus SINV.ΔRII is viable and represents a means by which the importance of the CP/IRAK1 interaction to infection and pathogenesis may be tested during genuine viral infections *in vivo*.

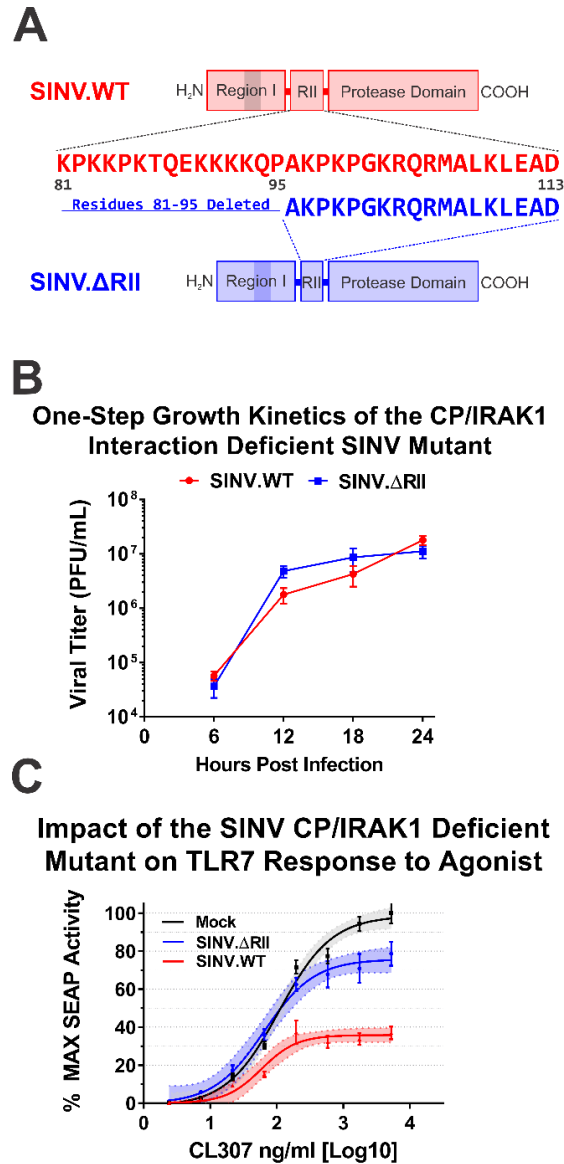


Figure 4.4 Deletion of RII Ablates the IRAK1 Interaction Without Disrupting Viral Replication

(A) Amino acid map of RII, the leading 15 amino acids were deleted to make SINV.ΔRII. (B) Deletion of the RII segment had no impact on viral growth kinetics. (C) Infection of TLR7 reporter cells with SINV.ΔRII shows restored TLR activity for all but the highest concentrations of agonist.

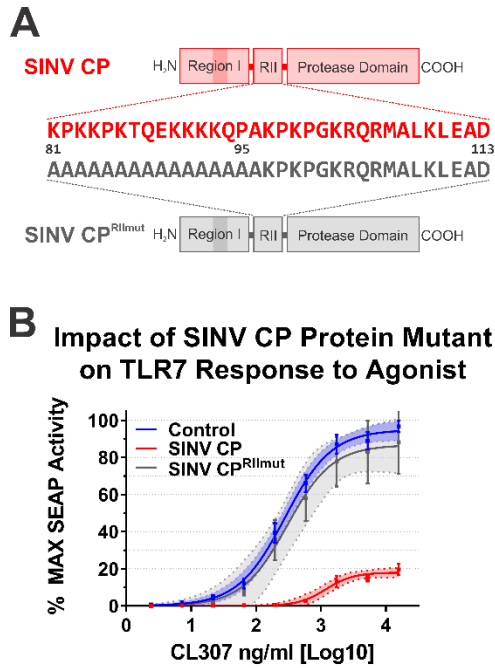


Figure 4.5 Mutation of the Leading 15 Amino Acids of RII Ablates TLR Repression

(A) Genomic map of RII and the 15 amino acids mutated to alanine for SINV CP^{RIImut} expression plasmid. (B) When TLR 7 reporter cells were transfected with SINV CP^{RIImut} they had no loss in TLR activity across all measured concentrations of agonist.

The SINV Δ RII Mutant is Significantly Attenuated *In Vivo*

Knowing that the CP protein of SINV. Δ RII is incapable of repressing IRAK1-dependent signaling leading we next sought to determine the role of the CP/IRAK1 interaction, and the importance of the inhibition of IRAK1-dependent signaling, to alphaviral pathogenesis *in vivo*. To this end, 4-week-old C57BL/6J mice were inoculated via rear footpad injection with either sterile PBS (as a mock infection), SINV.WT, or SINV. Δ RII at a dose of 10^4 PFU in a volume of 10ul. After inoculation, the mice were monitored for signs of neurological pathogenesis, including weakness; limb dragging; paralysis; and weight loss or gain. As shown in Fig 4.6A, mice that were infected with SINV.WT had a mean survival time (MST) of approximately 6 days post-infection (dpi) and showed significant weight loss compared to mock-infected animals (Fig. 4.6B). In contrast to infections of SINV.WT, all mice infected with SINV. Δ RII via footpad injection survived the infection, suggesting that the SINV. Δ RII virus is heavily attenuated *in vivo*. In parallel with the survival analyses, the development of clinical disease was quantified via an established scoring system. Like the aforescribed survival and weight-loss observations, mice infected with SINV.WT exhibited pronounced neurological disease as all mice exhibited limb paralysis in at least one limb, whereas mice infected with SINV. Δ RII showed no signs of neurological clinical disease (Fig. 4.6C).

To better understand the phenotypic consequences of allowing IRAK1-dependent signaling during SINV infection, the capacity of SINV. Δ RII to disseminate from the site of inoculation to the brain was assessed through the

quantitative analysis of viral loads in target tissues at several times post-infection. Specifically, ankle, quadricep, blood, and brain samples were taken at 1-, 3-, and 5dpi, and viral titers were quantitatively assessed. As shown in Figs. 4.6D and E, the viral titers of SINV. Δ RII were approximately 100-fold lower than those of SINV.WT in infected ankle tissues at 1- and 3-dpi, respectively. Despite reduced replication in tissues proximal to the site of inoculation, SINV. Δ RII was able to disseminate into the blood, albeit to levels approximately 100-fold lower than those observed for SINV.WT (Fig. 4.6F). Nonetheless, despite being able to cause viremia, SINV. Δ RII failed to disseminate into other tissues as evidenced by the absence of detectable infectious virus in either the quadriceps muscle or the brain, at 1- and 3-; and 5dpi, respectively (Figs. 4.6G, H, and I).

These data illustrate the importance of the SINV RII domain to SINV neurovirulence, as the SINV. Δ RII mutant exhibited reduced titers *in vivo* and a failure to disseminate into other target tissues following the development of viremia. Accordingly, a major conclusion from these data is that the CP/IRAK1 interaction, and by extension the loss of IRAK1-dependent signaling, is critical to SINV neuroinvasion and pathogenesis.

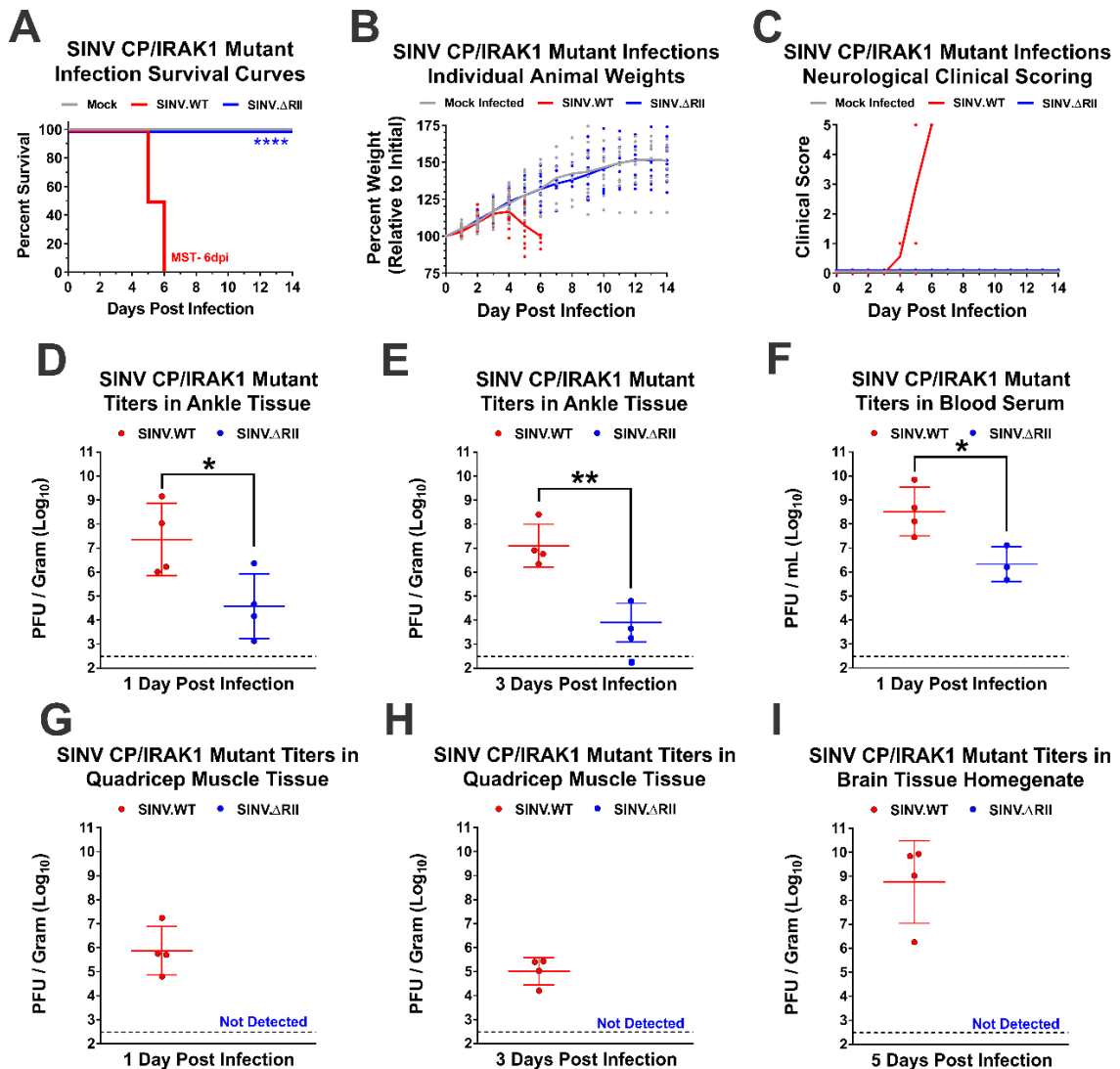


Figure 4.6- *In Vivo* infections of SINV.ΔRII Shows Attenuation of the Virus

(A) SINV.WT infected mice succumbed to infection after 6dpi while the SINV.ΔRII mice survived. (B) SINV.ΔRII infected mice showed weight gains comparable to mock infected mice while SINV.WT mice rapidly lost weight. (C) SINV.ΔRII showed no neurological scoring during infection while SINV.WT infected mice showed severe neurological defects. (D&E) Viral replication was measured for 1 and 3dpi in the ankle but at both time points SINV.ΔRII was significantly lower than SINV.WT. (F) SINV.ΔRII escapes into the blood to cause

viremia but titers are lower than SINV.WT. (G, H, & I) While SINV. Δ R11 was able to escape into the blood it fails to disseminate to secondary sites of infection including quadriceps and brain.

Bypassing Neuroinvasion via Intracranial Infection Results in Neuropathogenesis

As the above data indicated that SINV. Δ R11 was failing to disseminate from the site of inoculation to the brain, we sought to determine whether neurovirulence would be restored following direct inoculation of the virus into the brain. To test this, 4-week-old C57BL/6J mice were given intracranial (IC) injections with either PBS (as Mock infected), SINV.WT, or SINV. Δ R11 at a dose of 10^4 PFU in 10 μ l. As above, the experimentally infected animals were monitored for signs of morbidity and mortality, including signs of neurological disease and weight loss. As shown in Fig. 4.7A, SINV.WT-infected animals exhibited an MST of 4dpi, whereas SINV. Δ R11 infected animals had an MST of 5.5dpi. Despite exhibiting mortality in these studies, the SINV. Δ R11 infected mice displayed a different course of clinical illness from those infected with SINV.WT. As depicted in Fig. 4.7B, the SINV. Δ R11 infected animals had a more gradual weight loss profile than SINV.WT infected animals, and whereas all SINV.WT animals exhibited pronounced neurological disease only moderate clinical signs (yet moribund as per our euthanasia criteria) was observed in two experimentally infected SINV. Δ R11 animals (Fig. 4.7C). The remaining SINV. Δ R11 infected animals met weight loss criteria despite demonstrating no outward signs of neurological disease other than limited limb weakness. The weight loss observed in these experimentally infected mice may be alternatively explained by dehydration rather than infection per se (as the animals displayed signs of clinical dehydration, including tenting of the skin when gently pinched).

While these data indicate that SINV. Δ R11 has the capacity to be neurovirulent if directly introduced into the brain, to be thorough in our analyses we quantitatively evaluated the brains of the infected animals for viral replication. Specifically, at 1- and 3dpi the brains of the experimentally infected animals were harvested and measured for viral titer. Interestingly, following IC infection the titers observed for SINV. Δ R11 were still approximately 100-fold less than that of SINV.WT (Fig. 4.7D and E); however, it is notable that the levels of SINV. Δ R11 in the brain of the infected animals were roughly equivalent to that observed in the brains of animals infected with SINV.WT via footpad injection (Fig. 4.6I).

Transcriptomic Analyses Reveal Similar Inflammatory Profiles Despite Differing Viral Burdens

To better understand the consequences of, and inflammatory response to, SINV infection, next-generation sequencing of IC-infected brains 3dpi was performed. As shown in Fig. 4.8A, SINV.WT infection resulted in the differential expression of many host transcripts; and, as expected, SINV. Δ R11 infection also resulted in a similar expression profile relative to wild-type SINV (Fig. 4.8B). Indeed, comparative differential transcriptomic analysis between the SINV.WT and SINV. Δ R11 IC infections reveals a high degree of overall similarity between the experimentally infected groups, as comparatively few host transcripts were differentially expressed beyond the customary 2-fold change window relative to the comparisons involving mock-infected animals (Fig. 4.8C).

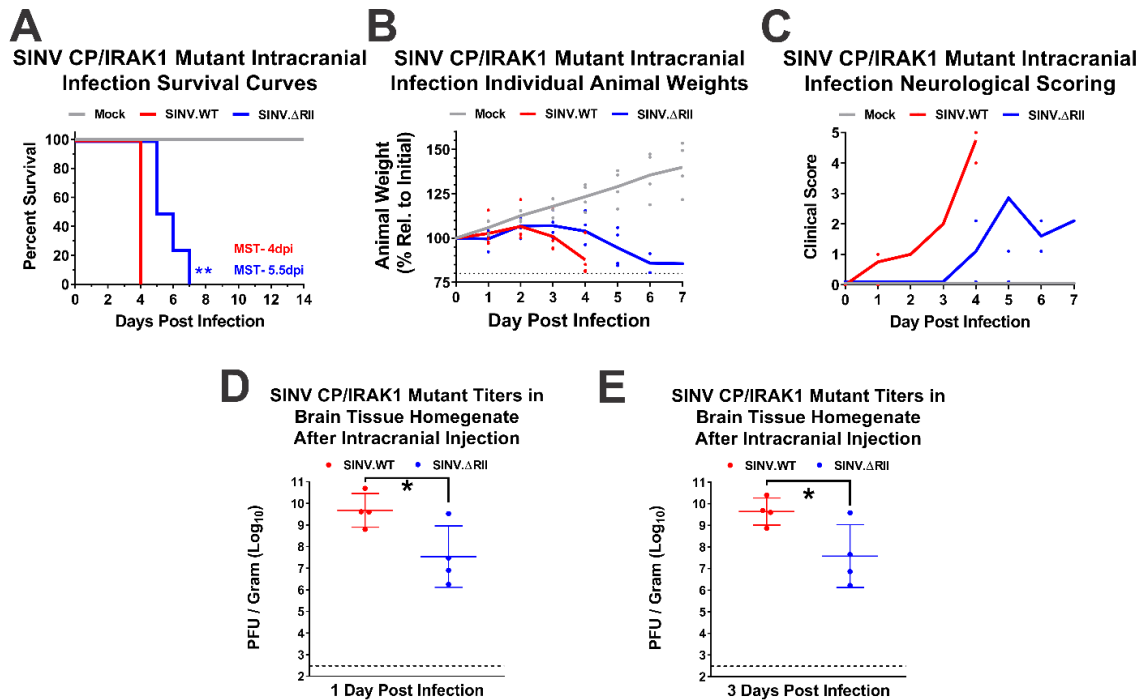


Figure 4.7- Intracranial Infections with SINV.ΔRII Cause a Less Severe Disease Than SINV.WT

(A) SINV.WT mice succumbed to infection at MST of 4dpi. While the intracranial injection of SINV.ΔRII was lethal it was delayed compared to SINV.WT with a MST of 5.5dpi. (B) SINV.ΔRII infected mice showed severe weight loss but it was delayed compared to SINV.WT. (C) SINV.ΔRII neurological symptoms were not as severe as SINV.WT and mice were starting to recover from them by the end of the experiment. (D & E) At 1 and 3 dpi SINV.DRII showed lower titers compared to SINV.WT

Ontological analyses of the up-regulated transcripts detected in whole brain homogenates from SINV.WT and SINV. Δ RII experimentally infected mice revealed similar biological process enrichment profiles. Unsurprisingly, the majority of the statistically enriched biological process ontological categories found to be upregulated in both SINV.WT and SINV. Δ RII infections centered around the host antiviral and innate immune response (Fig. 4.8D). Surprisingly, however, is that similar magnitudes of inflammation were observed at the transcriptomic level despite viral burdens between the two infections differing by on average 100-fold, with a mean difference in fold change between the common ontological groups of $\sim 1.08 \pm 0.09$. The enrichments observed with SINV. Δ RII mutant infections were in modest excess relative to wild-type infections for several biological process ontological categories, including positive regulation of autophagy ($\sim 23\%$ in excess), antigen processing and presentation of exogenous peptide antigen by MHC class II ($\sim 19\%$), and cell surface signaling pathway ($\sim 17\%$); however, none of these differences were statistically different from the group. The enrichments of two biological process categories identified as commonly upregulated were decreased in SINV. Δ RII mutant infections relative to wild-type infections to a statistically significant extent compared to the group, including positive regulation of angiogenesis ($\sim 15\%$ in deficit) and response to cytokine ($\sim 10\%$). Nonetheless, while the majority of upregulated biological process categories were common, both SINV.WT and SINV. Δ RII infections resulted in unique upregulation profiles, as shown in Figs. 4.8E and F.

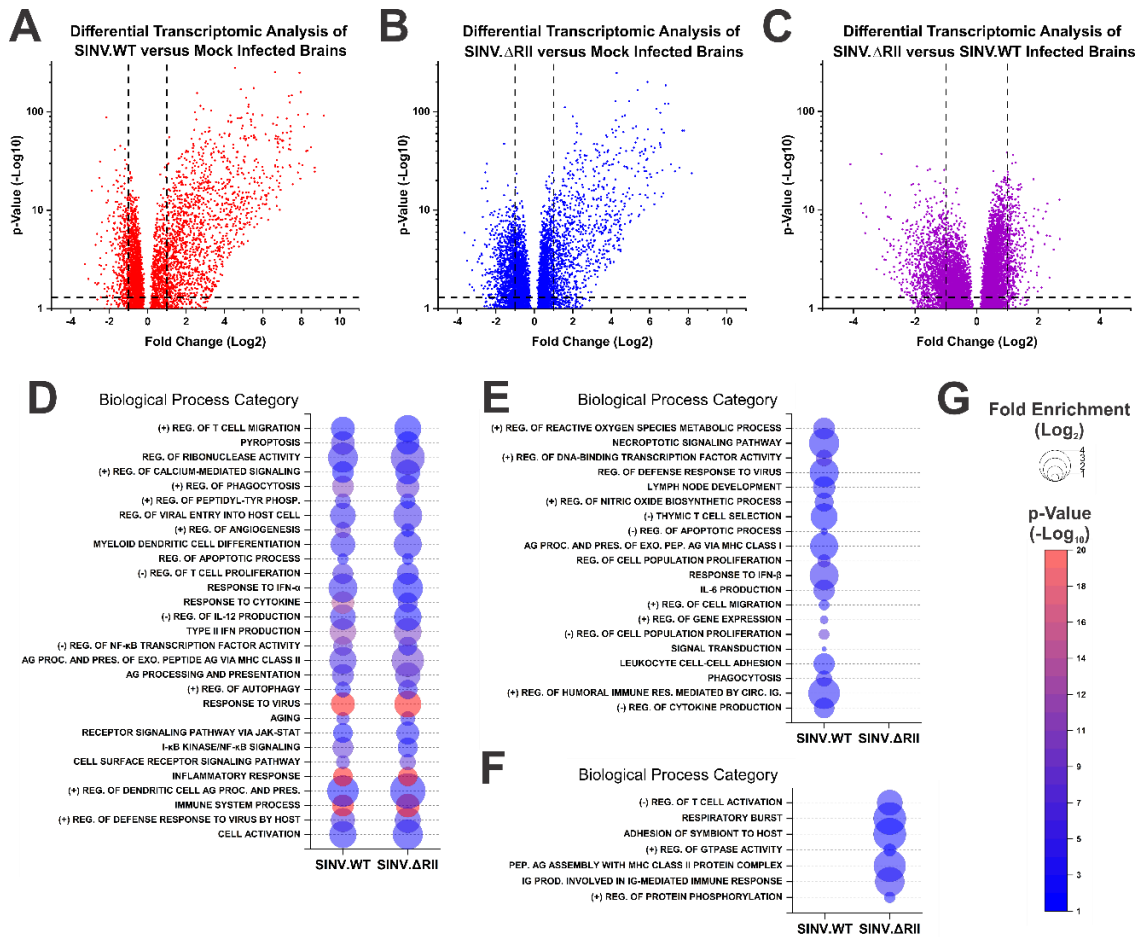


Figure 4.8- RNAseq of Intracranial Infected Brains 3dpi

(A, B, & C) Volcano plots differentially expressed transcripts of SINV.WT vs. Mock, SINV.ΔR11 vs. Mock, and SINV.ΔR11 vs. SINV.WT infection. This reveals there are differentially expressed genes between the SINV.WT and SINV.ΔR11. (D) The top upregulated Biological Processes shared between SINV.WT and SINV.ΔR11. (E & F) Uniquely upregulated biological process in SINV.WT or SINV.ΔR11. (G) Key for Fold enrichment circle diameter and p-value color scale.

Parallel biological process ontological analyses of down-regulated transcripts revealed little further insight into the underlying inflammatory process, as no biological process categories were shared between SINV.WT and SINV. Δ R11 infections, and the uniquely enriched categories were not directly related to host inflammation or the resolution of infection (Fig. 4.9).

The high degree of similarity between the transcriptomes of SINV.WT and SINV. Δ R11 infected brains is suggestive of differential inflammatory stimulation potentials with respect to viral burden. This assertion is based upon the fact that while a ~100-fold difference in viral titer is observed between the two experimental infections, the transcriptomic differences are exceptionally modest as shown in Fig. 4.8C. Nonetheless, from these data it cannot be directly concluded as to whether the SINV. Δ R11 mutant elicits a more pronounced antiviral response, or whether the response is equivalent between SINV.WT and SINV. Δ R11 yet the SINV. Δ R11 is acutely more sensitive to the innate immune response resulting in diminished viral loads.

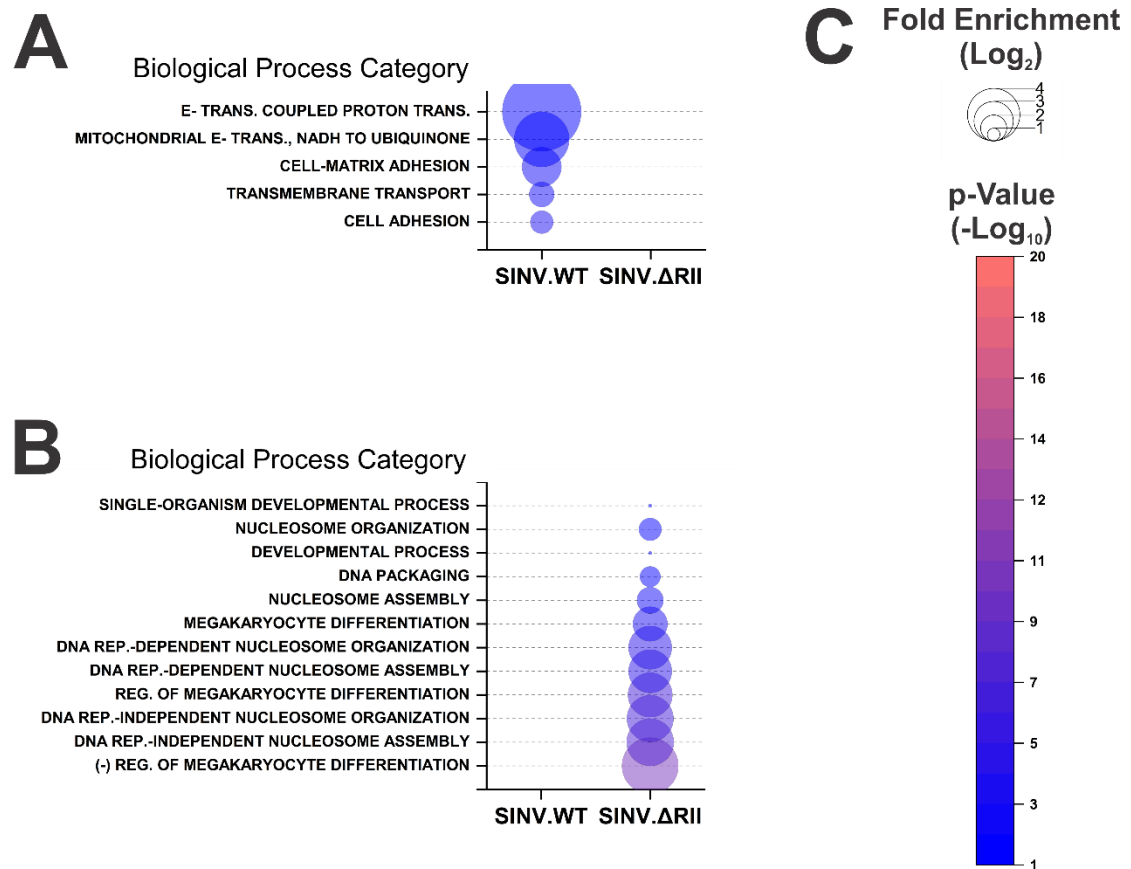


Figure 4.9 Down Regulated Biological Processes from Intracranial Infected Mice

(A & B) Uniquely downregulated biological process in SINV.WT or SINV.ΔRII. (C) Key for Fold enrichment circle diameter and p-value color scale.

The SINV ΔRII Mutant Induces Increased Type-I IFN Expression in Infected / Exposed Macrophages

As SINV.ΔRII was largely incapable of repressing IRAK1-dependent signaling during infection, we hypothesized that the inability of SINV.ΔRII to disseminate *in vivo* may be due to increased induction of Type-I IFN in an IRAK1-dependent manner. As IRAK1-dependent innate immune sensing relies on the detection of extracellular or vesicular PAMPs [349], the experimental design focused on evaluating the response to viral particle-associated PAMPs during wild-type and CP/IRAK1 interaction deficient infections.

To test the above hypotheses, C57BL/6-derived macrophages were either mock infected, infected with SINV.WT, or infected with SINV.ΔRII using equal numbers of viral particles (at an MOI of 10 genome equivalents per cell) to ensure equivalent delivery of any virion-associated PAMPs. At 4 hours post-infection the cells were harvested, and the total RNA was extracted via TRIzol for analysis of IFN β expression levels by way of qRT-PCR. As shown in Fig. 7A, macrophages infected with SINV.WT showed expression of IFN β mRNA at levels comparable to mock-infected cells. In contrast, SINV.ΔRII infections induced significantly higher levels of IFN β mRNA induction compared to SINV.WT (Fig. 7A). These data suggest that without the CP/IRAK1 interaction afforded by the RII domain of the SINV CP protein, the viral particle-associated PAMPs are more readily recognized and responded to by IRAK1-dependent innate immune sensors of viral infection, including the TLRs.

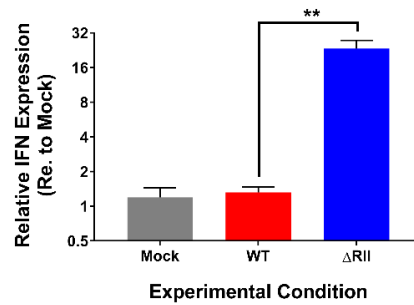
To confirm that the stimulation of IFN β expression observed during SINV. Δ R11 infection was specifically due to IRAK1-dependent signaling, we treated wild-type macrophages with JH-X-119-01, a small chemical inhibitor of IRAK1 that covalently binds to the active site and permanently blocks kinase activity and reassessed the capacity of the host to sense viral PAMPs and induce type-I IFN expression. As shown in Fig. 7B, mock, SINV.WT, and SINV. Δ R11 infections of wild-type macrophages treated with JH-X-119-01 elicited similar levels of IFN β mRNA expression, indicating that the induction of the innate immune response by viral particle-associated PAMPs was indeed IRAK1-dependent.

To further confirm that the trigger of IFN- β induction observed in SINV. Δ R11 infected macrophages was indeed an IRAK1-dependent TLR, MyD88^{-/-} macrophages were assessed using the same experimental conditions as the WT macrophages. As depicted by the data presented in Fig. 7C, MyD88^{-/-} macrophages infected with SINV. Δ R11 showed no increase in IFN β expression when compared to mock or SINV.WT-infected macrophages. These data suggest that all IFN β expression observed in the WT macrophages infected with SINV. Δ R11 comes from a MyD88-dependent signaling pathway.

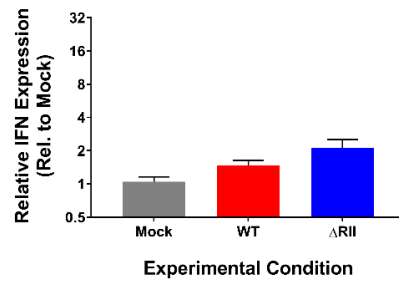
In conjunction with the *in vivo* data above, these *in vitro* data support the hypothesis that the CP/IRAK1 interaction is essential to evading the induction of an innate immune response through the detection of viral-associated PAMPs. Given that the differential induction of an innate immune response was largely lost in the absence of MyD88^{-/-}, it is probable that viral PAMP detection is occurring via one, or more, of the host TLRs responsive to positive-sense RNA virus PAMPs,

such as TLR7 and TLR8. Importantly, these *in vitro* observations are in firm alignment with the restricted dissemination of SINV.ΔRII as alphaviruses are exceptionally sensitive to the impacts of the host innate immune response.

A Induction of IFN β mRNA Expression During Infections of Wild Type Macrophages



B Induction of IFN β mRNA Expression During Infections of JH-X-119-01 Treated Macrophages



C Induction of IFN β mRNA Expression During Infections of MyD88^{-/-} Macrophages

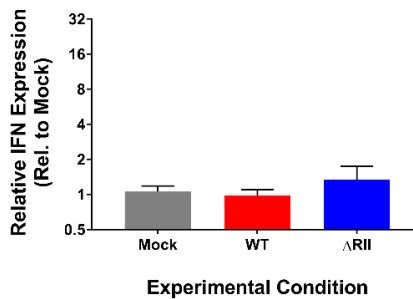


Figure 4.10- C57BL/6 Mice Derived Macrophages Showed Increased IFN- β Induction in SINV. Δ RII Infections

(A) WT macrophages from C57BL/6 mice were infected for four hours SINV.WT, or SINV. Δ RII or mock infected. IFN- β levels were measured by qPCR and showed that SINV. Δ RII induced significantly higher levels of IFN- β compared

to SINV.WT. (B) WT macrophages were treated with JH-X-119-01, an IRAK1 inhibitor, prior to the same infection conditions in A. These macrophages failed to induce IFN- β in the presence of SINV. Δ RII. (C) Macrophages from C57BL/6 MyD88^{-/-} mice were infected with the same conditions as A and when IFN- β levels were measured the SINV. Δ RII infected cells failed to induce INF- β .

Discussion

Here we have demonstrated that the CP/IRAK1 interaction, via the inhibition of IRAK1-dependent signaling, is a novel virulence determinant in alphaviral infection that is critical to the evasion of the innate immune response. This conclusion is supported by the body of evidence indicating that disruption of the functional consequence of the CP/IRAK1 interaction resulted in viral PAMP detection leading to the loss of neuroinvasion due to a severe restriction of SINV infection *in vivo*. As described earlier in the introduction, it has been classically believed that the inhibition of host macromolecular synthesis is the primary means by which the alphaviruses evade the effects of the type-I IFN system [90, 321]. Since this classical evasion mechanism requires viral gene expression, a window of opportunity for the host to detect viral PAMPs and mount an antiviral response existed early in infection and is ever present in non-permissive host cells[90, 281, 284, 318-320]. The data presented here represents one means by which the alphaviruses have closed this window, as the inhibition of IRAK1-dependent signaling effectively precludes the sensing of PAMPs by host TLRs without the need for viral gene expression. Thus, on the basis of all available data, we propose that the CP/IRAK1 interaction represents a means by which the detection of viral-associated PAMPs may be actively evaded prior to cessation of host macromolecular synthesis (Fig. 4.11).

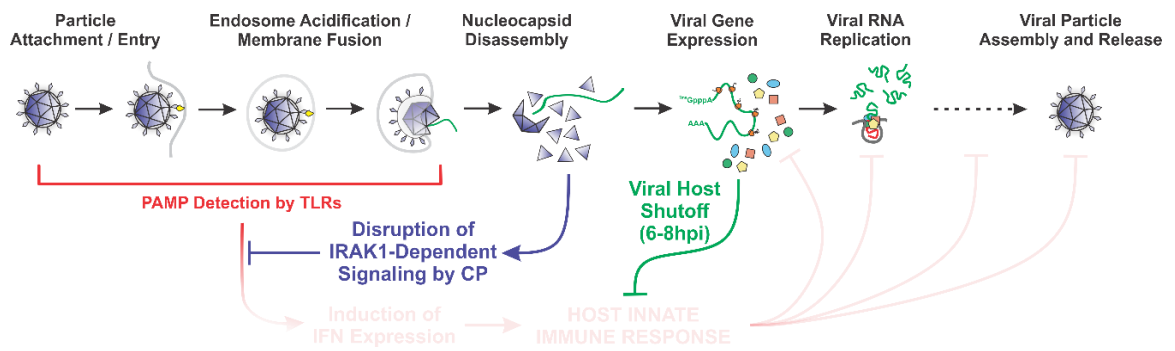


Figure 4.11- Proposed Model for SINV CP:IRAK1 Interaction

The Evasion of IRAK1-dependent PAMP Sensing is Critically Important to SINV Neuroinvasion and Pathogenesis

The data presented here indicates that the alphaviruses have evolved a means by which the activation of the innate immune response can be evaded prior to viral gene expression, enabling alphaviral infection to advance unperturbed during the window of host antiviral opportunity that precedes viral gene expression. Furthermore, as the CP/IRAK1 mediated evasion of IRAK1-dependent PAMP detection does not require viral gene expression, the CP/IRAK1 interaction represents a means by which the detection of viral-associated PAMPs may be masked in permissive and non-permissive cells thereby diffusing the induction of a limiting IFN response induced by exposed but uninfected host cells[335]. Crucially, in the absence of the CP/IRAK1 interaction, the recognition of viral particle-associated PAMPs resulted in the induction of a robust type-I IFN response which correlated with limited viral dissemination *in vivo*, which manifested as a loss of neuroinvasiveness. While it is currently unclear as to which specific host PAMP receptors are detecting which specific viral PAMPs, the receptors responsible for IFN induction during SINV.ΔR11 infection are IRAK1- and Myd88-dependent, leading us to conclude that they are members of the TLR family [213, 350]. For the reasons of alphaviruses being positive-sense RNA viruses, we hypothesize that TLRs 7 and 8 are the most likely TLRs that are sensing PAMPs associated with alphaviral particles [351-354]. As increased signaling was not detected in the TLR7 reporter cell line during SINV.ΔR11 infection it is likely that the primary sensor is TLR8. Nonetheless, the precise IRAK1-dependent sensor

remains unknown at this time, and work designed to identify and define the precise PAMPs, and their respective receptors, is ongoing.

When the need for dissemination to the brain was bypassed via intracranial inoculation, the CP/IRAK1 interaction deficient virus exhibited a unique pathological profile, suggesting that the CP/IRAK1 interaction may play additional roles in alphaviral pathogenesis beyond TLR evasion. While the control of SINV infection via PAMP detection in the brain likely contributes to this phenotype, it should be noted that the host IRAK1 protein is also a critical component of the signal transduction pathways of the host IL-1 superfamily cytokine receptors [324, 355]. Thus, an additional function of the CP/IRAK1 interaction may be to dysregulate the IL-1 response during infection, contributing towards alphaviral pathogenesis via the establishment of an aberrant pro-inflammatory state. Assessing the impact of the CP/IRAK1 interaction on IL-1 signaling during alphaviral infection is important, as IL-1 is known to be a key contributor to alphaviral pathogenesis [356-359]. Efforts aimed at teasing apart the importance of the CP/IRAK1 interaction to IL-1 dysregulation and alphaviral pathogenesis are a key ongoing focus of the Sokoloski Lab.

The RII Domain of the Alphaviral CP Protein is Functionally Complex and Involves the Interactions with Host Factors

These efforts identified a novel function of the alphaviral CP protein RII domain. Prior work in the field has determined that the RII domain is responsible

for the selection of the nucleocapsid cargo during assembly, and the disassembly of the nucleocapsid core during viral entry[115, 117, 118, 314, 348]. These earlier forays on the RII domain delineated the residues required for these nucleocapsid-associated functions of the CP protein, and largely concluded that the N-terminal residues were unimportant for viral infection in highly permissive cell models of infection[348]. Thus, despite the importance of the RII domain to critical assembly and disassembly events in the viral lifecycle, we were still able to develop a mutant virus that abrogated the interaction with IRAK1 while having no appreciable impact on viral growth kinetics.

Using BiMC, the RII domains of several arthritogenic Old World alphaviruses were assessed for their capacity to interact with the host IRAK1 protein. Together these efforts revealed that the capacity of the RII domain to instigate the CP/IRAK1 interaction was conserved across multiple members of the genus. Whether individual *Alphavirus* species differ in their capacity to restrict IRAK1-dependent PAMP detection, perhaps in a manner that correlates with clinical severity or viremia, is unknown at this time. One could envision a scenario where the affinity of the CP/IRAK1 interaction, or the tenacity with which the CP protein negatively impacts IRAK1-dependent signaling, contributes meaningfully to the development of high viral loads and disease *in vivo*. This possibility is particularly worthy of evaluation as it would represent a novel virulence determinant that may be fine-tuned towards the development or improvement of vaccine candidates.

Curiously, despite an apparent functional conservation regarding the CP/IRAK1 interaction, the N-terminal region of the RII domain exhibits a high degree of sequence diversity [117]. Regardless, bioinformatic alignments of the N-terminal regions of the RII domains of the aforementioned viruses putatively identify a conserved motif centered around a conserved threonine residue, specifically Thr87 in the SINV CP protein. Further predictive bioinformatic analysis of this threonine residue motif indicates that it is a likely substrate for cellular Tyrosine Kinase Like (TKL) kinases, including IRAK1. As the phosphorylation of the alphaviral CP protein is known to contribute to CP protein function [287, 288], the potential phosphorylation of the CP protein by IRAK1 may be an important switch during the alphaviral lifecycle, such as during the disassembly or assembly processes. Nonetheless, the precise importance of this potential RII motif, and its potential to act as a substrate for phosphorylation by the IRAK1 kinase remains unknown.

Implications for the Evasion of the Invertebrate Innate Immune System

Though the alphaviral CP protein RII domains exhibit limited sequence conservation, the homologs of the TLRs and IRAK1 kinase demonstrate a high degree of structural and functional similarity across the vertebrate and invertebrate alphavirus hosts [360-364]. Indeed, the mosquito IRAK1 homolog Pelle is synonymous with the IRAK1 protein regarding its role as a critical component of the Toll signal transduction pathway [365-369]. The conservation of the CP/IRAK1 interaction across multiple alphaviruses, the robustness of its consequence to

IRAK1-dependent signaling, and the conservation of the IRAK1 protein across multiple host species are all highly suggestive of a potentially important role for the alphaviral CP protein regarding the evasion of mosquito innate immunity. As invertebrates lack an interferon response, they are heavily reliant on the Toll and IMD pathways to respond to microbial pathogens [370-374]. It is known that alphaviruses are sensitive to Toll and IMD effector proteins, however, the Toll pathway is not appreciably activated during alphaviral infection [375-377]. Thus, given the parallels between the narratives observed for the vertebrate and invertebrate hosts, we postulate that the alphaviral CP protein similarly interacts with the mosquito Pelle protein to evade the induction of the Toll innate immune pathway. The importance of a putative CP/Pelle interaction is unknown at this time, but one could envision the evasion of Toll sensing as being critical to dissemination in the mosquito host, as is required for subsequent transmission during a blood-meal.

Potential Mechanistic Insight into the Impairment of IRAK1-Dependent Signaling by the CP/IRAK1 Interaction

The assessment of the contributions of the individual domains of the SINV CP protein to the inhibition of IRAK1-dependent signaling provides valuable insight into the potential mechanism of inhibition. While the RII domain is a necessary interaction determinant, expression of the RII domain alone is unable to cause the full robust inhibition of IRAK1-dependent signaling that is observed with the full-length SINV CP protein. Inclusion of either the RI or Protease domains alongside

the RII domain failed to recapitulate the phenotype associated with the expression of the full-length SINV CP protein. All together, these data imply that the mechanism of inhibition is facilitated by the presence of both the RI and Protease domains; and although further studies are needed to elucidate the exact mechanism(s) by which the SINV CP protein inhibits IRAK1-dependent signaling, the need for a full-length CP protein suggests that steric hindrance of IRAK1 activity / Protein:Protein interactions are at least partially responsible. Alternatively, it remains possible that the flanking domains of the CP protein serve to stabilize the primary interaction of the RII domain to block the catalytically active site of IRAK1.

CHAPTER 5

CONCLUSIONS AND FUTURE DIRECTIONS

Research Summary

Previous works on the CP proteins of *Alphaviruses* have focused heavily on its role in assembly and virion structure. This has left a gap in knowledge regarding the roles that CP is playing throughout the rest of the viral lifecycle, including those uninvolvement in the assembly of viral particles. This is curious as the CP is stoichiometrically the most concentrated viral product delivered to the cytoplasm of the host cell upon infection, and that during replication and viral gene expression excess CP is produced and remains largely freely available in the cytosol to interact with the host or viral factors to promote pathogenesis. Through our work utilizing the BioID biotin ligase system, we were able to identify a list of potential host factor interactions with CP as well as established that CP interacts with host the IRAK1 protein (Chapter 3). Upon identifying this interaction we validated and confirmed its veracity using nanoluc BiMC which also showed that the CP:IRAK1 interaction is conserved across a wide range of alphaviruses, suggesting this is a crucial interaction for the virus that has been evolutionarily conserved. When assessed using a TLR responsive cell line, IRAK1-dependent signaling was shown to be reduced with during both infections of live and inactive viral particles and

transfections of CP expression plasmids for both infection-relevant and irrelevant TLRs. Similar to the BiMC data, this loss of TLR/IRAK1 signaling when CP was present was found to be conserved across several *Alphavirus* species. These data contribute to a growing body of evidence that the alphaviral CP has significant roles outside of assembly and structure and is a vital virulence factor for helping establish infection and preventing detection by early innate PRRs.

In addition to establishing that CP interacts with IRAK1 to prevent TLR activation of innate immunity, we have been able to map the interaction site of the CP to the RII domain. The efforts into determining the necessary and sufficient residues in the CP have shown that the RII domain, the region responsible for vRNA selectivity as well as nucleation during viral assembly, is crucial to binding to IRAK1 and that no other domain on its own can inhibit IRAK1-dependent signaling. In addition to learning that the RII domain is crucial for this interaction, we have shown that while the RII domain in isolation is capable of some repression of IRAK1-related signaling, the full-length CP is necessary for the complete inhibitory effect of IRAK1-dependent signaling. This could imply that this interaction is through a mechanism involving steric hindrance, and that when RII directs the interaction with IRAK1 the remainder of CP blocks the interaction of IRAK1 with as-of-yet identified factors in the IRAK1-related signaling cascade. Upon identification of the necessary interactant on CP, we were able to develop a mutant virus that lacked the capacity to interact with IRAK1 and the inhibition of IRAK1 signaling (Δ RII). *In vitro* infections of WT C57BL/6-derived macrophages with this virus showed the induction of IFN β at significantly higher levels compared to

infections with the WT virus; in contrast macrophages from MyD88^{-/-} mice or WT mice macrophages treated with an IRAK1 inhibitor showed no IFN β induction, revealing that it was through IRAK1-dependent signaling that this IFN β response was produced. When *in vivo* experiments were performed with Δ RII, it was found that Δ RII infections via a footpad inoculation route exhibited no clinical signs of infection, and while the virus was able to cause mild viremia there was no escape into distal tissues, including the brain whereas wild type SINV rapidly disseminated to the brain within 3dpi.

When it was revealed that footpad infections of Δ RII failed to disseminate to the brain, we bypassed this barrier with direct intracranial injections of the virus to determine the native virulence of the Δ RII mutant. In this experiment, Δ RII showed that it retained lethality, but the onset of disease was significantly delayed compared to WT, unique from WT infection in regard to clinical manifestations of disease, and there was significantly less viral replication in the brain. An RNAseq experiment was performed on the brains of infected mice, which revealed that there were a few enriched biological processes in the Δ RII infected mice compared to WT infections including autophagy and antigen presentation. More interesting than what was different across the two infections, was the observation that the inflammation profiles for both Δ RII and WT infected mice were mostly the same, despite Δ RII titers being ~100-fold less than WT. This suggests that the Δ RII virus elicits a stronger immune response to infection than WT, presumably as the mutant is more readily recognized by TLRs and the host can mount a more robust immune response. While this alone is not enough to conclude that restored IRAK1-

dependent signaling via the loss of the CP:IRAK1 interaction by way of the Δ R11 mutant can generate a more robust immune response, it is in agreement with our *in vitro* data and offers insight into the potential roles of CP interacting with IRAK1 during infection and how this interaction is crucial for pathogenesis.

Mechanism of Action

Presented here is data that shows that the alphaviral CP protein interacts with IRAK1 to disrupt IRAK1-dependent signaling. Nonetheless, from these data we are not able to directly elucidate a mechanism of action for how CP blocks IRAK1-dependent signaling. The IRAK1 protein has several domains that are responsible for its protein interactions, as well as a kinase domain, for functional activity. Depending on where the CP binds to IRAK1 it could be disrupting recruitment to the Myddosome, kinase activity, or interactions with TRAF6 or IRF7 after activation by ligands binding to the TLRs. While the specifics of what stage of IRAK1 signaling CP disrupts remain unknown, we do have preliminary BiMC data that suggests that CP is interacting with the kinase domain of IRAK1. Interacting with the kinase domain is suggestive that CP may not be preventing IRAK1 from being recruited to the Myddosome, or even prevent activation by IRAK4, but is instead preventing any sort of phosphorylation event necessary for the activation of downstream effectors like TRAF6 or IRF7. This also has interesting implications for CP; if the interaction with IRAK1 puts it in or near the active site of the kinase domain, then perhaps the interaction with IRAK1 phosphorylates CP giving the interaction a second role beyond just inhibition of

PAMP detection. Phosphorylation of CP has been shown to be necessary for alphaviral life cycle with CP binding to vRNA and regulation of particle assembly [287, 288]. Whether IRAK1 phosphorylates the alphaviral CP, and to what extent it impacts viral biology, remains an area of active interest.

IRAK1 Interaction Conservation

From our data, we have shown that the interaction between IRAK1 and CP is conserved across several species of alphaviruses, suggesting that this interaction is conserved across the entire family. While the strength and importance of this interaction for other species of alphaviruses have yet to be evaluated, it could be a potential contributor to the range of phenotypic differences alphaviruses exhibit in TLR different systems. From the data presented in Chapter 3, there is a distinct phylogenetic difference in the amount of CP:IRAK1 engagement as measured by nanoluc activity in the BiMC experiments, as the encephalitic alphaviruses showed higher levels of nanoluc activity relative to the arthritogenic alphaviruses. From this, it is tempting to hypothesize that the CP:IRAK1 interaction is stronger and potentially more crucial for the encephalitic alphaviruses; however, there is the caveat that if the expression plasmid for the encephalitic viruses produced more protein than the arthritogenic virus expression plasmids, or that the encephalitic CP protein was inherently more stable, this would artefactually cause higher levels of nanoluc activity with the encephalitic CPs. Nevertheless, there is still a potential for this interaction to vary between species of alphaviruses, and it would be an interesting area of future study to see if this

interaction is a contributing factor to the differences in resistance to TLRs alphaviruses exhibited in the literature. Interestingly, while the interaction with IRAK1 is conserved across the members of the genus *Alphavirus* (Chapter 3) and that the RII domain is responsible for the interaction across several alphaviral species (Chapter 4), the leading 15 amino acids that were targeted for deletion to develop the RII mutant to ablate the interaction with IRAK1 are poorly conserved across the genus (Figure 5.1). This could suggest that the strength and importance of the CP:IRAK1 interaction does vary across the members of genus *Alphavirus*.

As previously mentioned, the TLR system is conserved in the invertebrate immune system as the Toll signaling pathway. In the Toll pathway, there is an analogous protein of IRAK1 called Pelle [366]. Like IRAK1, Pelle is a kinase that functions to phosphorylate I κ B-like inhibitor to free Rel, the invertebrate analog of NF- κ B [368]. Given the similar function of Pelle to IRAK1 and the structural similarities of the two proteins, it's possible that the CP:IRAK1 interaction is conserved to block immune signaling across both vertebrate and invertebrate host systems. Further evidence in support of this concept is that despite it having been shown that antiviral effectors produced by Rel are effective against alphaviruses, Toll signaling is not seen in alphaviral infection [376]. This is similar to the patterns of impact for the TLRs on alphaviral infection in vertebrates, where TLRs other than TLR3 tend to have diminished or no impact on alphaviral infection. Thus, the evolutionary conservation of the CP mediated interference of innate immune signaling is highly likely.

Preliminary data from our lab shows that the interaction with Pelle is indeed conserved, and that the RII domain is most likely to be the necessary interaction determinant. Unfortunately, the tools available to research the mosquito system aren't as developed or robust as the vertebrate systems, but the work done on the mammalian TLR system gives a starting point for further investigations into the importance of the CP:Pelle interaction. Understanding how alphaviruses interact with their mosquito host will ultimately offer a more robust understanding of the life cycle of alphaviruses and will illuminate potential targets for intervention to prevent the infection of mosquitos. Such understanding and efforts will become more important as the habitable zones of vector competent mosquitoes continue to expand.

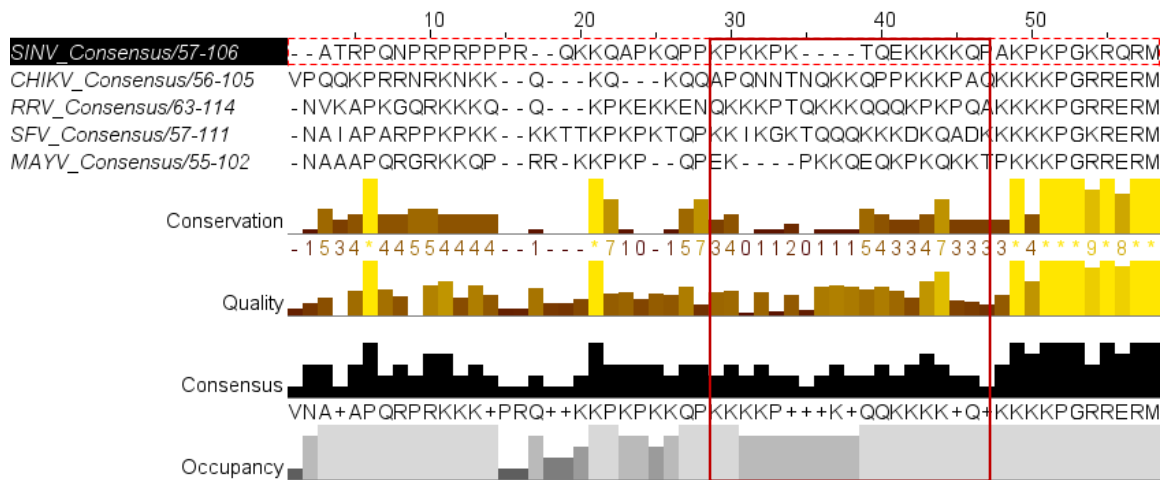


Figure 5.1- Conservation of RI and RII Regions Across Several Arthritogenic Alphaviruses

Alignments of consensus sequence of SINV, CHIKV, RRV, SFV, and MAYV CP protein RI and RII domains. Specifically shown is the region succeeding the alpha helical region of the RI domain, and the entirety of the RII domain. SINV sequence 29-47 (as highlighted by a red box) was deleted to develop the SINV. Δ RII mutant used in these studies. Despite low consensus and conservation in the RII region, a Threonine-centric motif is identifiable (Thr87 in SINV at position 39 in the alignment above).

IRAK1 Role in IL-1 Signaling

IRAK1 and the Myddosome are also crucial in the signaling of Interleukin-1 (IL-1) [378]. One of the key regulators and initiators of inflammation is the IL-1 produced by inflammasomes that are activated in response to PAMPs and DAMPs. While not addressed here, the conserved signaling pathways suggest that CP could just as easily be interacting and disrupting IL-1 signaling like it is for IRAK1-dependent TLRs. Long-term expression of IL-1 is related to a wide variety of diseases including rheumatoid arthritis, cancer, and heart disease. In the context of alphavirus pathogenesis studies that assessed IL-1 expression during infection, IL-1 levels are elevated higher than expected, especially given the negative regulation feedback loops that are supposed to control IL-1 and inflammation [357, 359]. If CP interacts with IRAK1 to cause a partial downregulation of IL-1 signaling this could cause prolonged inflammation and damage to tissues through the loss of a regulated IL-1 response. The prolonged arthritis experienced by some patients afflicted with alphaviruses is an ongoing area of interest for the field, and it has been shown despite clearance of the virus there are low levels of RNA present in cells for several weeks to months after infection [39, 141, 142]. While no replicating virus has yet to be observed despite the presence of viral RNAs, the mere presence of these viral materials could be indicative of low levels of translational products, such as CP, that contribute to dysregulation of the immune system. If CP is produced during this chronic phase, it could be a contributing factor to inflammation by continual interaction with IRAK1 to dysregulate IL-1 signaling.

Capsid:IRAK1 in Non-permissive Cells

From our data, we have shown that CP on its own is capable of inhibiting IRAK1-dependent signaling, and that non-replicative virus can impact IRAK1 signaling to a significant extent (Chapter 3). This means there are potential impacts on non-permissive cells which take up the virus, as if the CP is released out into the cytosol, their TLR and other IRAK1-dependent processes will have limited signaling, further protecting the virus from the innate immune system. As a key feature of Type-I IFN signaling is the paracrine signaling that alerts neighboring cells to infection to begin the translation of antiviral effectors, it is vital that the innate immune response be preempted. If CP can be picked up by non-permissive cells to block their signaling to produce Type-I IFNs via the detection of PAMPs, then this paracrine signaling could be severely limited in both infected and noninfected cells. This would lead to preventing a robust Type-I IFN response in both infected and non-infected cells.

Capsid:IRAK1 as Therapeutic Target

To date, there are no approved therapeutics for human use against any members of the *Alphavirus* genus. There are promising compounds in the testing stages that target viral entry or replication. From our *in vivo* data (Chapter 4), we've shown that the CP:IRAK1 interaction is crucial for pathogenesis, and without this interaction the virus is unable to cause any clinical disease through natural infection routes. This suggests that the CP:IRAK1 interaction could be an excellent

novel target for antiviral therapeutics; as by targeting the interaction between CP and IRAK1 protein with a small molecule you could restore a crucial signaling component in the innate immune system. This would help the patient mount an immune response to the virus in addition to any other antivirals that may eventually be approved for the treatment of alphaviral disease. As the CP:IRAK1 interaction seems to be conserved across the genus, compounds that targets this interaction could also exhibit potential to be broadly effective against multiple alphaviruses. A screen of small drugs or peptide inhibitors could be made by adapting the nanoluc BiMC assays employed to characterize the CP:IRAK1 interaction to test various compounds for their ability to disrupt this interaction and restore normal IRAK1 signaling. As further studies into this interaction are conducted, the exact interaction sites on CP and IRAK1 proteins can be better mapped so that the interaction site can be modeled *in silico* to allow for a computational prediction of compounds that might interfere with the interaction which can then be followed up with *in vitro* and *in vivo* studies of the compounds.

Capsid:IRAK1 as a Live-Attenuated Vaccine Candidate

The transcriptomic data obtained from RNAseq of infected brain tissues (Chapter 4) revealed differential expression of antigen processing and presentation biological pathways in the Δ R11 infected mice. If Δ R11 causes an improved phenotype of antigen processing and presentation, then it could possibly be used as a vaccine candidate to develop robust protection in vertebrates. There have been several candidate vaccines for specific alphaviruses, but none have

been successful enough for approval in human use. The leading candidate for CHIKV, named vaccine strain 181/clone 25 (181/25), is attenuated by two mutations in the E2 glycoprotein but failed as a vaccine for causing arthralgia in 8% of the recipients [379, 380]. VEEV had a promising live-attenuated vaccine, TC-83, but it showed poor seroconversion in trials and had high instances of side-effects and a potential to revert to pathogenic VEEV [381, 382]. Despite TC-83's flaws it is still used as a vaccine for those who work with wild strains VEEV in a research setting. There is an approved livestock vaccine for VEEV, but given the severity of alphaviral infection in equids it requires annual boosters to remain protective.

The majority of vaccines that have been tried for alphaviruses have generally failed clinical trials because the vaccine either doesn't invoke a durable and protective immune response to provide long-term protection, or they have severe side effects and risk reversion to a pathogenic virus. In the case of a live-attenuated virus trial for a VEEV vaccine in livestock, mosquito populations in the area started testing positive for the vaccine raising concerns that if the virus could revert then it could be a source for outbreak events [383]. It is possible Δ R11 on its own could cause a strong enough immune reaction to provide long-term protection, and with it being a deletion of fifteen amino acids there's little chance for a reversion. Seeing that antigen processing and presentation were enriched in Δ R11 compared to WT infected mice could indicate that Δ R11 is also able to bypass the issues of previous vaccines having low seroconversion and not being able to produce a long-lasting protective response. Even if it fails to be a good vaccine

candidate on its own, it could still be incorporated as one part of a series of mutations in an alphavirus to generate a robust long lasting protective vaccine.

RII as an Anti-inflammatory

Another interesting implication of the CP:IRAK1 interaction could be to utilize an RII peptide as an anti-inflammatory drug. Using virus-like particles (VLPs) as a method for drug delivery has already been proposed and is an active area of interest [384, 385]. If an engineered CP that could readily block IL-1 signaling were to be incorporated into the VLPs you could have a drug delivery system that targets specific cell types like macrophages or fibroblasts to limit their inflammation in diseases characterized by chronic or dysregulated inflammation.

Chronic inflammation and dysregulation are key factors in several diseases including rheumatoid arthritis, Crohn's disease, atherosclerosis, along with numerous genetic encoded diseases such as familial cold autoinflammatory syndrome and familial Mediterranean fever. With IL-1 being the key regulator and initiator of inflammation intervention with IL-1 blockers is either the approved treatment or proposed treatment for several autoinflammatory diseases. To date there are three approved IL-1 blockers including anakinra, a recombinant human IL-Ra; riloncept, a soluble decoy receptor; and canakinumab, a monoclonal antibody against IL-1. While these treatments are generally considered safe, they aren't always effective against every form of inflammatory disease. There are also issues with anakinra needing to be administered daily and the high cost associated

with therapy with canakinumab [386]. These methods while effective are also a blanket inhibition of IL-1 across the body, a cell targeted therapy with VLP could remove the limitations of having to inhibit the inflammatory response for the entire body which can leave the patient more susceptible to infections, including multidrug resistant tuberculosis. Furthermore, repeated systemic treatment with the above anti-inflammatory protein drugs eventually leads to the development of antibody responses to the drugs themselves, limiting their long-term treatment efficacy [387]. In contrast, targeted therapeutics that work internally to the target cell would be less likely to develop or be sensitive to host antibody responses.

Future Directions

The data presented here shows a novel host-pathogen interaction between the alphaviral CP and IRAK1 proteins. We have established that this interaction is conserved across several members of the *Alphavirus* genus, and that the interaction with IRAK1 is capable of disrupting TLR and PAMP detection for each of these viruses. Along with the data showing the importance of CP:IRAK1 interaction *in vivo*, these data opens up the possibility of studying CP:IRAK1 across several alphaviruses including both arthritogenic and encephalitic, to see how conserved the importance of this interaction is to pathogenesis. To do this first it would need to be shown that RII remains the conserved necessary interactant for IRAK1. While every alphaviral CP has an RII domain that serves the same function they are largely non-conserved at the amino acid level. This divergence could imply that different CP RIIs have varying degrees of strength when

interacting with IRAK1, influencing the importance of the interaction and how well that species of CP is capable of blocking IRAK1.

A remaining area of interest are stoichiometry, timing, location, and mechanisms by which the alphaviral CP protein effects the interference of IRAK1. While further experimental evidence will be needed to form direct conclusions regarding these areas of interest, specific inferences from the data presented here may be made allowing for the establishment of future research hypotheses.

Foremost is the question as to how much CP protein is needed to impact IRAK1-dependent signaling. The data presented here clearly indicates that the CP protein is capable of repressing IRAK1-dependent signaling in tissue culture models, but whether these conditions are directly synonymous to those observed during bona fide infections is unclear. In our tissue culture systems infection conditions were utilized to ensure total, or near total, infections of the cell monolayer with the number of infectious viral particles per cell following a Poisson distribution. In the context of a natural infection the MOI conditions are likely to vary from these experimental systems; however, it is likely that the experimental conditions used in these studies underrepresent those of natural infection. For instance, the viral load delivered during a mosquito feeding is approximated to be 10,000 infectious units. Thus, under these conditions a substantial bolus of viral particles is delivered to a relatively small population of cells, specifically the fibroblasts which are proximal to capillary impacted by the feeding event. Similarly, during a natural infection an infected cell will release progeny viral particles directly into the adjacent tissue space. As many of the tissue systems impacted by alphaviral

infection are inherently cell dense, this results in a scenario where the neighboring cells are being exposed to alphaviral particles at relatively high MOIs as the viral particles. It is also important to note that in addition to the infectious viral particles many non-infectious particles were co-delivered as alphaviral infections inherently produce viral particles inefficiently, as a typical particle-to-PFU ratio for vertebrate derived particles is ~80:1. Altogether, these data suggest that our experimental systems are probably underestimating the impact of the CP:IRAK1 interaction on IRAK1-dependent signaling as less CP protein is present in our experimental systems versus natural infection on a per cell basis. However, experiments measuring the effect of CP protein on IRAK1 over several MOIs and ratios of infectious to non-infectious particles could give further insight into how the initial dose of infection contributes to IRAK1 inhibition.

The timing of the CP:IRAK1 interaction, or more precisely whether the CP:IRAK1 interaction is critical during early or late stages of infection, is also unclear. From the data presented in this dissertation we know that the CP protein delivered solely from the incoming viral particles is sufficient to negatively impact IRAK1-dependent signaling. This is evidenced by the fact that CP protein derived from non-infectious viral particles suppressed IRAK1-dependent PAMP detection. Nonetheless, these effects were muted relative to fully replicative alphaviral infections indicating that the continued presence of CP protein or the increased abundance of CP protein afforded by structural gene expression. From these data, and the importance of IRAK1-dependent signaling, we speculate that the CP protein is critical towards evading PAMP detection during the earliest stages of

infection (such as immediately after nucleocapsid disassembly in the cytoplasm) and later during infection by way of disrupting other IRAK1-dependent signaling pathways, such as that of IL-1R. The impact of the CP protein on IRAK1-dependent signaling is also dependent on the capacity of the host to continue to express mRNAs and proteins late stages of infection, such as is observed in persistently infected cells such as macrophages. Future experiments to determine the timing of importance will undoubtedly need to utilize highly sensitive methods to dissect the precise timing of the establishment of the CP:IRAK1 interaction.

The question of where the CP:IRAK1 interaction occurs in the host cell is also unanswered. Nonetheless, by critically examining the alphaviral lifecycle several suppositions can be made, which in conjunction with our presented data, enable hypotheses to be formed. During infection the CP protein is present at high local concentrations during two specific instances- i) immediately after disassembly where 240 copies of CP protein are released per particle from the endosome, and ii) after structural gene expression where the intracellular concentration of CP likely exceeds micromolar concentrations. Importantly, the capacity of the CP protein to impact IRAK1-dependent signaling was not dependent on the infectious potential of the viral particles but was dependent on viral entry. As stated earlier, the evasion of PAMPs likely occurs by an interaction proximal to the particle-containing endosome. This is for several reasons, paramount of which is that this subcellular region contains all the necessary components, including the CP protein, the TLR, the Myddosome, and IRAK1. Another reason is that the viral associated PAMPs which are likely to be detected

by the endosomal TLRs are also within the endosome containing the infectious and non-infectious viral particles. Thus, the PAMP and the poison of IRAK1-dependent TLR signaling are co-delivered, but exist on opposing sides of the endosomal membrane. Later after the wholesale expression of the CP protein the CP:IRAK1 interaction is likely to form wherever IRAK1 protein may be found, and receptors at distal locations to the incoming endosomes are effected.

The exact stage of IRAK1 signaling that CP blocks, and the precise mechanism of action CP uses to block it is still also not fully understood. From the data we do have, full-length CP is necessary for the full robust levels of TLR inhibition. As such, we hypothesize that steric hindrance is the potential mechanism of action. It would be interesting to see if RII could be fused to other proteins to direct them to IRAK1 and if this would cause inhibition of IRAK1 signaling similar to what is seen with CP. IRAK1 contains several domains that facilitate protein/protein interactions and CP interacting with any of them could cause loss of recruitment to the Myddosome or interactions with downstream targets like IRF7 or TRAF6. From the mapping data we have done with IRAK1, it is suggestive that the kinase domain is the site that CP binds during the interaction. Further experiments will need to be done to see if this interaction takes place before or after IRAK1 is activated by IRAK4. But if CP is genuinely interacting with the kinase domain and blocking its activity then that also opens up the possibility of CP being phosphorylated by IRAK1. It has been shown previously that CP phosphorylation is necessary for the regulation of RNA interactions and this

interaction with IRAK1 could be another way the virus regulates itself in addition to the ability to evade the innate immune system.

In addition to the molecular mechanism, the biological mechanism remains to be completely described. Further *in vivo* experiments with IFNAR^{-/-}, TLR7/8^{-/-}, and IL-1R^{-/-} mice would be beneficial to further expanding our understanding of which IRAK1-dependent signaling cascades are being interrupted by the interaction with CP, as well as define how this interaction plays a role in evasion of TLR response as well as dysregulation of IL-1. Experiments with these mice would help identify which pathways inhibited by CP:IRAK1 are crucial for pathogenesis.

REFERENCES

1. Griffin, D.E., *Alphaviruses*, in *Fields Virology*, D.M.K.a. P.M.Howley, Editor. 2001, Lippincott-Raven: Philadelphia, PA. p. 917-962.
2. Kendrick, K., et al., *Notes from the field: transmission of chikungunya virus in the continental United States—Florida, 2014*. MMWR Morb Mortal Wkly Rep, 2014. **63**(48): p. 1137.
3. Weaver, S.C., *Urbanization and geographic expansion of zoonotic arboviral diseases: mechanisms and potential strategies for prevention*. Trends Microbiol, 2013. **21**(8): p. 360-3.
4. Johansson, M.A., et al., *Nowcasting the spread of chikungunya virus in the Americas*. PloS one, 2014. **9**(8): p. e104915.
5. Levi, L.I. and M. Vignuzzi, *Arthritogenic Alphaviruses: A Worldwide Emerging Threat?* Microorganisms, 2019. **7**(5).
6. Sissoko, D., et al., *Post-epidemic Chikungunya disease on Reunion Island: course of rheumatic manifestations and associated factors over a 15-month period*. PLoS Negl Trop Dis, 2009. **3**(3): p. e389.
7. Marimoutou, C., et al., *Morbidity and impaired quality of life 30 months after chikungunya infection: comparative cohort of infected and uninfected French military policemen in Reunion Island*. Medicine (Baltimore), 2012. **91**(4): p. 212-9.

8. Kurkela, S., et al., *Arthritis and arthralgia three years after Sindbis virus infection: clinical follow-up of a cohort of 49 patients*. Scand J Infect Dis, 2008. **40**(2): p. 167-73.
9. Thiberville, S.D., et al., *Chikungunya fever: epidemiology, clinical syndrome, pathogenesis and therapy*. Antiviral Res, 2013. **99**(3): p. 345-70.
10. Harley, D., A. Sleight, and S. Ritchie, *Ross River virus transmission, infection, and disease: a cross-disciplinary review*. Clinical microbiology reviews, 2001. **14**(4): p. 909-932.
11. Farnon, E.C., J.J. Sejvar, and J.E. Staples, *Severe disease manifestations associated with acute chikungunya virus infection*. Crit Care Med, 2008. **36**(9): p. 2682-3.
12. Cardona-Ospina, J.A., et al., *Estimating the burden of disease and the economic cost attributable to chikungunya, Colombia, 2014*. Trans R Soc Trop Med Hyg, 2015. **109**(12): p. 793-802.
13. Seyler, T., et al., *Estimating the burden of disease and the economic cost attributable to chikungunya, Andhra Pradesh, India, 2005-2006*. Trans R Soc Trop Med Hyg, 2010. **104**(2): p. 133-8.
14. Toivanen, A., *Alphaviruses: an emerging cause of arthritis?* Curr Opin Rheumatol, 2008. **20**(4): p. 486-90.
15. Kurkela, S., et al., *Clinical and laboratory manifestations of Sindbis virus infection: prospective study, Finland, 2002-2003*. J Infect Dis, 2005. **191**(11): p. 1820-9.

16. Kurkela, S., et al., *Sindbis virus infection in resident birds, migratory birds, and humans, Finland*. Emerg Infect Dis, 2008. **14**(1): p. 41-7.
17. Adouchief, S., et al., *Sindbis virus as a human pathogen-epidemiology, clinical picture and pathogenesis*. Rev Med Virol, 2016. **26**(4): p. 221-41.
18. Russell, R.C., *Ross River virus: ecology and distribution*. Annu Rev Entomol, 2002. **47**: p. 1-31.
19. Zuchi, N., et al., *Molecular detection of Mayaro virus during a dengue outbreak in the state of Mato Grosso, Central-West Brazil*. Mem Inst Oswaldo Cruz, 2014. **109**(6): p. 820-3.
20. Auguste, A.J., et al., *Evolutionary and Ecological Characterization of Mayaro Virus Strains Isolated during an Outbreak, Venezuela, 2010*. Emerging infectious diseases, 2015. **21**(10): p. 1742-1750.
21. Esposito, D.L.A. and B. Fonseca, *Will Mayaro virus be responsible for the next outbreak of an arthropod-borne virus in Brazil?* Braz J Infect Dis, 2017. **21**(5): p. 540-544.
22. Calisher, C.H., *Medically important arboviruses of the United States and Canada*. Clin Microbiol Rev, 1994. **7**(1): p. 89-116.
23. Goldfield, M., J.N. Welsh, and B.F. Taylor, *The 1959, outbreak of Eastern encephalitis in New Jersey. 4. CF reactivity following overt and inapparent infection*. American Journal of Epidemiology, 1968. **87**(1): p. 23-31.
24. de la Monte, S., et al., *The systemic pathology of Venezuelan equine encephalitis virus infection in humans*. Am J Trop Med Hyg, 1985. **34**(1): p. 194-202.

25. Ronca, S.E., K.T. Dineley, and S. Paessler, *Neurological Sequelae Resulting from Encephalitic Alphavirus Infection*. *Front Microbiol*, 2016. **7**: p. 959.
26. Griffin, D.E., *Emergence and re-emergence of viral diseases of the central nervous system*. *Prog Neurobiol*, 2010. **91**(2): p. 95-101.
27. Steele K., R.D., Glass P., Hart M., Ludwig G., Pratt W., Parker M., Smith J. , *Chapter 12: Alphavirus Encephalitides*. *Medical Aspects of Biological Warfare*, 2007: p. 241-270.
28. Control, C.f.D. and Prevention, *West Nile virus and other arboviral diseases--United States, 2012*. *MMWR. Morbidity and mortality weekly report*, 2013. **62**(25): p. 513-517.
29. Franz, A.W., et al., *Tissue Barriers to Arbovirus Infection in Mosquitoes*. *Viruses*, 2015. **7**(7): p. 3741-67.
30. Lim, E.X.Y., et al., *Mosquitoes as Suitable Vectors for Alphaviruses*. *Viruses*, 2018. **10**(2).
31. Dong, S., et al., *Infection pattern and transmission potential of chikungunya virus in two New World laboratory-adapted Aedes aegypti strains*. *Sci Rep*, 2016. **6**: p. 24729.
32. Pinggen, M., et al., *Host Inflammatory Response to Mosquito Bites Enhances the Severity of Arbovirus Infection*. *Immunity*, 2016. **44**(6): p. 1455-1469.

33. Surasombatpattana, P., et al., *Dengue virus replication in infected human keratinocytes leads to activation of antiviral innate immune responses*. Infection, Genetics and Evolution, 2011. **11**(7): p. 1664-1673.
34. Demeure, C.E., et al., *Anopheles Mosquito Bites Activate Cutaneous Mast Cells Leading to a Local Inflammatory Response and Lymph Node Hyperplasia*. The Journal of Immunology, 2005. **174**(7): p. 3932-3940.
35. Conway, M.J., et al., *Mosquito Saliva Serine Protease Enhances Dissemination of Dengue Virus into the Mammalian Host*. Journal of Virology, 2014. **88**(1): p. 164-175.
36. Cappuccio, L. and C. Maise, *Infection of Mammals and Mosquitoes by Alphaviruses: Involvement of Cell Death*. Cells, 2020. **9**(12).
37. Johnston, L.J., N.J. King, and G.M. Halliday, *Langerhans cells migrate to local lymph nodes following cutaneous infection with an arbovirus*. Journal of Investigative Dermatology, 2000. **114**(3): p. 560-568.
38. MacDonald, G.H. and R.E. Johnston, *Role of dendritic cell targeting in Venezuelan equine encephalitis virus pathogenesis*. Journal of virology, 2000. **74**(2): p. 914-922.
39. Soden, M., et al., *Detection of viral ribonucleic acid and histologic analysis of inflamed synovium in Ross River virus infection*. Arthritis Rheum, 2000. **43**(2): p. 365-9.
40. Linn, M.L., J.G. Aaskov, and A. Suhrbier, *Antibody-dependent enhancement and persistence in macrophages of an arbovirus associated with arthritis*. J Gen Virol, 1996. **77 (Pt 3)**: p. 407-11.

41. Way, S.J., B.A. Lidbury, and J.L. Banyer, *Persistent Ross River virus infection of murine macrophages: an in vitro model for the study of viral relapse and immune modulation during long-term infection*. *Virology*, 2002. **301**(2): p. 281-92.
42. Charles, P.C., et al., *Mechanism of neuroinvasion of Venezuelan equine encephalitis virus in the mouse*. *Virology*, 1995. **208**(2): p. 662-671.
43. Salimi, H., et al., *Encephalitic Alphaviruses Exploit Caveola-Mediated Transcytosis at the Blood-Brain Barrier for Central Nervous System Entry*. *mBio*, 2020. **11**(1): p. e02731-19.
44. Strauss, J.H. and E.G. Strauss, *The alphaviruses: gene expression, replication, and evolution*. *Microbiol Rev*, 1994. **58**(3): p. 491-562.
45. Hyde, J.L., et al., *The 5' and 3' ends of alphavirus RNAs--Non-coding is not non-functional*. *Virus Res*, 2015. **206**: p. 99-107.
46. Hardy, R.W., *The role of the 3' terminus of the Sindbis virus genome in minus-strand initiation site selection*. *Virology*, 2006. **345**(2): p. 520-31.
47. Caspar, D.L. and A. Klug. *Physical principles in the construction of regular viruses*. in *Cold Spring Harbor symposia on quantitative biology*. 1962. Cold Spring Harbor Laboratory Press.
48. Von Bonsdorff, C. and S. Harrison, *Sindbis virus glycoproteins form a regular icosahedral surface lattice*. *Journal of Virology*, 1975. **16**(1): p. 141-145.
49. Von Bonsdorff, C. and S. Harrison, *Hexagonal glycoprotein arrays from Sindbis virus membranes*. *Journal of Virology*, 1978. **28**(2): p. 578-583.

50. Mukhopadhyay, S., et al., *Mapping the structure and function of the E1 and E2 glycoproteins in alphaviruses*. Structure (London, England : 1993), 2006. **14**(1): p. 63-73.
51. Westcott, C.E., et al., *Dancing with the Devil: A Review of the Importance of Host RNA-Binding Proteins to Alphaviral RNAs during Infection*. Viruses, 2023. **15**(1): p. 164.
52. Knipe, D., et al., *Fields Virology, Volumes 1 and 2*. 2013.
53. Schnierle, B.S., *Cellular attachment and entry factors for chikungunya virus*. Viruses, 2019. **11**(11): p. 1078.
54. Clark, L.E., et al., *VLDLR and ApoER2 are receptors for multiple alphaviruses*. Nature, 2022. **602**(7897): p. 475-480.
55. DeTulleo, L. and T. Kirchhausen, *The clathrin endocytic pathway in viral infection*. The EMBO journal, 1998. **17**(16): p. 4585-4593.
56. Dubuisson, J. and C.M. Rice, *Sindbis virus attachment: isolation and characterization of mutants with impaired binding to vertebrate cells*. Journal of virology, 1993. **67**(6): p. 3363-3374.
57. Schmid, S., et al., *Acidification of endosome subpopulations in wild-type Chinese hamster ovary cells and temperature-sensitive acidification-defective mutants*. J Cell Biol, 1989. **108**(4): p. 1291-300.
58. Mellman, I., R. Fuchs, and A. Helenius, *Acidification of the endocytic and exocytic pathways*. Annu Rev Biochem, 1986. **55**: p. 663-700.
59. Helenius, A., et al., *On the entry of semliki forest virus into BHK-21 cells*. Journal of Cell Biology, 1980. **84**(2): p. 404-420.

60. Wengler, G., et al., *Entry of alphaviruses at the plasma membrane converts the viral surface proteins into an ion-permeable pore that can be detected by electrophysiological analyses of whole-cell membrane currents*. J Gen Virol, 2003. **84**(Pt 1): p. 173-181.
61. Gibbons, D.L., et al., *Visualization of the target-membrane-inserted fusion protein of Semliki Forest virus by combined electron microscopy and crystallography*. Cell, 2003. **114**(5): p. 573-583.
62. Jose, J., J.E. Snyder, and R.J. Kuhn, *A structural and functional perspective of alphavirus replication and assembly*. Future microbiology, 2009. **4**(7): p. 837-856.
63. Singh, I. and A. Helenius, *Role of ribosomes in Semliki Forest virus nucleocapsid uncoating*. J Virol, 1992. **66**(12): p. 7049-58.
64. Shirako, Y. and J.H. Strauss, *Regulation of Sindbis virus RNA replication: uncleaved P123 and nsP4 function in minus-strand RNA synthesis, whereas cleaved products from P123 are required for efficient plus-strand RNA synthesis*. J Virol, 1994. **68**(3): p. 1874-85.
65. Rupp, J.C., et al., *Alphavirus RNA synthesis and non-structural protein functions*. J Gen Virol, 2015. **96**(9): p. 2483-500.
66. Firth, A.E., et al., *Discovery of frameshifting in Alphavirus 6K resolves a 20-year enigma*. Virology Journal, 2008. **5**(1): p. 108.
67. Sariola, M., J. Saraste, and E. Kuismanen, *Communication of post-Golgi elements with early endocytic pathway: regulation of endoproteolytic*

- cleavage of Semliki Forest virus p62 precursor. J Cell Sci, 1995. 108 (Pt 6): p. 2465-75.*
68. Snyder, J.E., et al., *Functional characterization of the alphavirus TF protein. Journal of virology, 2013. 87(15): p. 8511-8523.*
69. Wilkinson, T.A., et al., *Association of sindbis virus capsid protein with phospholipid membranes and the E2 glycoprotein: implications for alphavirus assembly. Biochemistry, 2005. 44(8): p. 2800-10.*
70. Skoging, U., et al., *Aromatic interactions define the binding of the alphavirus spike to its nucleocapsid. Structure, 1996. 4(5): p. 519-29.*
71. Lee, S., et al., *Identification of a protein binding site on the surface of the alphavirus nucleocapsid and its implication in virus assembly. Structure, 1996. 4(5): p. 531-41.*
72. Ferreira, A.C., et al., *Beyond Members of the Flaviviridae Family, Sofosbuvir Also Inhibits Chikungunya Virus Replication. Antimicrob Agents Chemother, 2019. 63(2).*
73. Chung, D.-H., et al., *Discovery of a novel compound with anti-Venezuelan equine encephalitis virus activity that targets the nonstructural protein 2. PLoS pathogens, 2014. 10(6): p. e1004213.*
74. Skidmore, A.M., et al., *Benzamidine ML336 inhibits plus and minus strand RNA synthesis of Venezuelan equine encephalitis virus without affecting host RNA production. Antiviral research, 2020. 174: p. 104674.*
75. LaPointe, A.T., et al., *Identification and Characterization of Sindbis Virus RNA-Host Protein Interactions. J Virol, 2018. 92(7).*

76. LaPointe, A.T., J. Moreno-Contreras, and K.J. Sokoloski, *Increasing the Capping Efficiency of the Sindbis Virus nsP1 Protein Negatively Affects Viral Infection*. MBio, 2018. **9**(6).
77. Sokoloski, K.J., et al., *Noncapped Alphavirus Genomic RNAs and Their Role during Infection*. J Virol, 2015. **89**(11): p. 6080-92.
78. LaPointe, A.T., et al., *Production of Noncapped Genomic RNAs Is Critical to Sindbis Virus Disease and Pathogenicity*. mBio, 2020. **11**(6).
79. Kujala, P., et al., *Biogenesis of the Semliki Forest virus RNA replication complex*. J Virol, 2001. **75**(8): p. 3873-84.
80. Jones, R., et al., *Capping pores of alphavirus nsP1 gate membranous viral replication factories*. Nature, 2021. **589**(7843): p. 615-619.
81. Zhang, K., et al., *Structural insights into viral RNA capping and plasma membrane targeting by Chikungunya virus nonstructural protein 1*. Cell Host Microbe, 2021. **29**(5): p. 757-764.e3.
82. Tan, Y.B., et al., *Molecular architecture of the Chikungunya virus replication complex*. Sci Adv, 2022. **8**(48): p. eadd2536.
83. Hardy, W.R. and J.H. Strauss, *Processing the nonstructural polyproteins of sindbis virus: nonstructural proteinase is in the C-terminal half of nsP2 and functions both in cis and in trans*. J Virol, 1989. **63**(11): p. 4653-64.
84. Karpf, A.R., et al., *Superinfection exclusion of alphaviruses in three mosquito cell lines persistently infected with Sindbis virus*. Journal of virology, 1997. **71**(9): p. 7119-7123.

85. Balistreri, G., et al., *Enzymatic defects of the nsP2 proteins of Semliki Forest virus temperature-sensitive mutants*. J Virol, 2007. **81**(6): p. 2849-60.
86. Gorbalenya, A.E., et al., *A novel superfamily of nucleoside triphosphate-binding motif containing proteins which are probably involved in duplex unwinding in DNA and RNA replication and recombination*. FEBS Lett, 1988. **235**(1-2): p. 16-24.
87. Vasiljeva, L., et al., *Identification of a novel function of the alphavirus capping apparatus. RNA 5'-triphosphatase activity of Nsp2*. J Biol Chem, 2000. **275**(23): p. 17281-7.
88. Akhrymuk, I., et al., *Novel Mutations in nsP2 Abolish Chikungunya Virus-Induced Transcriptional Shutoff and Make the Virus Less Cytopathic without Affecting Its Replication Rates*. J Virol, 2019. **93**(4).
89. Akhrymuk, I., S.V. Kulemzin, and E.I. Frolova, *Evasion of the innate immune response: the Old World alphavirus nsP2 protein induces rapid degradation of Rpb1, a catalytic subunit of RNA polymerase II*. Journal of virology, 2012. **86**(13): p. 7180-7191.
90. Frolova, E.I., et al., *Roles of nonstructural protein nsP2 and Alpha/Beta interferons in determining the outcome of Sindbis virus infection*. J Virol, 2002. **76**(22): p. 11254-64.
91. Varjak, M., E. Zusinaite, and A. Merits, *Novel functions of the alphavirus nonstructural protein nsP3 C-terminal region*. Journal of virology, 2010. **84**(5): p. 2352-2364.

92. Jayabalan, A.K., et al., *Stress granule formation, disassembly, and composition are regulated by alphavirus ADP-ribosylhydrolase activity*. Proceedings of the National Academy of Sciences, 2021. **118**(6): p. e2021719118.
93. Abraham, R., et al., *ADP-ribosyl-binding and hydrolase activities of the alphavirus nsP3 macrodomain are critical for initiation of virus replication*. Proc Natl Acad Sci U S A, 2018. **115**(44): p. E10457-E10466.
94. Eckeï, L., et al., *The conserved macrodomains of the non-structural proteins of Chikungunya virus and other pathogenic positive strand RNA viruses function as mono-ADP-ribosylhydrolases*. Sci Rep, 2017. **7**: p. 41746.
95. Atasheva, S., et al., *New PARP gene with an anti-alphavirus function*. J Virol, 2012. **86**(15): p. 8147-60.
96. Shin, G., et al., *Structural and functional insights into alphavirus polyprotein processing and pathogenesis*. Proceedings of the National Academy of Sciences, 2012. **109**(41): p. 16534-16539.
97. Tuittila, M. and A.E. Hinkkanen, *Amino acid mutations in the replicase protein nsP3 of Semliki Forest virus cumulatively affect neurovirulence*. J Gen Virol, 2003. **84**(Pt 6): p. 1525-1533.
98. Dé, I., et al., *Functional analysis of nsP3 phosphoprotein mutants of Sindbis virus*. J Virol, 2003. **77**(24): p. 13106-16.
99. Lastarza, M.W., A. Grakoui, and C.M. Rice, *Deletion and duplication mutations in the C-terminal nonconserved region of Sindbis virus nsP3*:

- effects on phosphorylation and on virus replication in vertebrate and invertebrate cells. Virology, 1994. 202(1): p. 224-32.*
100. Nowee, G., et al., *A Tale of 20 Alphaviruses; Inter-species Diversity and Conserved Interactions Between Viral Non-structural Protein 3 and Stress Granule Proteins. Front Cell Dev Biol, 2021. 9: p. 625711.*
 101. Vihinen, H., et al., *Elimination of phosphorylation sites of Semliki Forest virus replicase protein nsP3. J Biol Chem, 2001. 276(8): p. 5745-52.*
 102. Vihinen, H. and J. Saarinen, *Phosphorylation site analysis of Semliki forest virus nonstructural protein 3. J Biol Chem, 2000. 275(36): p. 27775-83.*
 103. Teppor, M., E. Žusinaite, and A. Merits, *Phosphorylation Sites in the Hypervariable Domain in Chikungunya Virus nsP3 Are Crucial for Viral Replication. Journal of virology, 2021. 95(9): p. e02276-20.*
 104. Panas, M.D., et al., *Viral and cellular proteins containing FGDF motifs bind G3BP to block stress granule formation. PLoS pathogens, 2015. 11(2): p. e1004659.*
 105. OBERSTE, M.S., M.D. PARKER, and J.F. SMITH, *Complete sequence of Venezuelan equine encephalitis virus subtype IE reveals conserved and hypervariable domains within the C terminus of nsP3. Virology, 1996. 219(1): p. 314-320.*
 106. Foy, N.J., et al., *Hypervariable domain of nonstructural protein nsP3 of Venezuelan equine encephalitis virus determines cell-specific mode of virus replication. J Virol, 2013. 87(13): p. 7569-84.*

107. Hahn, Y.S., et al., *Mapping of RNA- temperature-sensitive mutants of Sindbis virus: complementation group F mutants have lesions in nsP4*. J Virol, 1989. **63**(3): p. 1194-202.
108. Rubach, J.K., et al., *Characterization of purified Sindbis virus nsP4 RNA-dependent RNA polymerase activity in vitro*. Virology, 2009. **384**(1): p. 201-8.
109. de Groot, R.J., et al., *Sindbis virus RNA polymerase is degraded by the N-end rule pathway*. Proc Natl Acad Sci U S A, 1991. **88**(20): p. 8967-71.
110. Coffey, L.L., et al., *Arbovirus high fidelity variant loses fitness in mosquitoes and mice*. Proceedings of the National Academy of Sciences, 2011. **108**(38): p. 16038-16043.
111. Krupovic, M. and E.V. Koonin, *Multiple origins of viral capsid proteins from cellular ancestors*. Proc Natl Acad Sci U S A, 2017. **114**(12): p. E2401-E2410.
112. Hahn, C.S., E.G. Strauss, and J.H. Strauss, *Sequence analysis of three Sindbis virus mutants temperature-sensitive in the capsid protein autoprotease*. Proc Natl Acad Sci U S A, 1985. **82**(14): p. 4648-52.
113. Garoff, H., et al., *The capsid protein of Semliki Forest virus has clusters of basic amino acids and prolines in its amino-terminal region*. Proc Natl Acad Sci U S A, 1980. **77**(11): p. 6376-80.
114. Perera, R., et al., *Alphavirus nucleocapsid protein contains a putative coiled coil alpha-helix important for core assembly*. J Virol, 2001. **75**(1): p. 1-10.

115. Weiss, B., U. Geigenmuller-Gnirke, and S. Schlesinger, *Interactions between Sindbis virus RNAs and a 68 amino acid derivative of the viral capsid protein further defines the capsid binding site*. Nucleic Acids Res, 1994. **22**(5): p. 780-6.
116. Weiss, B., et al., *Evidence for specificity in the encapsidation of Sindbis virus RNAs*. Journal of virology, 1989. **63**(12): p. 5310-5318.
117. Owen, K.E. and R.J. Kuhn, *Identification of a region in the Sindbis virus nucleocapsid protein that is involved in specificity of RNA encapsidation*. J Virol, 1996. **70**(5): p. 2757-63.
118. Wengler, G. and G. Wengler, *In vitro analysis of factors involved in the disassembly of Sindbis virus cores by 60S ribosomal subunits identifies a possible role of low pH*. J Gen Virol, 2002. **83**(Pt 10): p. 2417-2426.
119. Wengler, G. and G. Wengler, *Identification of a transfer of viral core protein to cellular ribosomes during the early stages of alphavirus infection*. Virology, 1984. **134**(2): p. 435-42.
120. Atasheva, S., et al., *Venezuelan equine Encephalitis virus capsid protein forms a tetrameric complex with CRM1 and importin alpha/beta that obstructs nuclear pore complex function*. J Virol, 2010. **84**(9): p. 4158-71.
121. Sokoloski, K.J., et al., *Identification of Interactions between Sindbis Virus Capsid Protein and Cytoplasmic vRNA as Novel Virulence Determinants*. PLoS Pathog, 2017. **13**(6): p. e1006473.

122. Hashimoto, K., et al., *Evidence for a separate signal sequence for the carboxy-terminal envelope glycoprotein E1 of Semliki forest virus*. J Virol, 1981. **38**(1): p. 34-40.
123. Garoff, H., et al., *The signal sequence of the p62 protein of Semliki Forest virus is involved in initiation but not in completing chain translocation*. J Cell Biol, 1990. **111**(3): p. 867-76.
124. Snyder, A.J. and S. Mukhopadhyay, *The alphavirus E3 glycoprotein functions in a clade-specific manner*. Journal of virology, 2012. **86**(24): p. 13609-13620.
125. Anthony, R.P., A.M. Paredes, and D.T. Brown, *Disulfide bonds are essential for the stability of the Sindbis virus envelope*. Virology, 1992. **190**(1): p. 330-6.
126. Mulvey, M. and D.T. Brown, *Formation and rearrangement of disulfide bonds during maturation of the Sindbis virus E1 glycoprotein*. J Virol, 1994. **68**(2): p. 805-12.
127. Klimstra, W.B., H.W. Heidner, and R.E. Johnston, *The furin protease cleavage recognition sequence of Sindbis virus PE2 can mediate virion attachment to cell surface heparan sulfate*. J Virol, 1999. **73**(8): p. 6299-306.
128. Cheng, R.H., et al., *Nucleocapsid and glycoprotein organization in an enveloped virus*. Cell, 1995. **80**(4): p. 621-30.
129. Weger-Lucarelli, J., et al., *Dissecting the Role of E2 Protein Domains in Alphavirus Pathogenicity*. Journal of Virology, 2016. **90**(5): p. 2418-2433.

130. Lescar, J., et al., *The Fusion glycoprotein shell of Semliki Forest virus: an icosahedral assembly primed for fusogenic activation at endosomal pH*. Cell, 2001. **105**(1): p. 137-48.
131. Mendes, A. and R.J. Kuhn, *Alphavirus Nucleocapsid Packaging and Assembly*. Viruses, 2018. **10**(3).
132. Taylor, A., et al., *Effects of an In-Frame Deletion of the 6k Gene Locus from the Genome of Ross River Virus*. J Virol, 2016. **90**(8): p. 4150-4159.
133. Kendra, J.A., et al., *Ablation of Programmed -1 Ribosomal Frameshifting in Venezuelan Equine Encephalitis Virus Results in Attenuated Neuropathogenicity*. J Virol, 2017. **91**(3).
134. Hallengård, D., et al., *Novel attenuated Chikungunya vaccine candidates elicit protective immunity in C57BL/6 mice*. J Virol, 2014. **88**(5): p. 2858-66.
135. Wang, K., S. Xie, and B. Sun, *Viral proteins function as ion channels*. Biochim Biophys Acta, 2011. **1808**(2): p. 510-5.
136. Rogers, K.J., et al., *TF protein of Sindbis virus antagonizes host type I interferon responses in a palmitoylation-dependent manner*. Virology, 2020. **542**: p. 63-70.
137. Ramsey, J., et al., *Palmitoylation of Sindbis Virus TF Protein Regulates Its Plasma Membrane Localization and Subsequent Incorporation into Virions*. J Virol, 2017. **91**(3).

138. Dey, D., et al., *The effect of amantadine on an ion channel protein from Chikungunya virus*. PLoS Neglected Tropical Diseases, 2019. **13**(7): p. e0007548.
139. Gardner, J., et al., *Chikungunya virus arthritis in adult wild-type mice*. J Virol, 2010. **84**(16): p. 8021-32.
140. Morrison, T.E., et al., *A Mouse Model of Chikungunya Virus–Induced Musculoskeletal Inflammatory Disease: Evidence of Arthritis, Tenosynovitis, Myositis, and Persistence*. The American Journal of Pathology, 2011. **178**(1): p. 32-40.
141. Hoarau, J.J., et al., *Persistent chronic inflammation and infection by Chikungunya arthritogenic alphavirus in spite of a robust host immune response*. J Immunol, 2010. **184**(10): p. 5914-27.
142. Niklasson, B., A. Espmark, and J. Lundström, *Occurrence of arthralgia and specific IgM antibodies three to four years after Ockelbo disease*. J Infect Dis, 1988. **157**(4): p. 832-5.
143. Couderc, T., et al., *A mouse model for Chikungunya: young age and inefficient type-I interferon signaling are risk factors for severe disease*. PLoS Pathog, 2008. **4**(2): p. e29.
144. Morrison, T.E., et al., *Characterization of Ross River Virus Tropism and Virus-Induced Inflammation in a Mouse Model of Viral Arthritis and Myositis*. Journal of Virology, 2006. **80**(2): p. 737-749.

145. Seymour, R.L., et al., *A Rodent Model of Chikungunya Virus Infection in RAG1 -/- Mice, with Features of Persistence, for Vaccine Safety Evaluation*. PLoS Negl Trop Dis, 2015. **9**(6): p. e0003800.
146. Morrison, T.E., J.D. Simmons, and M.T. Heise, *Complement Receptor 3 Promotes Severe Ross River Virus-Induced Disease*. Journal of Virology, 2008. **82**(22): p. 11263-11272.
147. Morrison, T.E., et al., *Complement Contributes to Inflammatory Tissue Destruction in a Mouse Model of Ross River Virus-Induced Disease*. Journal of Virology, 2007. **81**(10): p. 5132-5143.
148. Lidbury, B.A. and S. Mahalingam, *Specific ablation of antiviral gene expression in macrophages by antibody-dependent enhancement of Ross River virus infection*. J Virol, 2000. **74**(18): p. 8376-81.
149. Thach, D.C., T. Kimura, and D.E. Griffin, *Differences between C57BL/6 and BALB/cBy mice in mortality and virus replication after intranasal infection with neuroadapted Sindbis virus*. J Virol, 2000. **74**(13): p. 6156-61.
150. Taylor, A., et al., *Mouse models of alphavirus-induced inflammatory disease*. Journal of General Virology, 2015. **96**(2): p. 221-238.
151. Burdeinick-Kerr, R., J. Wind, and D.E. Griffin, *Synergistic roles of antibody and interferon in noncytolytic clearance of Sindbis virus from different regions of the central nervous system*. J Virol, 2007. **81**(11): p. 5628-36.

152. Burdeinick-Kerr, R. and D.E. Griffin, *Gamma interferon-dependent, noncytolytic clearance of sindbis virus infection from neurons in vitro*. J Virol, 2005. **79**(9): p. 5374-85.
153. Kerr, D.A., et al., *BCL-2 and BAX protect adult mice from lethal Sindbis virus infection but do not protect spinal cord motor neurons or prevent paralysis*. J Virol, 2002. **76**(20): p. 10393-400.
154. Jackson, A.C., et al., *The pathogenesis of spinal cord involvement in the encephalomyelitis of mice caused by neuroadapted Sindbis virus infection*. Lab Invest, 1987. **56**(4): p. 418-23.
155. Jackson, A.C., et al., *Basis of neurovirulence in Sindbis virus encephalomyelitis of mice*. Lab Invest, 1988. **58**(5): p. 503-9.
156. Jan, J.T., S. Chatterjee, and D.E. Griffin, *Sindbis virus entry into cells triggers apoptosis by activating sphingomyelinase, leading to the release of ceramide*. J Virol, 2000. **74**(14): p. 6425-32.
157. Nargi-Aizenman, J.L. and D.E. Griffin, *Sindbis virus-induced neuronal death is both necrotic and apoptotic and is ameliorated by N-methyl-D-aspartate receptor antagonists*. J Virol, 2001. **75**(15): p. 7114-21.
158. Binder, G.K. and D.E. Griffin, *Interferon-gamma-mediated site-specific clearance of alphavirus from CNS neurons*. Science, 2001. **293**(5528): p. 303-6.
159. Levine, B., et al., *Antibody-mediated clearance of alphavirus infection from neurons*. Science, 1991. **254**(5033): p. 856-60.

160. Tyor, W.R., et al., *Long term intraparenchymal Ig secretion after acute viral encephalitis in mice*. J Immunol, 1992. **149**(12): p. 4016-20.
161. Liang, X.H., et al., *Protection against fatal Sindbis virus encephalitis by beclin, a novel Bcl-2-interacting protein*. Journal of virology, 1998. **72**(11): p. 8586-8596.
162. Judith, D., et al., *Species-specific impact of the autophagy machinery on Chikungunya virus infection*. EMBO reports, 2013. **14**(6): p. 534-544.
163. Fros, J.J., et al., *Chikungunya virus nonstructural protein 2 inhibits type I/II interferon-stimulated JAK-STAT signaling*. Journal of virology, 2010. **84**(20): p. 10877-10887.
164. Harding, H.P., Y. Zhang, and D. Ron, *Protein translation and folding are coupled by an endoplasmic-reticulum-resident kinase*. Nature, 1999. **397**(6716): p. 271-274.
165. Sanz, M.A., E. González Almela, and L. Carrasco, *Translation of Sindbis Subgenomic mRNA is Independent of eIF2, eIF2A and eIF2D*. Scientific Reports, 2017. **7**(1): p. 43876.
166. Kawasaki, T. and T. Kawai, *Toll-Like Receptor Signaling Pathways*. Frontiers in Immunology, 2014. **5**.
167. Goubau, D., S. Deddouche, and C.R. e Sousa, *Cytosolic sensing of viruses*. Immunity, 2013. **38**(5): p. 855-869.
168. Hu, Y., et al., *Distribution and Evolution of Yersinia Leucine-Rich Repeat Proteins*. Infection and Immunity, 2016. **84**(8): p. 2243-2254.

169. Shiu, S.-H., et al., *Comparative analysis of the receptor-like kinase family in Arabidopsis and rice*. The plant cell, 2004. **16**(5): p. 1220-1234.
170. Sakamoto, T., et al., *The tomato RLK superfamily: phylogeny and functional predictions about the role of the LRRIL-RLK subfamily in antiviral defense*. BMC plant biology, 2012. **12**: p. 1-18.
171. Liu, J., et al., *Soybean kinome: functional classification and gene expression patterns*. Journal of experimental botany, 2015. **66**(7): p. 1919-1934.
172. Burch-Smith, T.M. and S.P. Dinesh-Kumar, *The functions of plant TIR domains*. Sci STKE, 2007. **2007**(401): p. pe46.
173. Anderson, K.V., L. Bokla, and C. Nüsslein-Volhard, *Establishment of dorsal-ventral polarity in the drosophila embryo: The induction of polarity by the Toll gene product*. Cell, 1985. **42**(3): p. 791-798.
174. Hashimoto, C., S. Gerttula, and K.V. Anderson, *Plasma membrane localization of the Toll protein in the syncytial Drosophila embryo: importance of transmembrane signaling for dorsal-ventral pattern formation*. Development, 1991. **111**(4): p. 1021-1028.
175. Stein, D., et al., *The polarity of the dorsoventral axis in the drosophila embryo is defined by an extracellular signal*. Cell, 1991. **65**(5): p. 725-735.
176. Ozinsky, A., et al., *The repertoire for pattern recognition of pathogens by the innate immune system is defined by cooperation between Toll-like receptors*. Proceedings of the National Academy of Sciences, 2000. **97**(25): p. 13766-13771.

177. Lee, B.L., et al., *UNC93B1 mediates differential trafficking of endosomal TLRs*. eLife, 2013. **2**: p. e00291.
178. Huh, J.-W., et al., *UNC93B1 is essential for the plasma membrane localization and signaling of Toll-like receptor 5*. Proceedings of the National Academy of Sciences, 2014. **111**(19): p. 7072-7077.
179. Yang, Y., et al., *Heat shock protein gp96 is a master chaperone for toll-like receptors and is important in the innate function of macrophages*. Immunity, 2007. **26**(2): p. 215-226.
180. Takahashi, K., et al., *A protein associated with Toll-like receptor (TLR) 4 (PRAT4A) is required for TLR-dependent immune responses*. The Journal of experimental medicine, 2007. **204**(12): p. 2963-2976.
181. Nakatsu, F. and H. Ohno, *Adaptor protein complexes as the key regulators of protein sorting in the post-Golgi network*. Cell structure and function, 2003. **28**(5): p. 419-429.
182. Sasai, M., M.M. Linehan, and A. Iwasaki, *Bifurcation of Toll-like receptor 9 signaling by adaptor protein 3*. Science, 2010. **329**(5998): p. 1530-1534.
183. Sepulveda, F.E., et al., *Critical role for asparagine endopeptidase in endocytic Toll-like receptor signaling in dendritic cells*. Immunity, 2009. **31**(5): p. 737-748.
184. Maschalidi, S., et al., *Asparagine endopeptidase controls anti-influenza virus immune responses through TLR7 activation*. 2012.
185. Ewald, S.E., et al., *Nucleic acid recognition by Toll-like receptors is coupled to stepwise processing by cathepsins and asparagine*

- endopeptidase*. *Journal of Experimental Medicine*, 2011. **208**(4): p. 643-651.
186. Barton, G.M., J.C. Kagan, and R. Medzhitov, *Intracellular localization of Toll-like receptor 9 prevents recognition of self DNA but facilitates access to viral DNA*. *Nature immunology*, 2006. **7**(1): p. 49-56.
187. Li, W.-W., et al., *Ubiquitination of TLR3 by TRIM3 signals its ESCRT-mediated trafficking to the endolysosomes for innate antiviral response*. *Proceedings of the National Academy of Sciences*, 2020. **117**(38): p. 23707-23716.
188. Kurt-Jones, E.A., et al., *Pattern recognition receptors TLR4 and CD14 mediate response to respiratory syncytial virus*. *Nature immunology*, 2000. **1**(5): p. 398-401.
189. Bieback, K., et al., *Hemagglutinin protein of wild-type measles virus activates toll-like receptor 2 signaling*. *Journal of virology*, 2002. **76**(17): p. 8729-8736.
190. Landais, I., et al., *Human Cytomegalovirus miR-UL112-3p Targets TLR2 and Modulates the TLR2/IRAK1/NFκB Signaling Pathway*. *PLoS pathogens*, 2015. **11**(5): p. e1004881-e1004881.
191. Uyangaa, E., et al., *Dual TLR2/9 Recognition of Herpes Simplex Virus Infection Is Required for Recruitment and Activation of Monocytes and NK Cells and Restriction of Viral Dissemination to the Central Nervous System*. *Frontiers in Immunology*, 2018. **9**.

192. Krutzik, S.R., et al., *Activation and regulation of Toll-like receptors 2 and 1 in human leprosy*. *Nature medicine*, 2003. **9**(5): p. 525-532.
193. Ferwerda, G., et al., *Dectin-1 synergizes with TLR2 and TLR4 for cytokine production in human primary monocytes and macrophages*. *Cellular Microbiology*, 2008. **10**(10): p. 2058-2066.
194. Zheng, M., et al., *TLR2 senses the SARS-CoV-2 envelope protein to produce inflammatory cytokines*. *Nature Immunology*, 2021. **22**(7): p. 829-838.
195. Aliprantis, A.O., et al., *Cell activation and apoptosis by bacterial lipoproteins through toll-like receptor-2*. *Science*, 1999. **285**(5428): p. 736-9.
196. Yoshimura, A., et al., *Cutting Edge: Recognition of Gram-Positive Bacterial Cell Wall Components by the Innate Immune System Occurs Via Toll-Like Receptor 21*. *The Journal of Immunology*, 1999. **163**(1): p. 1-5.
197. Massari, P., et al., *Cutting Edge: Immune Stimulation by Neisserial Porins Is Toll-Like Receptor 2 and MyD88 Dependent1*. *The Journal of Immunology*, 2002. **168**(4): p. 1533-1537.
198. Ikeda, Y., et al., *Dissociation of Toll-Like Receptor 2-Mediated Innate Immune Response to Zymosan by Organic Solvent-Treatment without Loss of Dectin-1 Reactivity*. *Biological and Pharmaceutical Bulletin*, 2008. **31**(1): p. 13-18.
199. Takeuchi, O., et al., *Discrimination of bacterial lipoproteins by Toll-like receptor 6*. *International Immunology*, 2001. **13**(7): p. 933-940.

200. Schröder, N.W., et al., *Lipoteichoic acid (LTA) of Streptococcus pneumoniae and Staphylococcus aureus activates immune cells via Toll-like receptor (TLR)-2, lipopolysaccharide-binding protein (LBP), and CD14, whereas TLR-4 and MD-2 are not involved.* Journal of biological chemistry, 2003. **278**(18): p. 15587-15594.
201. Barbalat, R., et al., *Toll-like receptor 2 on inflammatory monocytes induces type I interferon in response to viral but not bacterial ligands.* Nature Immunology, 2009. **10**(11): p. 1200-1207.
202. Alexopoulou, L., et al., *Recognition of double-stranded RNA and activation of NF- κ B by Toll-like receptor 3.* Nature, 2001. **413**(6857): p. 732-738.
203. Matsumoto, M., et al., *Establishment of a monoclonal antibody against human Toll-like receptor 3 that blocks double-stranded RNA-mediated signaling.* Biochemical and biophysical research communications, 2002. **293**(5): p. 1364-1369.
204. Akira, S. and K. Takeda, *Toll-like receptor signalling.* Nature reviews immunology, 2004. **4**(7): p. 499-511.
205. Jin, M.S. and J.O. Lee, *Structures of TLR-ligand complexes.* Curr Opin Immunol, 2008. **20**(4): p. 414-9.
206. Agrawal, S. and E.R. Kandimalla, *Synthetic agonists of Toll-like receptors 7, 8 and 9.* Biochemical Society Transactions, 2007. **35**(6): p. 1461-1467.
207. Carlsson, E., J.L. Ding, and B. Byrne, *SARM modulates MyD88-mediated TLR activation through BB-loop dependent TIR-TIR interactions.* Biochim Biophys Acta, 2016. **1863**(2): p. 244-53.

208. Carty, M., et al., *The human adaptor SARM negatively regulates adaptor protein TRIF-dependent Toll-like receptor signaling*. Nature Immunology, 2006. **7**(10): p. 1074-1081.
209. Fitzgerald, K.A., et al., *Mal (MyD88-adaptor-like) is required for Toll-like receptor-4 signal transduction*. Nature, 2001. **413**(6851): p. 78-83.
210. Lin, S.-C., Y.-C. Lo, and H. Wu, *Helical assembly in the MyD88-IRAK4-IRAK2 complex in TLR/IL-1R signalling*. Nature, 2010. **465**(7300): p. 885-890.
211. Ferrao, R., et al., *IRAK4 dimerization and trans-autophosphorylation are induced by Myddosome assembly*. Molecular cell, 2014. **55**(6): p. 891-903.
212. Kollwe, C., et al., *Sequential autophosphorylation steps in the interleukin-1 receptor-associated kinase-1 regulate its availability as an adapter in interleukin-1 signaling*. Journal of Biological Chemistry, 2004. **279**(7): p. 5227-5236.
213. Cao, Z., W.J. Henzel, and X. Gao, *IRAK: a kinase associated with the interleukin-1 receptor*. Science, 1996. **271**(5252): p. 1128-31.
214. Uematsu, S., et al., *Interleukin-1 receptor-associated kinase-1 plays an essential role for Toll-like receptor (TLR) 7-and TLR9-mediated interferon- α induction*. The Journal of experimental medicine, 2005. **201**(6): p. 915-923.
215. Verstak, B., C.J. Arnot, and N.J. Gay, *An alanine-to-proline mutation in the BB-loop of TLR3 Toll/IL-1R domain switches signalling adaptor specificity*

- from TRIF to MyD88*. Journal of immunology (Baltimore, Md. : 1950), 2013. **191**(12): p. 6101-6109.
216. Oshiumi, H., et al., *TICAM-1, an adaptor molecule that participates in Toll-like receptor 3-mediated interferon-beta induction*. Nat Immunol, 2003. **4**(2): p. 161-7.
217. Tseng, P.-H., et al., *Different modes of ubiquitination of the adaptor TRAF3 selectively activate the expression of type I interferons and proinflammatory cytokines*. Nature immunology, 2010. **11**(1): p. 70-75.
218. Häcker, H., et al., *Specificity in Toll-like receptor signalling through distinct effector functions of TRAF3 and TRAF6*. Nature, 2006. **439**(7073): p. 204-207.
219. Oganessian, G., et al., *Critical role of TRAF3 in the Toll-like receptor-dependent and-independent antiviral response*. Nature, 2006. **439**(7073): p. 208-211.
220. Sun, S.C., *The noncanonical NF- κ B pathway*. Immunological reviews, 2012. **246**(1): p. 125-140.
221. Deng, L., et al., *Activation of the I κ B kinase complex by TRAF6 requires a dimeric ubiquitin-conjugating enzyme complex and a unique polyubiquitin chain*. Cell, 2000. **103**(2): p. 351-361.
222. Conze, D.B., et al., *Lys63-linked polyubiquitination of IRAK-1 is required for interleukin-1 receptor-and toll-like receptor-mediated NF- κ B activation*. Molecular and cellular biology, 2008. **28**(10): p. 3538-3547.

223. Jiang, Z., et al., *Interleukin-1 (IL-1) receptor-associated kinase-dependent IL-1-induced signaling complexes phosphorylate TAK1 and TAB2 at the plasma membrane and activate TAK1 in the cytosol*. *Molecular and cellular biology*, 2002. **22**(20): p. 7158-7167.
224. Oeckinghaus, A. and S. Ghosh, *The NF- κ B family of transcription factors and its regulation*. Cold Spring Harbor perspectives in biology, 2009. **1**(4): p. a000034.
225. Karin, M. and M. Delhase. *The I κ B kinase (IKK) and NF- κ B: key elements of proinflammatory signalling*. in *Seminars in immunology*. 2000. Elsevier.
226. Sun, S.-C. and S.C. Ley, *New insights into NF- κ B regulation and function*. *Trends in immunology*, 2008. **29**(10): p. 469-478.
227. Adli, M., et al., *IKK α and IKK β Each Function to Regulate NF- κ B Activation in the TNF-Induced/Canonical Pathway*. *PLOS ONE*, 2010. **5**(2): p. e9428.
228. McNab, F., et al., *Type I interferons in infectious disease*. *Nature Reviews Immunology*, 2015. **15**(2): p. 87-103.
229. Fitzgerald, K.A., et al., *IKK ϵ and TBK1 are essential components of the IRF3 signaling pathway*. *Nature Immunology*, 2003. **4**(5): p. 491-496.
230. Hu, X., et al., *The JAK/STAT signaling pathway: from bench to clinic*. *Signal Transduction and Targeted Therapy*, 2021. **6**(1): p. 402.
231. Kessler, D.S., et al., *Interferon-alpha regulates nuclear translocation and DNA-binding affinity of ISGF3, a multimeric transcriptional activator*. *Genes Dev*, 1990. **4**(10): p. 1753-65.

232. Schindler, C., D.E. Levy, and T. Decker, *JAK-STAT signaling: from interferons to cytokines*. Journal of Biological Chemistry, 2007. **282**(28): p. 20059-20063.
233. Wollish, A.C., et al., *An attenuating mutation in a neurovirulent Sindbis virus strain interacts with the IPS-1 signaling pathway in vivo*. Virology, 2013. **435**(2): p. 269-80.
234. Li, Y.G., et al., *Poly (I:C), an agonist of toll-like receptor-3, inhibits replication of the Chikungunya virus in BEAS-2B cells*. Virol J, 2012. **9**: p. 114.
235. Rudd, P.A., et al., *Interferon response factors 3 and 7 protect against Chikungunya virus hemorrhagic fever and shock*. J Virol, 2012. **86**(18): p. 9888-98.
236. Neighbours, L.M., et al., *Myd88-dependent toll-like receptor 7 signaling mediates protection from severe Ross River virus-induced disease in mice*. Journal of virology, 2012. **86**(19): p. 10675-10685.
237. Gao, X., R. Nasci, and G. Liang, *The neglected arboviral infections in mainland China*. PLoS Negl Trop Dis, 2010. **4**(4): p. e624.
238. Turunen, M., et al., *Pogosta disease: clinical observations during an outbreak in the province of North Karelia, Finland*. Br J Rheumatol, 1998. **37**(11): p. 1177-80.
239. Rico-Hesse, R., et al., *Emergence of a new epidemic/epizootic Venezuelan equine encephalitis virus in South America*. Proc Natl Acad Sci U S A, 1995. **92**(12): p. 5278-81.

240. Salas, R.A., et al., *Ecological studies of enzootic Venezuelan equine encephalitis in north-central Venezuela, 1997-1998*. Am J Trop Med Hyg, 2001. **64**(1-2): p. 84-92.
241. Weaver, S.C., et al., *Re-emergence of epidemic Venezuelan equine encephalomyelitis in South America*. VEE Study Group. Lancet, 1996. **348**(9025): p. 436-40.
242. Weaver, S.C., et al., *Genetic evidence for the origins of Venezuelan equine encephalitis virus subtype IAB outbreaks*. Am J Trop Med Hyg, 1999. **60**(3): p. 441-8.
243. Sidwell, R.W., L.P. Gebhardt, and B.D. Thorpe, *Epidemiological aspects of venezuelan equine encephalitis virus infections*. Bacteriol Rev, 1967. **31**(1): p. 65-81.
244. Powers, A.M., et al., *Repeated emergence of epidemic/epizootic Venezuelan equine encephalitis from a single genotype of enzootic subtype ID virus*. J Virol, 1997. **71**(9): p. 6697-705.
245. Cauchemez, S., et al., *Local and regional spread of chikungunya fever in the Americas*. Euro Surveill, 2014. **19**(28): p. 20854.
246. Renault, P., et al., *Epidemiology of Chikungunya infection on Reunion Island, Mayotte, and neighboring countries*. Med Mal Infect, 2012. **42**(3): p. 93-101.
247. Renault, P., et al., *A major epidemic of chikungunya virus infection on Reunion Island, France, 2005-2006*. Am J Trop Med Hyg, 2007. **77**(4): p. 727-31.

248. Ligon, B.L., *Reemergence of an unusual disease: the chikungunya epidemic*. Semin Pediatr Infect Dis, 2006. **17**(2): p. 99-104.
249. Jacups, S.P., P.I. Whelan, and B.J. Currie, *Ross River virus and Barmah Forest virus infections: a review of history, ecology, and predictive models, with implications for tropical northern Australia*. Vector Borne Zoonotic Dis, 2008. **8**(2): p. 283-97.
250. Rulli, N.E., et al., *The molecular and cellular aspects of arthritis due to alphavirus infections: lesson learned from Ross River virus*. Ann N Y Acad Sci, 2007. **1102**: p. 96-108.
251. Hawman, D.W., et al., *Chronic joint disease caused by persistent Chikungunya virus infection is controlled by the adaptive immune response*. J Virol, 2013. **87**(24): p. 13878-88.
252. Schwartz, O. and M.L. Albert, *Biology and pathogenesis of chikungunya virus*. Nat Rev Microbiol, 2010. **8**(7): p. 491-500.
253. Weaver, S.C., et al., *Venezuelan equine encephalitis*. Annu Rev Entomol, 2004. **49**: p. 141-74.
254. Zhang, R., et al., *4.4 A cryo-EM structure of an enveloped alphavirus Venezuelan equine encephalitis virus*. EMBO J, 2011. **30**(18): p. 3854-63.
255. Ramsey, J. and S. Mukhopadhyay, *Disentangling the Frames, the State of Research on the Alphavirus 6K and TF Proteins*. Viruses, 2017. **9**(8).
256. Kim, D.I., et al., *An improved smaller biotin ligase for BioID proximity labeling*. Mol Biol Cell, 2016. **27**(8): p. 1188-96.

257. Roux, K.J., et al., *BioID: A Screen for Protein-Protein Interactions*. *Curr Protoc Protein Sci*, 2018. **91**: p. 19 23 1-19 23 15.
258. Gottipati, S., N.L. Rao, and W.P. Fung-Leung, *IRAK1: a critical signaling mediator of innate immunity*. *Cell Signal*, 2008. **20**(2): p. 269-76.
259. Flannery, S. and A.G. Bowie, *The interleukin-1 receptor-associated kinases: critical regulators of innate immune signalling*. *Biochem Pharmacol*, 2010. **80**(12): p. 1981-91.
260. Melancon, P. and H. Garoff, *Processing of the Semliki Forest virus structural polyprotein: role of the capsid protease*. *J Virol*, 1987. **61**(5): p. 1301-9.
261. Mo, X., et al., *AKT1, LKB1, and YAP1 Revealed as MYC Interactors with NanoLuc-Based Protein-Fragment Complementation Assay*. *Mol Pharmacol*, 2017. **91**(4): p. 339-347.
262. Frolova, E., et al., *Formation of nsP3-specific protein complexes during Sindbis virus replication*. *J Virol*, 2006. **80**(8): p. 4122-34.
263. Mayuri, et al., *Role for conserved residues of sindbis virus nonstructural protein 2 methyltransferase-like domain in regulation of minus-strand synthesis and development of cytopathic infection*. *J Virol*, 2008. **82**(15): p. 7284-97.
264. Sokoloski, K.J., et al., *Encapsidation of host-derived factors correlates with enhanced infectivity of Sindbis virus*. *J Virol*, 2013. **87**(22): p. 12216-26.

265. Kim, D.I., S.C. Jensen, and K.J. Roux, *Identifying Protein-Protein Associations at the Nuclear Envelope with BioID*. *Methods Mol Biol*, 2016. **1411**: p. 133-46.
266. Roux, K.J., D.I. Kim, and B. Burke, *BioID: a screen for protein-protein interactions*. *Curr Protoc Protein Sci*, 2013. **74**: p. Unit 19 23.
267. Wang, M., et al., *Version 4.0 of PaxDb: Protein abundance data, integrated across model organisms, tissues, and cell-lines*. *Proteomics*, 2015. **15**(18): p. 3163-8.
268. Szklarczyk, D., et al., *The STRING database in 2017: quality-controlled protein-protein association networks, made broadly accessible*. *Nucleic Acids Res*, 2017. **45**(D1): p. D362-D368.
269. Huang da, W., B.T. Sherman, and R.A. Lempicki, *Bioinformatics enrichment tools: paths toward the comprehensive functional analysis of large gene lists*. *Nucleic Acids Res*, 2009. **37**(1): p. 1-13.
270. Huang da, W., B.T. Sherman, and R.A. Lempicki, *Systematic and integrative analysis of large gene lists using DAVID bioinformatics resources*. *Nat Protoc*, 2009. **4**(1): p. 44-57.
271. Casella, C.R. and T.C. Mitchell, *Putting endotoxin to work for us: monophosphoryl lipid A as a safe and effective vaccine adjuvant*. *Cell Mol Life Sci*, 2008. **65**(20): p. 3231-40.
272. Casella, C.R. and T.C. Mitchell, *Inefficient TLR4/MD-2 heterotetramerization by monophosphoryl lipid A*. *PLoS One*, 2013. **8**(4): p. e62622.

273. Szklarczyk, D., et al., *STRING v10: protein-protein interaction networks, integrated over the tree of life*. Nucleic Acids Res, 2015. **43**(Database issue): p. D447-52.
274. Schilte, C., et al., *Type I IFN controls chikungunya virus via its action on nonhematopoietic cells*. J Exp Med, 2010. **207**(2): p. 429-42.
275. Neighbours, L.M., et al., *Myd88-dependent toll-like receptor 7 signaling mediates protection from severe Ross River virus-induced disease in mice*. J Virol, 2012. **86**(19): p. 10675-85.
276. Fujita, Y., et al., *6-(4-Amino-2-butyl-imidazoquinolyl)-norleucine: Toll-like receptor 7 and 8 agonist amino acid for self-adjuvanting peptide vaccine*. Amino Acids, 2016. **48**(5): p. 1319-29.
277. Haile, L.A., et al., *Detection of innate immune response modulating impurities in therapeutic proteins*. PLoS One, 2015. **10**(4): p. e0125078.
278. Salyer, A.C., et al., *Identification of Adjuvant Activity of Amphotericin B in a Novel, Multiplexed, Poly-TLR/NLR High-Throughput Screen*. PLoS One, 2016. **11**(2): p. e0149848.
279. Schuster, L., et al., *Reporter cell assay-based functional quantification of TNF-alpha-antagonists in serum - a proof-of-principle study for adalimumab*. Anal Biochem, 2020. **596**: p. 113646.
280. Blasius, A.L. and B. Beutler, *Intracellular toll-like receptors*. Immunity, 2010. **32**(3): p. 305-15.

281. Garmashova, N., et al., *The Old World and New World alphaviruses use different virus-specific proteins for induction of transcriptional shutoff*. J Virol, 2007. **81**(5): p. 2472-84.
282. Helenius, A., M. Marsh, and J. White, *Inhibition of Semliki forest virus penetration by lysosomotropic weak bases*. J Gen Virol, 1982. **58 Pt 1**: p. 47-61.
283. Warner, N.L., et al., *Mammarenaviral Infection Is Dependent on Directional Exposure to and Release from Polarized Intestinal Epithelia*. Viruses, 2018. **10**(2).
284. Garmashova, N., et al., *Analysis of Venezuelan equine encephalitis virus capsid protein function in the inhibition of cellular transcription*. J Virol, 2007. **81**(24): p. 13552-65.
285. Atasheva, S., et al., *Venezuelan equine encephalitis virus capsid protein inhibits nuclear import in Mammalian but not in mosquito cells*. J Virol, 2008. **82**(8): p. 4028-41.
286. Atasheva, S., et al., *Venezuelan equine encephalitis virus variants lacking transcription inhibitory functions demonstrate highly attenuated phenotype*. J Virol, 2015. **89**(1): p. 71-82.
287. Carey, B.D., et al., *Protein Kinase C subtype delta interacts with Venezuelan equine encephalitis virus capsid protein and regulates viral RNA binding through modulation of capsid phosphorylation*. PLoS Pathog, 2020. **16**(3): p. e1008282.

288. Carey, B.D., et al., *Protein Phosphatase 1alpha Interacts with Venezuelan Equine Encephalitis Virus Capsid Protein and Regulates Viral Replication through Modulation of Capsid Phosphorylation*. J Virol, 2018. **92**(15).
289. Fonseca, B.D., et al., *La-related Protein 1 (LARP1) Represses Terminal Oligopyrimidine (TOP) mRNA Translation Downstream of mTOR Complex 1 (mTORC1)*. J Biol Chem, 2015. **290**(26): p. 15996-6020.
290. Lahr, R.M., et al., *La-related protein 1 (LARP1) binds the mRNA cap, blocking eIF4F assembly on TOP mRNAs*. Elife, 2017. **6**.
291. Hong, S., et al., *LARP1 functions as a molecular switch for mTORC1-mediated translation of an essential class of mRNAs*. Elife, 2017. **6**.
292. Philippe, L., et al., *La-related protein 1 (LARP1) repression of TOP mRNA translation is mediated through its cap-binding domain and controlled by an adjacent regulatory region*. Nucleic Acids Res, 2018. **46**(3): p. 1457-1469.
293. Aoki, K., et al., *LARP1 specifically recognizes the 3' terminus of poly(A) mRNA*. FEBS Lett, 2013. **587**(14): p. 2173-8.
294. Vikesaa, J., et al., *RNA-binding IMPs promote cell adhesion and invadopodia formation*. EMBO J, 2006. **25**(7): p. 1456-68.
295. Wachter, K., et al., *Subcellular localization and RNP formation of IGF2BPs (IGF2 mRNA-binding proteins) is modulated by distinct RNA-binding domains*. Biol Chem, 2013. **394**(8): p. 1077-90.
296. Park, E. and L.E. Maquat, *Staufen-mediated mRNA decay*. Wiley Interdiscip Rev RNA, 2013. **4**(4): p. 423-35.

297. Balistreri, G., et al., *The host nonsense-mediated mRNA decay pathway restricts Mammalian RNA virus replication*. Cell Host Microbe, 2014. **16**(3): p. 403-11.
298. Fukushima, M., et al., *TDP-43 accelerates deadenylation of target mRNAs by recruiting Caf1 deadenylase*. FEBS Lett, 2019. **593**(3): p. 277-287.
299. Garneau, N.L., et al., *The 3' untranslated region of sindbis virus represses deadenylation of viral transcripts in mosquito and Mammalian cells*. J Virol, 2008. **82**(2): p. 880-92.
300. Sokoloski, K.J., et al., *Sindbis virus usurps the cellular HuR protein to stabilize its transcripts and promote productive infections in mammalian and mosquito cells*. Cell Host Microbe, 2010. **8**(2): p. 196-207.
301. Wang, X., et al., *N6-methyladenosine-dependent regulation of messenger RNA stability*. Nature, 2014. **505**(7481): p. 117-20.
302. Wang, X., et al., *N(6)-methyladenosine Modulates Messenger RNA Translation Efficiency*. Cell, 2015. **161**(6): p. 1388-99.
303. Du, H., et al., *YTHDF2 destabilizes m(6)A-containing RNA through direct recruitment of the CCR4-NOT deadenylase complex*. Nat Commun, 2016. **7**: p. 12626.
304. Park, O.H., et al., *Endoribonucleolytic Cleavage of m(6)A-Containing RNAs by RNase P/MRP Complex*. Mol Cell, 2019. **74**(3): p. 494-507 e8.
305. Xu, C., et al., *Structural Basis for the Discriminative Recognition of N6-Methyladenosine RNA by the Human YT521-B Homology Domain Family of Proteins*. J Biol Chem, 2015. **290**(41): p. 24902-13.

306. Wojtas, M.N., et al., *Regulation of m(6)A Transcripts by the 3'-->5' RNA Helicase YTHDC2 Is Essential for a Successful Meiotic Program in the Mammalian Germline*. *Mol Cell*, 2017. **68**(2): p. 374-387 e12.
307. Ye, P., et al., *DEXH-Box protein DHX30 is required for optimal function of the zinc-finger antiviral protein*. *Protein Cell*, 2010. **1**(10): p. 956-64.
308. Bick, M.J., et al., *Expression of the zinc-finger antiviral protein inhibits alphavirus replication*. *J Virol*, 2003. **77**(21): p. 11555-62.
309. Guo, X., et al., *The zinc finger antiviral protein directly binds to specific viral mRNAs through the CCCH zinc finger motifs*. *J Virol*, 2004. **78**(23): p. 12781-7.
310. Guo, X., et al., *The zinc-finger antiviral protein recruits the RNA processing exosome to degrade the target mRNA*. *Proc Natl Acad Sci U S A*, 2007. **104**(1): p. 151-6.
311. Tang, Q., X. Wang, and G. Gao, *The Short Form of the Zinc Finger Antiviral Protein Inhibits Influenza A Virus Protein Expression and Is Antagonized by the Virus-Encoded NS1*. *J Virol*, 2017. **91**(2).
312. Hong, E.M., R. Perera, and R.J. Kuhn, *Alphavirus capsid protein helix I controls a checkpoint in nucleocapsid core assembly*. *J Virol*, 2006. **80**(18): p. 8848-55.
313. Warriar, R., et al., *Role of sindbis virus capsid protein region II in nucleocapsid core assembly and encapsidation of genomic RNA*. *J Virol*, 2008. **82**(9): p. 4461-70.

314. Lulla, V., et al., *The amino-terminal domain of alphavirus capsid protein is dispensable for viral particle assembly but regulates RNA encapsidation through cooperative functions of its subdomains*. J Virol, 2013. **87**(22): p. 12003-19.
315. Reynaud, J.M., et al., *The SD1 Subdomain of Venezuelan Equine Encephalitis Virus Capsid Protein Plays a Critical Role in Nucleocapsid and Particle Assembly*. J Virol, 2016. **90**(4): p. 2008-20.
316. Forsell, K., G. Griffiths, and H. Garoff, *Preformed cytoplasmic nucleocapsids are not necessary for alphavirus budding*. EMBO J, 1996. **15**(23): p. 6495-505.
317. Forsell, K., M. Suomalainen, and H. Garoff, *Structure-function relation of the NH2-terminal domain of the Semliki Forest virus capsid protein*. J Virol, 1995. **69**(3): p. 1556-63.
318. Gorchakov, R., et al., *PKR-dependent and -independent mechanisms are involved in translational shutoff during Sindbis virus infection*. J Virol, 2004. **78**(16): p. 8455-67.
319. Gorchakov, R., E. Frolova, and I. Frolov, *Inhibition of transcription and translation in Sindbis virus-infected cells*. J Virol, 2005. **79**(15): p. 9397-409.
320. Garmashova, N., et al., *Sindbis virus nonstructural protein nsP2 is cytotoxic and inhibits cellular transcription*. J Virol, 2006. **80**(12): p. 5686-96.

321. Frolov, I., et al., *Early events in alphavirus replication determine the outcome of infection*. J Virol, 2012. **86**(9): p. 5055-66.
322. Sims, J.E. and D.E. Smith, *The IL-1 family: regulators of immunity*. Nat Rev Immunol, 2010. **10**(2): p. 89-102.
323. Mantovani, A., et al., *Interleukin-1 and Related Cytokines in the Regulation of Inflammation and Immunity*. Immunity, 2019. **50**(4): p. 778-795.
324. Dinarello, C.A., *Overview of the IL-1 family in innate inflammation and acquired immunity*. Immunol Rev, 2018. **281**(1): p. 8-27.
325. Dinarello, C.A., *Interleukin-1 in the pathogenesis and treatment of inflammatory diseases*. Blood, 2011. **117**(14): p. 3720-32.
326. Michael, B.D., et al., *The Interleukin-1 Balance During Encephalitis Is Associated With Clinical Severity, Blood-Brain Barrier Permeability, Neuroimaging Changes, and Disease Outcome*. J Infect Dis, 2016. **213**(10): p. 1651-60.
327. Assuncao-Miranda, I., M.T. Bozza, and A.T. Da Poian, *Pro-inflammatory response resulting from sindbis virus infection of human macrophages: implications for the pathogenesis of viral arthritis*. J Med Virol, 2010. **82**(1): p. 164-74.
328. Kelvin, A.A., et al., *Inflammatory cytokine expression is associated with chikungunya virus resolution and symptom severity*. PLoS Negl Trop Dis, 2011. **5**(8): p. e1279.

329. Tappe, D., et al., *Increased Proinflammatory Cytokine Levels in Prolonged Arthralgia in Ross River Virus Infection*. *Emerg Infect Dis*, 2017. **23**(4): p. 702-704.
330. Gardner, C.L., et al., *Type I interferon induction is correlated with attenuation of a South American eastern equine encephalitis virus strain in mice*. *Virology*, 2009. **390**(2): p. 338-347.
331. Griffin, D., *The Togaviridae and Flaviviridae (S. Schlesinger and MJ Schlesinger, eds.) Plenum Press*. New York, 1986: p. 209-249.
332. Griffin, D.E., *Molecular pathogenesis of Sindbis virus encephalitis in experimental animals*. *Advances in virus research*, 1989. **36**: p. 255-271.
333. Ryman, K.D. and W.B. Klimstra, *Host responses to alphavirus infection*. *Immunological reviews*, 2008. **225**(1): p. 27-45.
334. Janeway Jr, C.A. and R. Medzhitov, *Innate immune recognition*. *Annual review of immunology*, 2002. **20**(1): p. 197-216.
335. Landers, V.D., et al., *The Alphaviral Capsid Protein Inhibits IRAK1-Dependent TLR Signaling*. *Viruses*, 2021. **13**(3): p. 377.
336. Linger, B.R., et al., *Sindbis virus nucleocapsid assembly: RNA folding promotes capsid protein dimerization*. *Rna*, 2004. **10**(1): p. 128-138.
337. Choi, H.K., et al., *Structure of Semliki Forest virus core protein*. *Proteins: Structure, Function, and Bioinformatics*, 1997. **27**(3): p. 345-359.
338. Choi, H.-K., et al., *Structure of Sindbis virus core protein reveals a chymotrypsin-like serine proteinase and the organization of the virion*. *Nature*, 1991. **354**(6348): p. 37-43.

339. Aggarwal, M., et al., *Crystal structure of aura virus capsid protease and its complex with dioxane: new insights into capsid-glycoprotein molecular contacts*. PLoS One, 2012. **7**(12): p. e51288.
340. Aliperti, G. and M.J. Schlesinger, *Evidence for an autoprotease activity of Sindbis virus capsid protein*. Virology, 1978. **90**(2): p. 366-369.
341. Thomas, S., et al., *Functional dissection of the alphavirus capsid protease: sequence requirements for activity*. Virology journal, 2010. **7**(1): p. 1-7.
342. Barreto, G., et al., *Lumican is upregulated in osteoarthritis and contributes to TLR4-induced pro-inflammatory activation of cartilage degradation and macrophage polarization*. Osteoarthritis Cartilage, 2020. **28**(1): p. 92-101.
343. Grabowski, M., et al., *Identification and validation of a novel dual small-molecule TLR2/8 antagonist*. Biochem Pharmacol, 2020. **177**: p. 113957.
344. Hankins, J.V., et al., *Amino acid addition to Vibrio cholerae LPS establishes a link between surface remodeling in gram-positive and gram-negative bacteria*. Proc Natl Acad Sci U S A, 2012. **109**(22): p. 8722-7.
345. Murase, M., et al., *Intravesicular Acidification Regulates Lipopolysaccharide Inflammation and Tolerance through TLR4 Trafficking*. J Immunol, 2018. **200**(8): p. 2798-2808.
346. Rahiman, S.S.F., et al., *Inhibitory effects of dynorphin 3-14 on the lipopolysaccharide-induced toll-like receptor 4 signalling pathway*. Peptides, 2017. **90**: p. 48-54.

347. Satta, N., et al., *Toll-like receptor 2 mediates the activation of human monocytes and endothelial cells by antiphospholipid antibodies*. *Blood*, 2011. **117**(20): p. 5523-31.
348. Warriar, R., et al., *Role of Sindbis Virus Capsid Protein Region II in Nucleocapsid Core Assembly and Encapsidation of Genomic RNA*. *Journal of Virology*, 2008. **82**(9): p. 4461-4470.
349. Jain, A., S. Kaczanowska, and E. Davila, *IL-1 Receptor-Associated Kinase Signaling and Its Role in Inflammation, Cancer Progression, and Therapy Resistance*. *Frontiers in immunology*, 2014. **5**: p. 553-553.
350. Oda, K. and H. Kitano, *A comprehensive map of the toll-like receptor signaling network*. *Molecular systems biology*, 2006. **2**(1): p. 2006.0015.
351. Diebold, S.S., et al., *Innate antiviral responses by means of TLR7-mediated recognition of single-stranded RNA*. *Science*, 2004. **303**(5663): p. 1529-31.
352. Greulich, W., et al., *TLR8 Is a Sensor of RNase T2 Degradation Products*. *Cell*, 2019. **179**(6): p. 1264-1275.e13.
353. Heil, F., et al., *Species-specific recognition of single-stranded RNA via toll-like receptor 7 and 8*. *Science*, 2004. **303**(5663): p. 1526-9.
354. Krüger, A., et al., *Human TLR8 senses UR/URR motifs in bacterial and mitochondrial RNA*. *EMBO reports*, 2015. **16**(12): p. 1656-1663.
355. Wesche, H., et al., *MyD88: An Adapter That Recruits IRAK to the IL-1 Receptor Complex*. *Immunity*, 1997. **7**(6): p. 837-847.

356. Chen, W., et al., *Specific inhibition of NLRP3 in chikungunya disease reveals a role for inflammasomes in alphavirus-induced inflammation*. *Nature microbiology*, 2017. **2**(10): p. 1435-1445.
357. Liang, X.H., et al., *Resistance of interleukin-1beta-deficient mice to fatal Sindbis virus encephalitis*. *Journal of virology*, 1999. **73**(3): p. 2563-2567.
358. Ng, L.F.P., et al., *IL-1beta, IL-6, and RANTES as biomarkers of Chikungunya severity*. *PloS one*, 2009. **4**(1): p. e4261-e4261.
359. Wolf, S., et al., *Inhibition of Interleukin-1 β Signaling by Anakinra Demonstrates a Critical Role of Bone Loss in Experimental Arthritogenic Alphavirus Infections*. *Arthritis & Rheumatology*, 2019. **71**(7): p. 1185-1190.
360. Belvin, M.P. and K.V. Anderson, *A conserved signaling pathway: the Drosophila toll-dorsal pathway*. *Annual review of cell and developmental biology*, 1996. **12**(1): p. 393-416.
361. Horng, T. and R. Medzhitov, *Drosophila MyD88 is an adapter in the Toll signaling pathway*. *Proceedings of the National Academy of Sciences*, 2001. **98**(22): p. 12654-12658.
362. Lemaitre, B., et al., *The dorsoventral regulatory gene cassette spätzle/Toll/cactus controls the potent antifungal response in Drosophila adults*. *Cell*, 1996. **86**(6): p. 973-983.
363. Medzhitov, R., P. Preston-Hurlburt, and C.A. Janeway Jr, *A human homologue of the Drosophila Toll protein signals activation of adaptive immunity*. *nature*, 1997. **388**(6640): p. 394-397.

364. Moynagh, P.N., *The Pellino family: IRAK E3 ligases with emerging roles in innate immune signalling*. Trends in immunology, 2009. **30**(1): p. 33-42.
365. Daigneault, J., L. Klemetsaune, and S.A. Wasserman, *The IRAK homolog Pelle is the functional counterpart of I κ B kinase in the Drosophila Toll pathway*. PloS one, 2013. **8**(9): p. e75150-e75150.
366. Großhans, J., et al., *Activation of the kinase Pelle by Tube in the dorsoventral signal transduction pathway of Drosophila embryo*. Nature, 1994. **372**(6506): p. 563-566.
367. Hecht, P.M. and K.V. Anderson, *Genetic characterization of tube and pelle, genes required for signaling between Toll and dorsal in the specification of the dorsal-ventral pattern of the Drosophila embryo*. Genetics, 1993. **135**(2): p. 405-17.
368. Towb, P., A. Bergmann, and S.A. Wasserman, *The protein kinase Pelle mediates feedback regulation in the Drosophila Toll signaling pathway*. Development, 2001. **128**(23): p. 4729-36.
369. Valanne, S., J.H. Wang, and M. Rämetsä, *The Drosophila Toll signaling pathway*. J Immunol, 2011. **186**(2): p. 649-56.
370. Barletta, A.B.F., et al., *Microbiota activates IMD pathway and limits Sindbis infection in Aedes aegypti*. Parasites & Vectors, 2017. **10**(1): p. 103.
371. De Gregorio, E., et al., *The Toll and Imd pathways are the major regulators of the immune response in Drosophila*. The EMBO journal, 2002. **21**(11): p. 2568-2579.

372. Hoffmann, J.A., *The immune response of Drosophila*. Nature, 2003. **426**(6962): p. 33-38.
373. Rutschmann, S., A. Kilinc, and D. Ferrandon, *Cutting edge: the toll pathway is required for resistance to gram-positive bacterial infections in Drosophila*. The Journal of Immunology, 2002. **168**(4): p. 1542-1546.
374. Tanji, T., et al., *Toll and IMD pathways synergistically activate an innate immune response in Drosophila melanogaster*. Molecular and cellular biology, 2007. **27**(12): p. 4578-4588.
375. Avadhanula, V., et al., *A novel system for the launch of alphavirus RNA synthesis reveals a role for the Imd pathway in arthropod antiviral response*. PLoS pathogens, 2009. **5**(9): p. e1000582.
376. Fragkoudis, R., et al., *Semliki Forest virus strongly reduces mosquito host defence signaling*. Insect molecular biology, 2008. **17**(6): p. 647-656.
377. Huang, Z., et al., *An antiviral role for antimicrobial peptides during the arthropod response to alphavirus replication*. Journal of virology, 2013. **87**(8): p. 4272-4280.
378. Fields, J.K., S. Günther, and E.J. Sundberg, *Structural Basis of IL-1 Family Cytokine Signaling*. Frontiers in Immunology, 2019. **10**.
379. Gorchakov, R., et al., *Attenuation of Chikungunya virus vaccine strain 181/clone 25 is determined by two amino acid substitutions in the E2 envelope glycoprotein*. J Virol, 2012. **86**(11): p. 6084-96.

380. Edelman, R., et al., *Phase II safety and immunogenicity study of live chikungunya virus vaccine TSI-GSD-218*. Am J Trop Med Hyg, 2000. **62**(6): p. 681-5.
381. Pittman, P.R., et al., *Long-term duration of detectable neutralizing antibodies after administration of live-attenuated VEE vaccine and following booster vaccination with inactivated VEE vaccine*. Vaccine, 1996. **14**(4): p. 337-343.
382. Kautz, T.F., et al., *Low-fidelity Venezuelan equine encephalitis virus polymerase mutants to improve live-attenuated vaccine safety and efficacy*. Virus Evol, 2018. **4**(1): p. vey004.
383. PEDERSEN, C.E., JR., D.M. ROBINSON, and F.E. COLE, JR., *ISOLATION OF THE VACCINE STRAIN OF VENEZUELAN EQUINE ENCEPHALOMYELITIS VIRUS FROM MOSQUITOES IN LOUISIANA*. American Journal of Epidemiology, 1972. **95**(5): p. 490-496.
384. Nooraei, S., et al., *Virus-like particles: preparation, immunogenicity and their roles as nanovaccines and drug nanocarriers*. Journal of Nanobiotechnology, 2021. **19**(1): p. 59.
385. Urakami, A., et al., *Development of a Novel Virus-Like Particle Vaccine Platform That Mimics the Immature Form of Alphavirus*. Clinical and vaccine immunology : CVI, 2017. **24**(7): p. e00090-17.
386. Malcova, H., et al., *IL-1 Inhibitors in the Treatment of Monogenic Periodic Fever Syndromes: From the Past to the Future Perspectives*. Frontiers in Immunology, 2021. **11**.

387. Wikén, M., et al., *Development and effect of antibodies to anakinra during treatment of severe CAPS: sub-analysis of a long-term safety and efficacy study*. *Clinical Rheumatology*, 2018. **37**(12): p. 3381-3386.

GLOSSARY

181/25	181/clone 25
5' TOP	5' terminal oligopyrimidine motif
ADE	Antibody-dependent enhancement
ANOVA	Analysis of variance
AP	Adapter proteins
Arbovirus	Arthropod-borne virus
AUD	Alphavirus-unique domain
BiMC	BiMolecular complementation
CHIKV	Chikungunya virus
CNS	Central nervous system
COPII	Coat protein complex II
CP	Capsid protein
DAMP	Damage-associated molecular pattern
DD	Death Domain
DMEM	Dulbecco's Modified Eagle Medium
dpi	Days post infection

DTT	DiThioThreitol
EEE	Easter Equine Encephalitis virus
ER	Endoplasmic reticulum
FBS	Fetal Bovine Serum
FPKM	Fragments per kilobase million
gp96	Glycoprotein 96
hpt	hours post treatment
HVD	Hypervariable domain
IC	Intracranial
IFN	Type-I interferon
IFNAR	IFN α receptor
IKK	I κ B kinase
IRAK	IL-1 receptor-associated kinase
IRF	IFN-regulatory factor
ISG	Interferon response genes
ISRE	Interferon-sensitive response element
JAK	Janus kinase
LRR	Leucine rich repeats

m6A	N6-methyladenosine readers
Macro	Macrodomain
MAL	MyD88-adaptor like
MAYV	Mayaro virus
MEM	Minimal Essential Media
MST	Mean survival time
naCP-RNA	non-assembly CP-RNA
NC	Nucleocapsid core
NEAA	Non-essential amino acids
NEMO	NF- κ B essential modulator
NF- κ B	Nuclear factor κ B
NLS	Nuclear localization signal
NMD	Non-sense mediated decay
PAMP	Pathogen-associated molecular pattern
PBS	Phosphate Buffered Saline
Pen/Strep	Penicillin/Streptomycin
PERK	PKR-like ER kinase
PKR	dsRNA-dependent protein kinase

Poly(I:C)	Polyinosinic acid: polycytidylic acid
PRAT4A	Protein Associated with TLR4 A
Pro	Protease domain
PRR	Pathogen recognition receptor
RdRP	Rna-dependent RNA-polymerase
RI	Region I
RII	Region II
RLE	Relative log expression
RRM	RNA-Recognition motifs
RRV	Ross River virus
SARM	Sterile α - and amafillo-motif-containing protein
SDS	Sodium Dodecyl Sulfate
SDS-PAGE	SDS-poly acrylmide gel electrophoresis
SEAP	Secreted embryonic alkaline phosphotase
SFV	Semliki Forest virus
SINV	Sindbis virus
SMD	Staufen-Mediated Decay
Spz	Spätzle

STAT	Signal transducer and activator of transcription
TAB2	TGF-beta activated kinase
TAK1	Transforming growth factor beta-activated kinase 1
TANK	TRAF associated NF-kB activator
TBK1	TANK binding kinase 1
TCA	TriChloroactic acid
TIR	Toll/IL-1 receptor
TIRAP	TIR domain-containing adptor protein
TKL	Tyrosine kinase like
TLR	Toll-like receptor
TNF α	Tumor necrosis factor α
TNFR	TNF α receptor
TRAF	Tumor necrosis factor receptor-associated factor
TRAM	TRIF-related adptor molecule
TRIF	TIR-domain containing adaptor molecule
TRIM3	Tripartite motif-containing protein 3
UPR	Unfolded Protein Response
VEE	Venezuelan Equine Encephalitis virus

VLP	Virus-like particles
WEE	Western Equine Encephalitis virus
WT	Wild-type
YFV	Yellow Fever virus
ZAP	Zinc-finger antiviral protein

CURRICULUM VITAE

V "Trey" Landers
505 S. Hancock St. room
642E Louisville, KY, 40202
v.landerson@louisville.edu

EDUCATION

2011-2015 B.S. Molecular Biology, Lipscomb University, Nashville, TN
2015-2016 M.S. Biomolecular Science, Lipscomb University, Nashville,
TN
2017-current Ph.D. Microbiology and Immunology, University of Louisville,
Louisville, KY

PROFESSIONAL MEMBERSHIPS AND ACTIVITIES

2018-2021 American Society for Microbiology
2019- 2022 Microbiology Society
2019-current American Society for Virology

HONORS AND AWARDS

2014 Summer research fellowship in infectious disease, Lipscomb
University, Nashville, TN
2020 American Society for Virology Student Travel Award (meeting
canceled due to COVID-19 pandemic)
2021 American Society for Virology Student Registration Award
2022 American Society for Virology Student Travel Award
2019-2021 T32 Inflammation and pathogenesis NIH-T32 AI132146 Fellow

ABSTRACTS AND PRESENTATIONS

Oral Presentations

National/International Meetings

1. Identifying the role of sindbis capsid IRAK1 interactions during viral life cycle **Landers, Trey**, Sokoloski, Kevin, American Society of Virology annual conference, Minneapolis, MN 2019
2. Identifying and characterizing a novel Sindbis virus capsid and IRAK1 interaction **Landers, Trey**, Sokoloski, Kevin, Microbiology Society annual conference Edinburgh, UK 2020 (canceled due to COVID-19 pandemic)
3. The Alphavirus Capsid Protein disrupts TLR and Il-1 Signaling by Interactions with IRAK1 **Landers, Trey**, Sokoloski, Kevin American Society of Virology annual conference, virtual, 2021
4. The Alphaviral Capsid Protein Inhibits IRAK1-Dependent TLR Signaling to Promote Pathogenesis **Landers, Trey**, Thomas, Milton, Sokoloski, Kevin. Microbiology Society annual conference Belfast, UK 2022
5. The Alphavirus Capsid Protein Inhibits IRAK1-Dependent TLR Signaling to Promote Pathogenesis **Landers, Trey**, Thomas, Milton, Sokoloski, Kevin American Society of Virology annual conference, Madison, WI, 2022

Local/Regional Meetings

1. Identifying the effect of alphavirus capsid on IRAK1 signaling **Landers, Trey**, Sokoloski, Kevin, KY-TN ASM Branch Meeting, virtual meeting 2020

Invited Seminars

1. The Ohio State University, Columbus, OH (2022) “The Alphaviral Capsid Protein Inhibits IRAK1-Dependent TLR Signaling to Promote Pathogenesis”
2. University of Massachusetts Chen Medical School, Worcester, MA (2023) “The Alphaviral Capsid Protein Inhibits IRAK1-Dependent TLR Signaling to Promote Pathogenesis”
3. University of Colorado Anschutz, Aurora CO (2023) “The Alphaviral Capsid Protein Inhibits IRAK1-Dependent TLR Signaling to Promote Pathogenesis”

Poster Presentations

National/International Meetings

1. The JAK/STAT Pathway is Responsible for Immunoproteasome Activation and Potentially MHCI presentation with both TNF- α and IFN- γ in Murine Macrophages, but not Murine Dendritic Cells. **Landers, Trey**, Williams,

Amanda, Keystone Symposia Cytokine JAK-STAT Signaling in Immunity and Disease, Steamboat Springs, CO January 2016

2. Characterizing a Novel Interaction Between Sindbis Virus Capsid and IRAK1 **Landers, Trey**, Sokoloski, Kevin, American Society for Virology annual conference 2020 (canceled due to COVID-19 pandemic)
3. The Alphavirus Capsid Protein Inhibits IRAK1-Dependent Signaling to Promote Infection, Neuroinvasion, and Pathogenesis **Landers, Trey**, Thomas, Milton, Sokoloski, Kevin Positive-Sense RNA Viruses Keystone Symposia, Keystone, CO 2022

Local/Regional Meetings

1. Determining the Potential Role of NF- κ B in Immunoproteasome Subunit Expression Induced by TNF- α Association of Southeastern Biologist **Landers, Trey**, Williams, Amanda, Chattanooga, TN April 2015
2. Identifying Sindbis virus host factor interactions through use of a biotin ligase strategy **Landers, Trey**, Sokoloski, Kevin, Research!Louisville Louisville, KY October 2018
3. Identifying Sindbis virus host factor interactions through use of a biotin ligase strategy **Landers, Trey**, Sokoloski, Kevin, KY-TN ASM Branch Meeting Murfreesboro, TN November 2018
4. Identifying the role of sindbis capsid IRAK1 interactions during viral life cycle **Landers, Trey**, Sokoloski, Kevin, Research!Louisville Louisville, KY September 2019
5. Identifying the role of sindbis capsid IRAK1 interactions during viral life cycle **Landers, Trey**, Sokoloski, Kevin, Midwest Virology Symposium Columbus, OH, October 2019
6. Identifying Sindbis Virus Host Factor Interactions Through Use of a Biotin Ligase Strategy **Landers, Trey**, Sokoloski, Kevin, Research!Louisville, Louisville, KY 2021
7. The Alphavirus Capsid Protein Inhibits IRAK1-Dependent Signaling to Promote Infection, Neuroinvasion, and Pathogenesis **Landers, Trey**, Thomas, Milton, Sokoloski, Kevin, Research!Louisville, Louisville, KY, 2022

PUBLICATIONS

1. Zhang, Y., Hao, J., Zeng, J., Li, Q., Rao, E., Sun, Y., Liu, L., Mandal, A., **Landers, V D.**, Morris, R., Cleary, M., Suttles, J., and Li, B. Epidermal FABP prevents chemical-induced skin tumorigenesis by regulation of TPA-induced IFN/p53/SOX2 pathway in keratinocytes. *Journal of Investigative Dermatology*, 138(9), 1925-1934
2. LaPointe, A. T., **Landers, V D.**, Westcott, C. E., & Sokoloski, K. J. (2020). Production of Noncapped Genomic RNAs is Critical to Sindbis Virus Disease and Pathogenicity. *Mbio*, 11(6).
3. **Landers, V D.**, Wilkey, D. W., Merchant, M. L., Mitchell, T. C., & Sokoloski, K. J. (2021). The Alphaviral Capsid Protein Inhibits IRAK1-Dependent TLR Signaling. *Viruses*, 13(3), 377.
4. **Landers, V D.**, Thomas, Milton, Isom, Cierra, Sokoloski, Kevin J. The Alphavirus Capsid Protein Promotes Neuroinvasion and Pathogenesis by Inhibiting IRAK1-Dependent Pathways, In preparation.